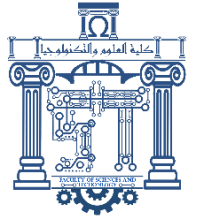الجمهورية الجزائرية الديمقراطية الشعبية

Republique Algerienne Democratique Et Populaire

وزارة التعليم العالي والبحث العلمي

Ministère de l'Enseignement Supérieur et de la Recherche Scientifique

جامعة العربي التبسي – تبسة

Université Larbi Tébessi – Tébessa –

Faculté des Sciences et de la Technologie

Département de Génie Civil

MEMOIRE

Présenté pour l'obtention du **diplôme** de **Master Académique**

En : Filière Génie Civil

Spécialité : Structures

Par : **Chifa Merabti**

Sujet

The mechanical behaviour of hollow clay brick masonry under normal compression

Présenté et soutenu publiquement, le :12 /06 /2022, devant le jury composé de :

Ali MESSABHIA	**Professeur**	**Président**
Ismail LAYADI	**Maître Conférence B**	**Rapporteur**
Abdelouaheb BOUDJELLAL	**Maître Conférence b**	**Examinateur 1**

Promotion : 2021/2022

Acknowledgements

In recognition, I would like to express my sincere thanks to all those who contributed directly or indirectly to this study,

In the impossibility of mentioning all the names, our sincere thanks go to all those who, from near or far, have allowed by their advice and their skills the realization of this thesis

My sincere gratitude to **Dr Layadi** , the completion of this study could not have been possible without his expertise and **patience**, he has been an ideal teacher, mentor, and thesis supervisor, offering advice and encouragement, representing a role model of honest work and dedication.

I would like to thank the members of the civil engineering department at Chikh Larbi Tebessi University for the tremendous work they are doing to create the most favorable conditions for us to conduct our studies and for generously sharing their knowledge, I am very grateful for being taught and educated by them, and I regret not taking advantage of every moment I could've spent in class, knowing that I might not find instructors with such dedication again.

I would like to express my gratitude to the members of CTC-Tebessa, for sharing their expertise and mentoring me through the internship, it was my pleasure to be surrounded by proficient engineers, Especially Mr; Boudjellal Elhadi, who have been more than just a mentor, I would like to thank Mr. Amoura Mohamed for providing this opportunity.

And last but not least, I would like to thank my parents, my sister Bouchra and Wafa, My brothers, and my friends Yasmin, Ikram, Aicha, Ghizlaine, Taima, Marwa, and Nesrine, for being supportive through this journey.

Abstract:

Hollow clay brick masonry is the most common used building material for infill, Bricks and Mortar, chief constituents of masonry, makes masonry non-homogeneous and offers complexity during experimental as well as numerical investigations. The present work focusses on the determination of mechanical properties of Hollow Clay Brick Masonry under normal uniaxial compression loading. A numerical approach is developed using the Abaqus software to capture the inelastic behaviour of masonry specimens under uniaxial compression loadings. The Concrete Damage Plasticity (CDP) model implemented in Abaqus is adopted in this case to model the masonry wall. An existing experimental program is used for the validation of the numerical approach. The numerical model developed showed a good correlation with the experimental results.

Résumé :

La maçonnerie en brique d'argile creuse est le matériau de construction le plus couramment utilisé pour le remplissage, les briques et le mortier, principaux constituants de la maçonnerie, rend la maçonnerie non homogène et offre de la complexité lors d'enquêtes expérimentales et numériques. Le présent travail est axé sur la détermination des propriétés mécaniques de la maçonnerie en brique d'argile creuse sous charge de compression uniaxiale normale. Une approche numérique est développée à l'aide du logiciel Abaqus pour capturer le comportement inélastique des échantillons de maçonnerie sous des charges de compression uniaxiale. Le modèle de plasticité des dommages au béton (CDP) mis en œuvre à Abaqus est adopté dans ce cas pour modéliser le mur de maçonnerie. Un programme expérimental existant est utilisé pour la validation de l'approche numérique. Le modèle numérique développé a montré une bonne corrélation avec les résultats expérimentaux.

Mot- clés :

Maçonnerie, brique creuse en terre cuite, maçonnerie non renforcée, maçonnerie de briques, comportement uniaxial, comportement en compression, compression normale, compression uniaxiale, modélisation numérique, micro-modélisation, Concrete damaged plasticity.

الملخص:

الطوب الطيني المجوف هو أكثر مواد البناء المستخدمة شيوعًا لبناء الجدران، والطوب والملاط، المكونات الرئيسية للجدار تجعله غير متجانس وتوفر تعقيدًا أثناء التحقيقات التجريبية وكذلك العددية. يركز العمل الحالي على تحديد الخصائص الميكانيكية لـ Hollow Clay Brick Masonry تحت تحميل ضغط موحد عادي. يتم تطوير نهج عددي باستخدام برنامج Abaqus لالتقاط السلوك غير المرن لعينات البناء تحت تحميل ضغط موحد. تم اعتماد نموذج مرونة الضرر الخرساني (CDP) المطبق في Abaqus في هذه الحالة لنمذجة جدار البناء. يتم استخدام برنامج تجريبي قائم للتحقق من صحة النهج العددي. أظهر النموذج العددي الذي تم تطويره ارتباطًا جيدًا بالنتائج التجريبية.

الكلمات المفتاحية:

البناء، الطوب الطيني المجوف، البناء غير المقوى، البناء بالطوب، السلوك أحادي المحور، السلوك في الانضغاط، الضغط العادي، الضغط أحادي المحور، النمذجة العددية، النمذجة الدقيقة، اللدونة التالفة للخرسانة.

Table of Figures

Table of Tables

List of symbols

ε — Total strain rate

ε^{el} — Elastic part of strain rate

ε^{pl} — Plastic part of strain rate

d — Scalar stiffness degradation variable

D_0^{el} — Initial (undamaged) elastic stiffness of the material

D^{el} — Degraded elastic stiffness

d_c — Damage factor during compression

d_t — Damage factor during tension

$\tilde{\varepsilon}_t^{pl}$ — Hardening factor (Tension Damage)

$\tilde{\varepsilon}_c^{pl}$ — Hardening factor (Compression damage)

σ — Cauchy stress

$\overline{\sigma}$ — Effective Stress

α/γ — Dimensionless material constants

I — Effective hydrostatic pressure

$\overline{q}$ — Hydrostatic pressure

$\overline{S}$ — Mises equivalent effective pressure

$\overline{\sigma}$ — Deviatoric part of the effective stress tensor

$\hat{\overline{\sigma}}max$ — Algebraically maximum Eigen value of $\overline{\sigma}$

$\overline{\sigma}_c$ — Effective compressive cohesion stress

$\overline{\sigma}_t$ — Effective tensile stress

σ_{b0} — Initial equibiaxial compressive yield stress

σ_{c0} — Initial uniaxial compressive yield stress

G — Flow potential

ψ — Dilation angle

ε — Flow potential eccentricity

e — Eccentricity parameter

$\dot{\lambda}$ — Plastic multiplier

$\overline{q}_{(TM)}$ — Tensile meridian

$\overline{q}_{(CM)}$ — Compressive meridian

K_c — Stress Ratio

μ — the viscosity parameter

k/λ — Material constants

ϕ — Friction angle

J_2 — Second invariant of the stress deviator tensor

σ'_{oct} — Octahedral normal stress

τ_{oct} — Octahedral shear stress

c — Cohesion intercept

ε_c^{-in} — Inelastic strain

ε_{0c}^{el} — Elastic strain of undamaged material

σ_c — Stress of the strain

E_0 — Elasticity modulus

ε_t^{-ck} Cracking strain

ε_t Total strain

ε_{0t}^{el} Elastic strain corresponding to the undamaged material

K Tensile meridian

v Viscosity parameter

ε Flow potential eccentricity

ψ Dilation angle

fb0   Biaxial compressive yield stress

fc0   Uniaxial compressive yield stress

R   Compressive breaking strength of a wall

σ_m Mortar compressive strength

σ_b Brick compressive strength

E_{bo} Elasticity modulus of the brick 'orthogonal to holes direction.'

E_{bp} Elasticity modulus of the brick 'Parallel to holes direction.'

E_b Elasticity modulus of the brick

E_m Elasticity modulus of the mortar

E_M Elasticity modulus of the wall

h   Height of the product

e   Thickness of the product

Table of Contents

Chapter 1

Introduction

Chapter 1: Introduction

1.1   Background and aims

Masonry is the component of separate units bonded together by mortar. Even though they have a substantial impact on the structure's in-plane behaviour and seismic performance, masonry walls are frequently considered non-structural features. Researchers studied this aspect in recent years to resolve this dispute. In order to do so, the resistance of masonry must be tested, examined, and evaluated so that it would be possible to measure its reliability. However, due to the complexity in implementing and testing such a large element, it is most usual to employ formulations found in regulations, such as [1], which is based on the material properties of the component.

Recently, an increasing number of academics are integrating experimental testing findings with numerical simulations to obtain absolute results using a more developed technique. Numerical models have become a feasible alternative to actual experiments in recent years. To perform numerical analysis and simulate linear and non-linear behaviour of masonry, several numerical approaches have been used, including the finite element method (FEM), discrete element method (DEM), limit analysis, and the applied element method (AEM).

1.2   Methodology

The work consists of to study the mechanical behaviour of hollow clay masonry under uniaxial compression loading, using a combination of experimental and numerical approaches, the masonry selected for this study is single panel hollow clay brick masonry, because it is the most common to use for infill in Algeria.

1.2.1   Experimental Approach

The experimental approach adopted for numerical validations consists of a two-stage experimental investigation performed by [2]. The first stage is an initial masonry components characterization through a two different loading direction compression test on brick units, and three-point bending test in addition to compression test on mortar. The second stage of experimental characterization is additional test on the wall, three different load orientation compression tests have been carried out to obtain the compressive behaviour results of hollow clay brick masonry wall submitted to normal loading.

These experimental investigations provide the necessary data for numerical modelling.

1.2.1   Numerical Approach:

The adopted numerical approach using Abaqus/CAE is a block-based FEM detailed micro-modelling technique, using concrete damaged plasticity model for material properties definition, it consists of a similar strategy to the experimental investigation, and it is also divided into two stages:

The first stage is the initial components numerical properties defining, creating models of the initial experimental tests respecting the specimen's dimensions, starting by defining the elastic properties, then plastic properties, and eventually adopting Concrete Damaged Plasticity models for each test after a sensitivity analysis to determine the rest of the necessary properties for this model.

The second stage concerns using the first stage results to create a numerical simulation for the experimental tests realized on the wallets scale and using sensitivity analysis to adapt the initial material properties so that it simulates the experimental results.

The theoretical formulas provided and recommended by Algerian construction regulation [1] is tested and compared by the experimental results to evaluate their precision and reliability to determine the compressive strength of masonry walls without using the additional experimental tests.

1.3   Thesis Structure

- The first chapter presents a general introduction to the thesis, aim of the study, and the methodology adopted to accomplish it.
- The second chapter represents a background information about varieties of masonry that exist, as well as their component, and their mechanical behaviour.
- The third chapter is a bibliographic overview on the most common experimental approaches of masonry.
- The fourth chapter is a bibliographic overview on the numerical investigation approaches.
- The fifth chapter presents the experimental test for numerical validation, their protocols, and results.
- The sixth chapter presents focuses on numerical analysis and simulation, which involves converting experimental data to a numerical model in order to acquire correct findings.
- The seventh chapter discusses the previous two chapter's results and compare the two theoretical results, concluding the mechanical behaviour of hollow clay brick masonry under normal compression.

Chapter 2

Masonry Background

Chapter 2: Masonry Background

2.1   Introduction

This chapter aims to highlight prior research on the mechanical behaviour of masonry infill.

The masonry infill is considered a non-structural element; therefore, its behaviour was not evaluated in the calculation process. Engineers have lately observed the impacts of earthquakes, differential settlement, and other variables on masonry walls, showing cracking and instability, indicating that this element has a contribution in sustaining loads and solicitations. As a result, there has been a greater focus on studying the mechanical behaviour of masonry infill under various solicitations using a variety of methodologies, including numerical modelling.

The masonry infill walls are a complicated element that is formed by masonry units, assembled together by horizontal and vertical joints. Because of the various properties of vertical and horizontal joints, and particularly on the fact that the properties of masonry units frequently contrast in the vertical and horizontal direction, the masonry infill walls are anisotropic. The behaviour of masonry infill walls is determined by the geometry and mechanical behaviour of its constituents, which are the masonry units and mortar joints, as well as the assembly and the type and direction of solicitation.

2.2   The different types of masonry walls:

According to the Algerian regulation of conception and calculation of masonry [1], there are two types of masonry based on their function:

2.2.1   Load Bearing Masonry

Its structure must not undergo any modification or unacceptable deformation while transmitting to the foundations the pressure of the loads that exert it.

2.2.2   Non-Load-Bearing Masonry

In general, its function is to fill a load-bearing structure (reinforced concrete steel, load-bearing wall, etc.) It must be able to bear its weight as well as that of ordinary equipment such as doors, windows, sinks, pipes, etc.

A variety of materials combined with mortar of varying strength can be used for masonry construction. Some of the common materials used are brick, stones, concrete, veneer, gabion, etc.

Based on the type of individual units used for masonry walls, the main types of masonry walls are:

2.2.2.1   Brick Masonry walls

Brick masonry is an exceptionally durable form of construction. It is built by placing bricks on mortar in a systematic manner to construct a solid mass that withstands exerted loads **Figure 2-1**, There are several types of bricks and several mortars that can be used to construct brick masonry. The bond in brick masonry, which adheres bricks together, is produced by filling joints between bricks with suitable mortar. The Overall performance depends on the type of brick chosen, the size, position, and the number of openings provided to the masonry structure.

Many construction systems have adopted clay brick masonry due to its thermal and acoustic properties.

Figure 2-1 Brick Masonry Construction

2.2.2.2   Concrete Masonry walls

Similar to brick masonry, concrete blocks are pressed on top of each other in concrete masonry buildings as indicated in **Figure 2-2**, As a result, the configuration becomes staggered. Concrete blocks take less time to lay than bricks since their dimensions are larger.

Concrete block construction hence is popular as it is affordable and gains high fire resistance. The concrete masonry blocks come in diverse sizes, shapes, and special forms thus making them a versatile construction material.

Figure 2-2 Concrete Masonry Construction

2.2.2.3   Stone Masonry Walls

Stone is the most durable, strong, and weather-resistant construction material compared with any others. These are less affected by daily wear and tear. Masonry structures are made out of stone hence last for a longer period. It has a life period of 300 to 1000 plus years. Due to its numerous advantages, it is widely used in masonry construction. However, this type of masonry is less used because of the heavyweight of its units, the difficulty of assembly and the extremely excessive cost of construction.

Figure 2-3 Stone Masonry Construction

2.3   Types of masonry units

According to the Algerian masonry construction regulation [1] masonry units differ into three categories.

2.3.1   Bricks of usual shape (silico-limestone brick, Clay brick)

-   The hollow brick: is the most used and adapts to any work, it is common for being solid, lightweight, and cheap.
-   The red brick: Its cost is a little high, formed from clay and sand. Exceptionally good insulation and used outside and inside.

- Facing brick: Fits perfectly to the outside and is used for building facades.

| a) | b) | c) |
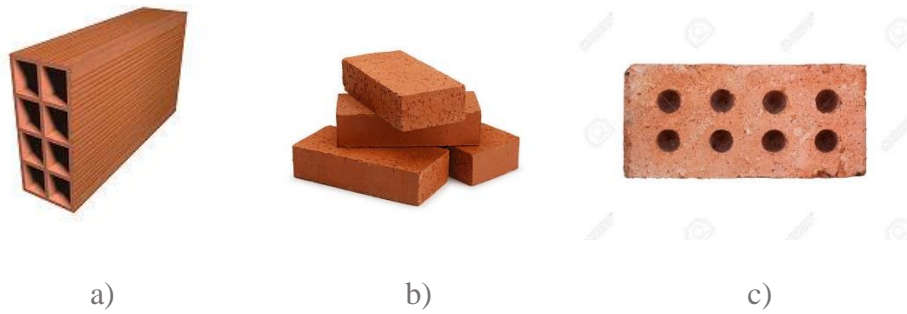
Figure 2-4 Usual shape bricks: a) hollow clay brick, b) red bricks, c)
Facing brick

2.3.2 Big size blocks (Cellular concrete)

Cellular concrete is a mixture of cement, water, and preformed foam. The cause of the foam is to deliver a mechanism through which a relatively high percentage of strong air voids may be induced into the combination and bring a cellular or porous solid upon curing of the mixture. Cellular concrete is light, resistant to freezing and thawing, with good thermal and acoustic insulation.

Figure 2-5 Cellular concrete brick

2.3.3 Brick or Block from Concrete Vibro-Treatment (Compressed Stabilized Earth Blocks, Cinder blocks)

- Compressed Stabilized Earth Blocks (CSEB), commonly called, Pressed Earth Blocks, are a mix of soil, sand, a stabilizer (often 5% of cement), and water. They are compressed in a press (manual or motorised) and cured for 28 days.

- Ordinary cinder blocks are mainly composed of grits, sand, cement, and gravel. However, some subspecies of blocks incorporate insulating materials such as expanded clay, shale (expanded and then fired clay), or pumice (porous volcanic rock). In addition, other types of blocks have siliceous sand, plaster, aluminium powder, or lime. In general, 87% of the ordinary block consists of aggregates, 7% of cement and 6% of water, which components are moulded to obtain a solid and more or less homogeneous structure.

a)   b)

Figure 2-6 a) CSEB Blocks, b) Cinder block

2.4   Types of Mortar

Mortar is a vital paste made of Ca(OH)2 and other modules that are used to bind construction blocks together and fill gaps between them. When it sets, it solidifies, resulting in a rigid and robust agglomerate. Modern mortars are typically made from a mixture of sand, a binder such as lime/cement, and water.

Cement, hydraulic and fat lime, gypsum, gauged, surkhi, aerated cement, and mud mortar are the most common types of mortar, each of which is named after the binding ingredient employed. Each type of mortar has different features that make it useful in certain projects. For example, cement mortar is associated with a higher level of resistivity and resistance to water, while hydraulic lime water is particularly appropriate for moist areas that are saturated with water. Regardless of what type of mortar is used, the preparation of mortar will typically involve the addition of water to the binding material and fine aggregate to ultimately create the malleable paste.

2.4.1   Types of mortar according to their conception

According to [3] there are two types of mortar according to their conception:

2.4.1.1   *Performantial mortar (formulated)*

Mortar whose design and method of manufacture have been chosen by the manufacturer to obtain specific characteristics (performance concept). It is defined by its characteristics and performance. It can only be mixed in the factory (industrial mortar).

2.4.1.2   *Recipe Mortar*

Mortar is manufactured according to predetermined proportions and whose properties result from the proportions of declared constituents (recipe concept). It is defined by its composition. It can be mixed on-site (mortar) or in the factory (industrial mortar). This technical specification gives dosages —

binder(s) / sand(s) levels — of mortars of common uses on diverse types of masonry. The account of the moisture of the sand on-site is taken into consideration.

2.4.2   Applications of Mortar

2.4.2.1   Bricklaying Mortar

For masonry projects, bricklaying mortar is most typically used to bind bricks, stones, and concrete blocks together. As the structure is being constructed, bricklaying mortar can also be utilized as a bed to keep these building components from bearing an uneven weight distribution onto each other.

2.4.2.2   Finishing Mortar

Finishing mortar is commonly used in construction projects that require plastering as well as those that want to give the structure an aesthetically pleasing aspect. Finishing mortar, which frequently contains lime and/or cement as a binding element, is used to improve a structure's strength and mobility, as well as its resistance to destructive environmental events such as rain and wind.

2.4.2.3   Thinset Mortar

Thinset mortar can serve as an adhesive structure for projects requiring ceramic or stone installation.

2.5   Masonry wall conception
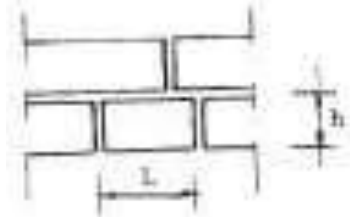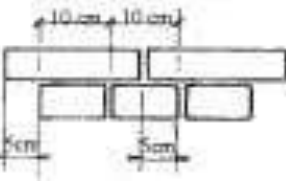
Rules concerning the conception of masonry infill walls are well described in the Algerian masonry construction regulation [1].

2.5.1   Joints and fitting:

Masonry wall joints and fitting must respect the rules represented in **Table 2-1**.

Table 2-1 Practical rules for masonry fitting [1]

Type of masonry	Joints thickness	The overlay	Schema
Large blockwork masonry	0,30 To 1 cm	>15cm for load-bearing masonry	- h : Represents the block height of the block

		> 0,75 h : for non-load-bearing masonry	- L: Represents the width of the block
Masonry of small manufactured elements	1 To 2 cm	5 cm Minimal binding	

2.5.2 Geometry and dimensions

When it comes to geometry and dimensions of masonry walls, a few rules are required:

- Horizontal and regular foundations are required to build a masonry infill. In the same wall, the ratio of openings to solids must not be less than 1/3, and it should be distributed as equally as possible

- Spans are typically restricted to 1.20 meters. For the greatest openings, lintels and jambs should be enlarged.

2.5.3 Masonry junctions

Joints are provided to prevent masonry problems caused by thermal expansion, shrinkage, or settlement, and the wall junctions complete these provisions. In the case of load-bearing walls, the floors are supported on the walls, and it is convenient to plan wall junctions that link all the vertical and horizontal elements of the building. These junctions are usually made of reinforced concrete, but sometimes they can be made of another material (metal or wood).

The wall junctions must be covered with a material of the same nature as the masonry. This material must be placed in the formwork and not be reported after the coup. Its thickness must not exceed 1/3 of the thickness of the wall [1]. Whether horizontal or vertical, all the junctions must comply with the specifications and regulations detailed in Algerian masonry construction regulations.

2.6   Common Defects in Brick Masonry Works

Brick masonry defects are frequently the result of shoddy workmanship, a failure to follow instructions or the use of inferior materials, sometimes it is a result of miscalculations. Age and prolonged exposure to the elements, natural phenomena such as earthquakes, on the other hand, can and will impact negatively on even the best-built masonry structures, therefore construction technical control organisation "CTC" provides a book [4] describing the common masonry defects :

- Poor execution of the mortar layer at the head of the walls
- Lack of joint filling
- Non-compliant thickness of assembly joints - Excessive thickness of joints
- Lack of horizontal and vertical stiffeners, large panels.
- Lack of connection between the reinforced concrete framework and the masonry element.
- Absence of bonding reinforcement at the junction between supports of different nature.
- no bonding between interior and exterior walls.
- installation of shunt ducts in the living rooms.
- Insufficient lintel support lengths
- Absence of window and bay ledges
- Absence of resilient footings at the base and top of interior masonry walls.

2.7   The Mechanical Behaviour of Brick Masonry walls

2.7.1   Brick masonry failure mechanisms

The typical failure mechanisms in masonry wall are characterized as unit failure mechanisms, joint failure mechanisms and combined mechanisms involving joints and units.

Masonry has five different failure mechanisms [5] as illustrated in

Figure 2-7 Masonry failure mechanisms: (a) joint tensile cracking (b) joint slipping (c) unit direct tensile cracking (d) unit diagonal tensile cracking (e) masonry crushing.

:

1- Tension failure of bricks: cracking of the units. Known as ***"Unit failure mechanism."***
2- Tension failure of joints: sliding of the bed or head joints (at a low value of normal stress). ***"Joint failure mechanism"***

3- Shear failure of joints: cracking of the joints (at a low value of normal stress). ***"Joint failure mechanism"***

4- Diagonal tensile failure of brick: happened under sufficient normal. It's a ***"Combined failure mechanism"***

5- The crushing failure of masonry. ***"Combined failure mechanism"***
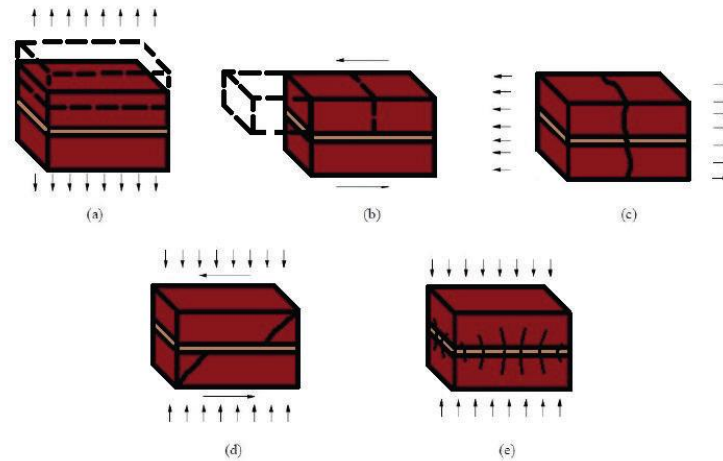
Figure 2-7 Masonry failure mechanisms: (a) joint tensile cracking (b) joint slipping (c) unit direct tensile cracking (d) unit diagonal tensile cracking (e) masonry crushing [5].

2.7.2   In-plane failure mechanisms of unreinforced brick masonry walls

Unreinforced masonry walls have three failure mechanisms [6]:

2.7.2.1   Diagonal Tensile failure:

It is a diagonal crack pattern that occurs when the principal tensile stress in the mortar surpasses the tensile strength of the joints, this is a typical failure mode in shear masonry walls, when a wall is subjected to significant normal compressive loads and a relatively large force is applied to it. It is typically for a wall with a 1 aspect ratio (which is defined as the ratio of the wall's height to its length, H/L), However, when strong vertical loads are also applied to the wall, it can occur in a panel with a higher aspect ratio.

2.7.2.2   Horizontal sliding shear failure:

Sliding shear failure: it is common in the situation of low vertical load and poor-quality mortar, seismic loads frequently cause shearing of the wall, causing sliding of the upper part of the wall at one of the horizontal mortar joints. This type of failure generally happens in walls with low aspect ratio.

2.7.2.3   Crushing Failure and rocking failure:

This mode of failure is most common for the walls with aspect ratio higher than one. In the case of a high moment/shear ratio or improved shear resistance, the wall may be set into rocking motion or toe crushing depending on the level of the applied normal force.

a)   b)   c)
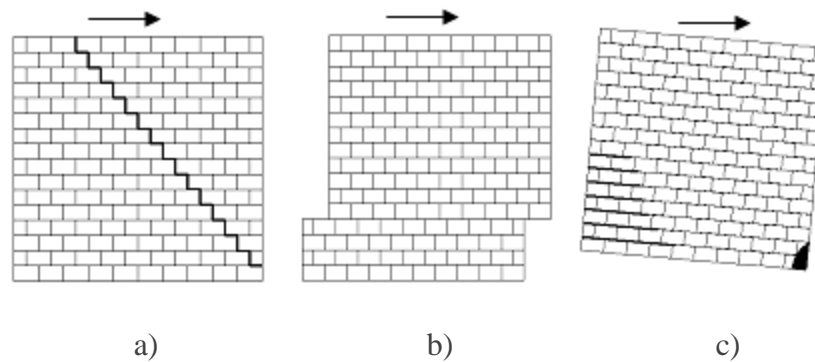
Figure 2-8 In-plane failure mechanisms of masonry walls a)Diagonal tensile failure, b) Sliding failure, c) Rocking/crushing toe failure [6]

2.7.3   Mechanical behaviour of masonry under compression

The majority of the standards recommend determining masonry compression resistance by applying uni-axial load on simple masonry prisms that are made from 3, 4 or 5 masonry units, combined together vertically.

(a) Configuration 1 (C1)   (b) Configuration 2 (C2)

(c) Configuration 3 (C3)   (d) Configuration 4 (C4)

(e) Configuration 5 (C5)   Configuration 6 (C6)

(f) Configuration 7 (C7)   (g) Configuration 8 (C8)
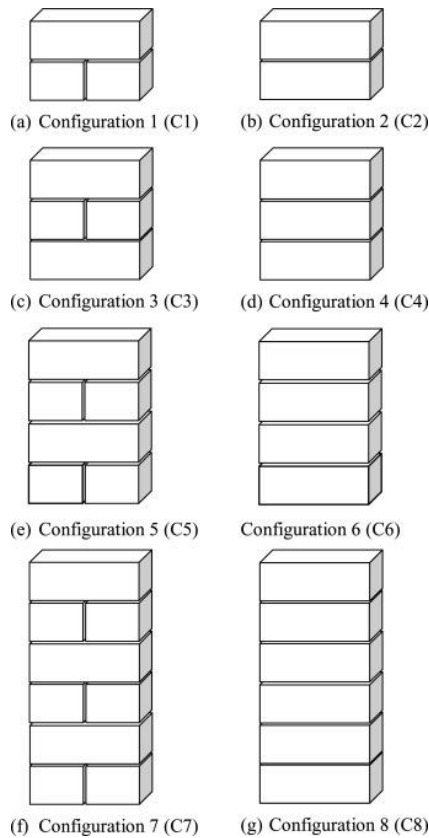
Figure 2-9 Geometrical configuration of prisms. [7]

In general, tests have shown that the compressive strength of prism is lower than the masonry unit but higher than the mortar's compressive strength results [8]. Other studies [7] [9] shown that the compressive strength of masonry prism increases with the increase in mortar strength and brick's strength.
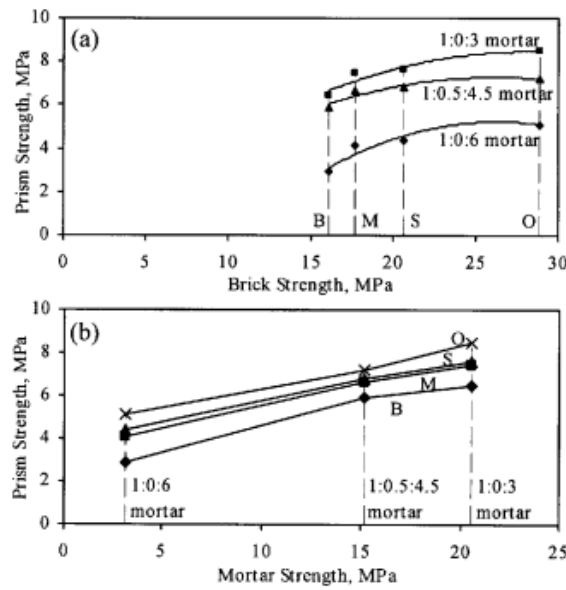
Figure 2-10 Relationship between: a) masonry prism strength and brick compressive strength for different mortar grades b) masonry prism strength and mortar compressive strength for different bricks [10]

The Algerian masonry construction standards suggests two methods to determine the compressive strength of masonry, the first and recommended one is using the formula [3.1]. That is based on the initial components characterization results. The second method is to determine the wall compressive strength by applying uni-axial load on wallet samples until failure.

$$R= 0.55\sqrt[3]{\sigma_m . \sigma_b^2}$$
[3.1]

Several fracture mechanisms were observed: crushing of masonry pieces, vertical cracking due to transverse stresses, and sudden rupture due to instability of the internal walls in hollow bricks [8]. The following conclusions can therefore be drawn:

- Tensile stresses causing cracking are due to deformations generated by the mortar.
- The nominal compressive strength of the bricks (standard tests) cannot be used directly to determine the strength of the bricks in the walls because the fracture modes of brick in both situations are different [10].
- Other experimental investigations [11] comes to conclusion that there are two types of failure modes due to compression loading; In the case of uniaxial compression, failure happened in a plane parallel to the panel's plane, as a result of cracking and sliding in the bed and/or head joints, or as a result of a combination mechanism including cracking in both brick and joint, depending on the orientation of the bed joints to the applied load as indicted in **Figure 2-11-**

a; in the case of biaxial compression failure occurred when the specimen split in a plane parallel to the free surface at mid-thickness, regardless of bed joint angle. Splitting failure occurred suddenly and in a brittle way, frequently starting at one of the loaded edges and spreading across the panel as illustrated in **Figure 2-11-b**.
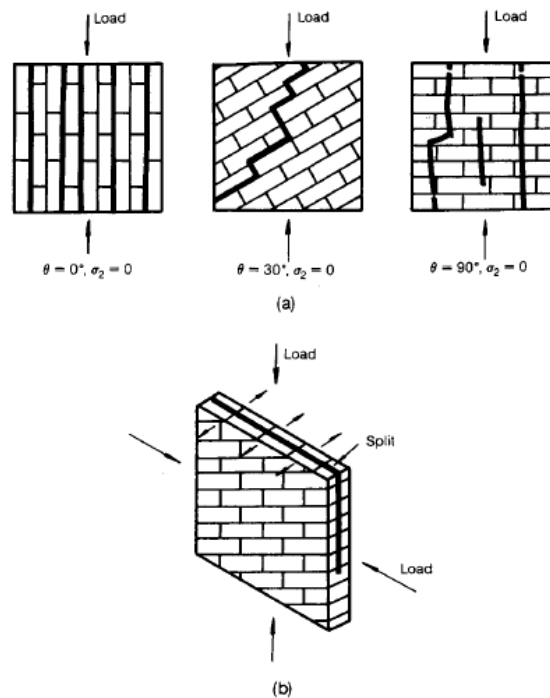
Figure 2-11 Failure modes for biaxial compression tests on brickwork: a) uniaxial compression, b)
biaxial compression [11]

2.7.4   Mechanical Behaviour of Masonry under Shear Load

Many standards recommend that this resistance be calculated using a "nominal" shear stress that can be measured experimentally [8]. Coulomb's law is used by Eurocode 6 to describe the characteristic shear strength of unreinforced masonry. The triplet test EN 1052-3 [12] has been recognized as the European standard laboratory test for determining initial shear strength under zero compressive stress.

However, there are diverse types of laboratory tests to determine the shear strength of a masonry. It has been found experimentally that bending forces are appearing which modify the desired shear conditions, meanwhile the test type **Figure 2-12-1** found to be the simplest and the easiest to execute [8].
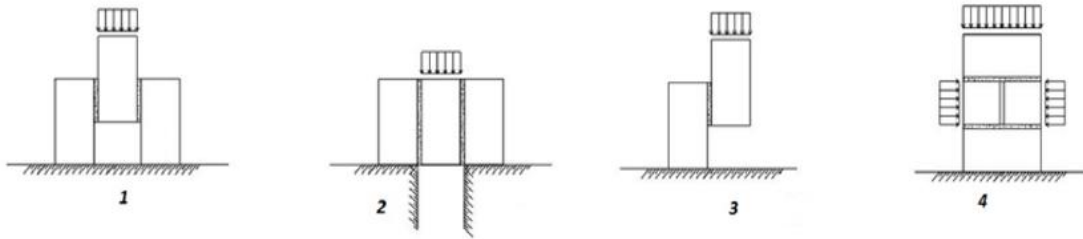
Figure 2-12 The different laboratory shear tests [8]

This type of test results in curves such as **Figure 2-13** determine the cohesion and friction coefficients (c and φ). The dispersion coefficients are high. References indicate that in this type of experiment, the failure occurs suddenly and brittle, making it impossible to observe the crack propagation.

$$\tau = 0.23\,\sigma + 1.06$$
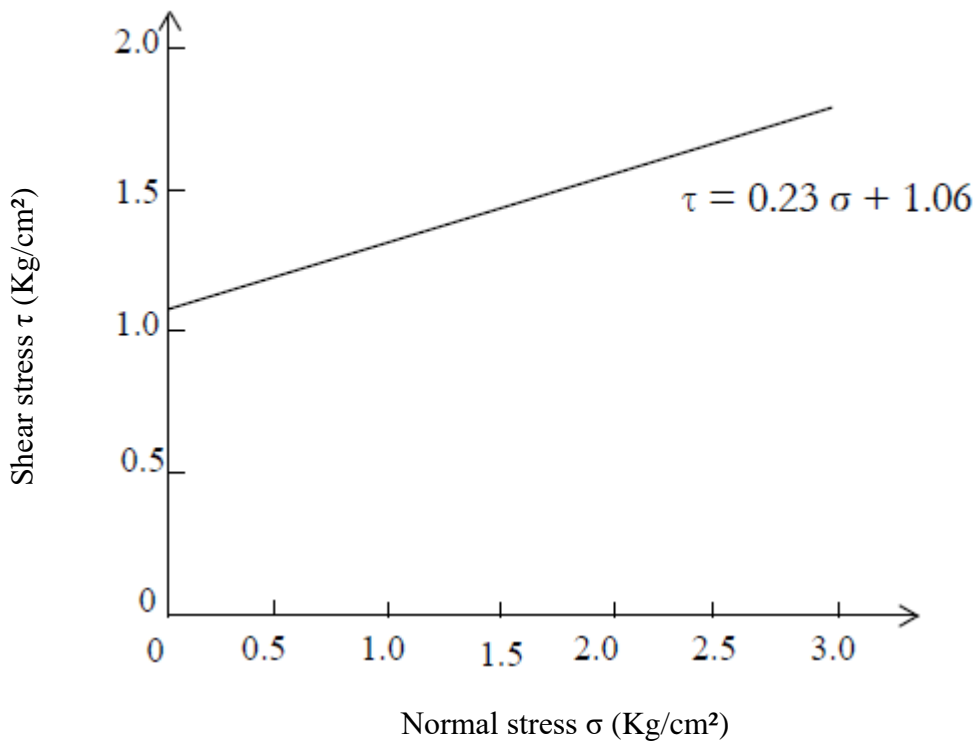
Figure 2-13 Shear strength as a function of load, [Lafuente, 1990]

2.7.5   Bending behaviour of masonry

The bond strength between masonry units and mortar has been of considerable interest to researchers for some time. The flexural bond strength of masonry is needed for the design of masonry walls subjected to out of plane loading, to study the bending behaviour of masonry **Figure 2-14**.

a)   b)
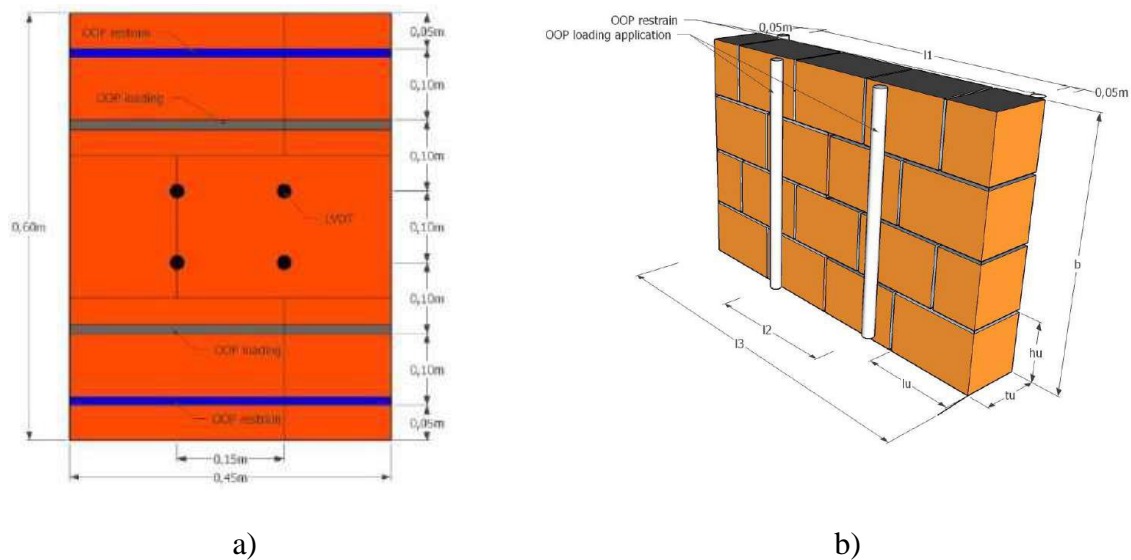
Figure 2-14 Flexural strength tests: a)Parallel to horizontal bed joints b) perpendicular to horizontal bed joints: specimens' dimensions according to NP EN1052-2 standard (CEN 1999) [13].

The analysis is divided into two pure bending states and a pure torsion:

- Bending around the axis perpendicular to the bed joint plane (horizontal bending)
- Bending around the axis parallel to the bed joint plane (vertical bending).
- Torsion.
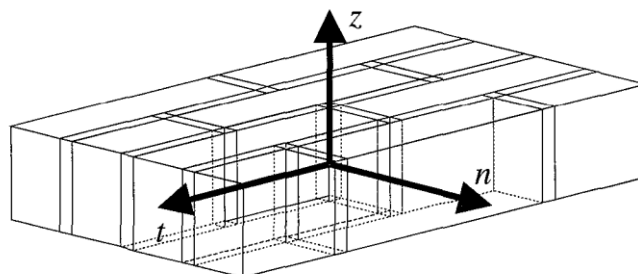
a)
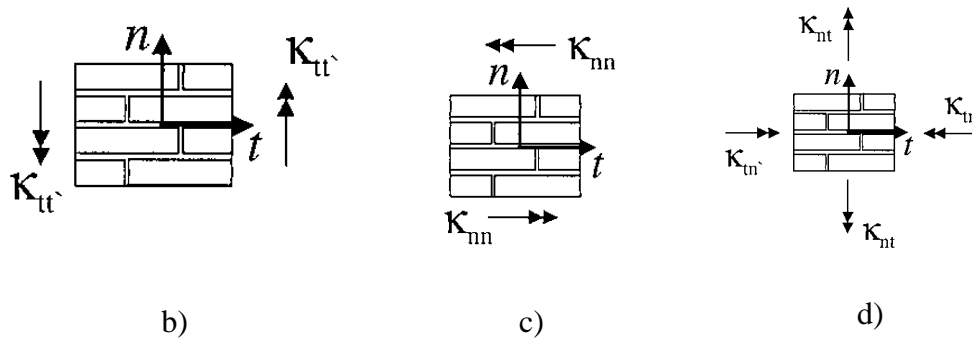
Figure 2-15 Masonry bending types : a) Definition of axes with respect to the bed joint direction and plane of masonry; b)Horizontal bending ; c) Vertical bending ; d) Torsion [14]
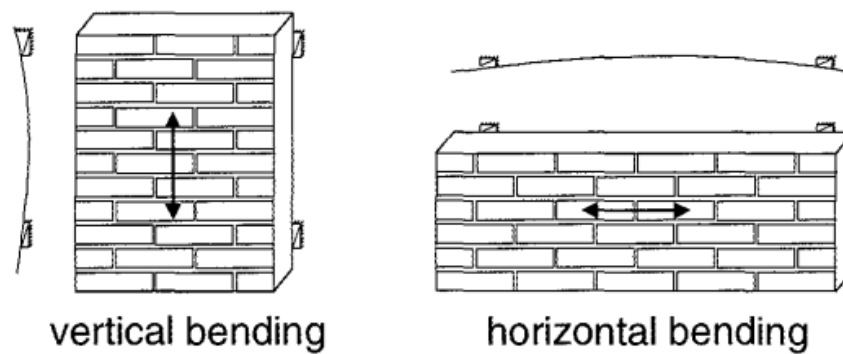
Figure 2-16 Definition of vertical and horizontal bending [14]

Experimental investigation realized by [13] show that the flexural strength test parallel to horizontal bed joints failure mechanisms were presented by a horizontal cracks/ rupture characterized by the detachment between the masonry units and the horizontal bed joint. However, the flexural test perpendicular to horizontal bed joints have presented different failure mechanism that looks like a vertical crack/rupture splitting the tested wallet in the middle and a detachment between masonry units and vertical bed joints along with a total rupture in the central masonry units.

a)   b)
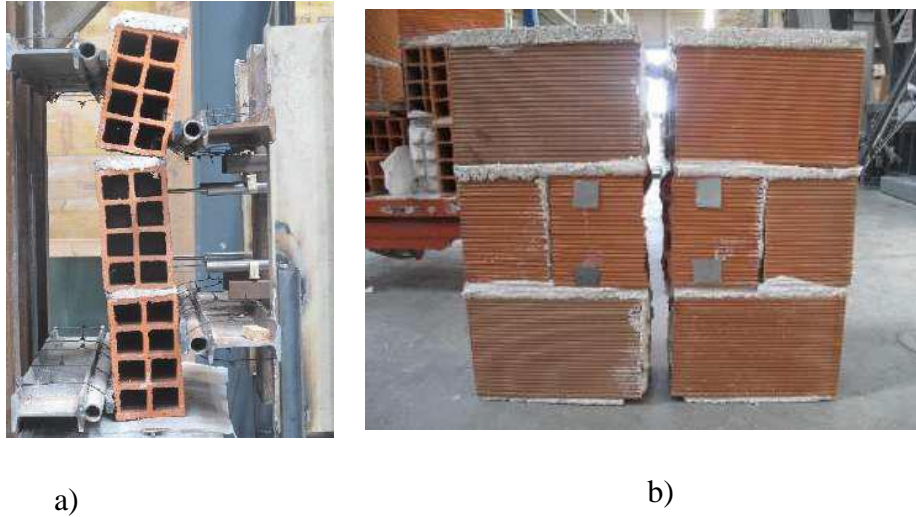
Figure 2-17 Typical failure mechanism to flexural strength test: a) parallel to horizontal bed joints;
b) perpendicular to horizontal bed joints

2.7.6   Mechanical behaviour of masonry subjected to Uniaxial and biaxial load

Several experimental investigations have been performed in order to study the mechanical behaviour of masonry wall under uniaxial and biaxial loading. Earlier investigations such as [15] [16] [8] [11] have outstand and became a foundation of later investigation. The failure mechanisms of masonry in uniaxial and biaxial loading are summarized in table 0-3.

Table 2-2 Modes of failure of solid clay units' masonry under biaxial loading [17]

Angle θ	Uniaxial tension	Tension/ compression	Uniaxial compression	Biaxial compression
0°				
22.5°				Splitting crack
45°				
67.5°				
90°				

2.7.6.1   *Masonry behaviour for uniaxial loading*

The results of the tests realized on masonry panels subjected to uni-axial compression load vary according to the direction of the lads in relation to the bed joints. The failure occurred in a plane parallel to the panel's plane. Failure occurred due to cracking and sliding in the bed and/or header joints, or a combined mechanism involving cracking in both brick and joint, depending on the orientation of the bed joints to the applied load.
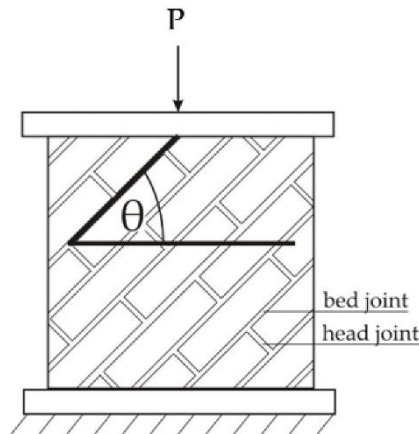
Figure 2-18 Description of θ angle measurements of tested samples. [18]
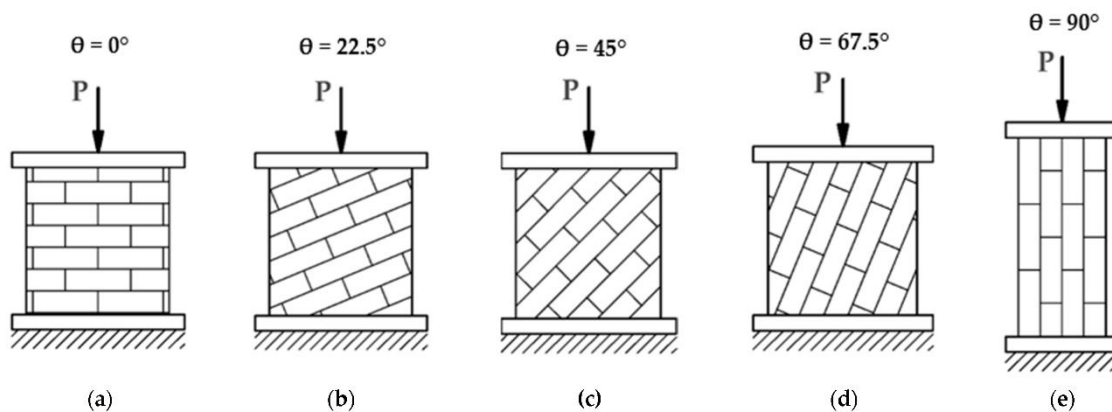
Figure 2-19 Load application diagram for compressed wall samples at different angles of bed joints

(a) θ = 0°, (b) θ = 22.5°, (c) θ = 45°, (d) θ = 67.5°, (e) θ = 90°. [18]

A minimal compressive strength has been obtained for the load acting at an angle θ = 67.5°. Its value is limited to 24% of the compressive strength for the load acting parallel to the bed joints (θ = 0°) [18]

2.7.6.2   Masonry Behaviour for biaxial loading

In the case of biaxial compression, the failure mode was prevented by the presence of the second principal compressive stress for most σ_1/σ_2 ratios. Failure occurred by splitting in a plane parallel to the free surface of the specimen at mid-thickness regardless of bed joint angle [11]

CHAPTER 3

EXPERIMENTAL APPROACHES OVERVIEW

Chapter 3: Experimental Approaches Overview

Because of the anisotropy of the hollow clay masonry walls, its behaviour severely depends on the behaviour of its components. For that reason, last research studies interested in the characterization of the masonry material properties and their impact on the whole behaviour.

The experimental characterization of masonry mechanical properties remains a challenging task. Despite the fact that a variety of experimental tests and setups have recently been developed, their reliability remains a topic of debate. Experimental masonry characterization is done on different scales.

3.1   Masonry Components Testing
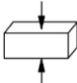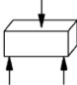
Because of the anisotropy of brick masonry walls, the first step of studying the mechanical behaviour of masonry wall is an experimental investigation on masonry wall components (block, mortar, and block-mortar bond), which is a necessary step in order to study its mechanical behaviour.
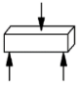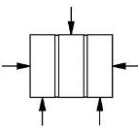
The initial experimental characterization tests are divided into three categories:

3.1.1   Tests on masonry units

Mainly the compression test on masonry units according to NF EN 771-1/CN: 2012 [1]. This type of test can be performed on three different loading direction [19]. Tests results shows that the brick have a higher compressive strength in parallel to holes loading direction, compared to the other two test load orientation. However, some researchers tend to conduct additional tests to determine Young modulus, Poisson's ratio and flexural strength [18] as indicated in **Table 3-1**.

Table 3-1 Masonry Components Tests Results [18]

No.	Load Diagram	Test	Material	Result
A		Compressive strength (EN 772-1)	Brick	f_b = 44.1 MPa
B		Young and Poisson	Brick	E = 11,850 MPa ν = 0.11
C		Flexural strength	Brick	f = 3.2 MPa

D		Flexural strength (EN 1015-11)	Mortar	$f = 3.3$ MPa
E		Compressive strength (EN 1015-11)	Mortar	$f_m = 10.9$ MPa
F		Young and Poisson	Mortar	$E = 10,580$ MPa $\nu = 0.17$
G		Shear strength (EN 1052-3)	Masonry	$f_{vo} = 0.50$ MPa $tg(\alpha) = 0.5$

3.1.2   Tests on Mortar:

To identify the mechanical characteristic of mortar joints, researchers conduct compression and flexural strength tests according to NF EN 1015-11 [20]. The three point flexural strength test is performed on a 40x40x160 mm specimens, and the compression test is performed on the previous tests leftover using a hydraulic compressor as indicated in **Figure 3-1**. However, some research conducts the compression test on a cylinder specimen instead of using the flexural prism [2]. Additional test might be conducted to determine young modulus, and Poisson's ratio as indicated in **Table 3-1**.

a)   b)   c)
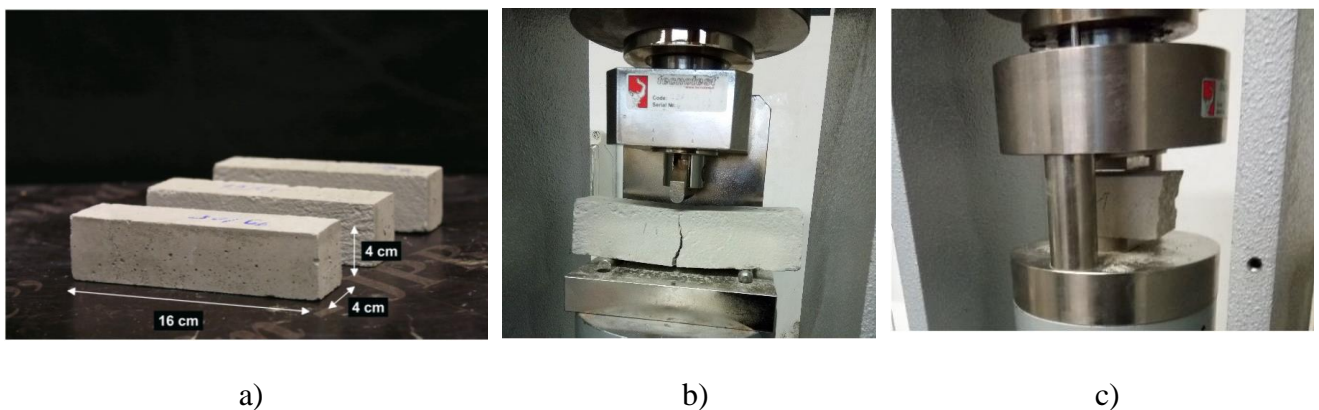
Figure 3-1 Experimental characterization of mortar : a) Mortar prism; b) Three point flexural test; c)Compression test [19]

3.1.3   Tests on masonry unit–mortar interface:

To determine the joint interface properties, shear test is often conducted to determine the shear strength of masonry, there are different kind of laboratory shear tests previously detailed in **Error! Reference**

source not found.. The most common test to determine shear strength is triplet test [18] according to NF EN 1052-3 [12] **Figure 3-2-a**. The cohesion as well as the dilation angle can be identified by applying a pre-load [19].

In order to determine the tensile strength of the interface, some researchers conduct additional brick-mortar interface test [19]. A three-point bending test on a composite prism of masonry unit and mortar is conducted in this case, as indicated in **Figure 3-2-b**.
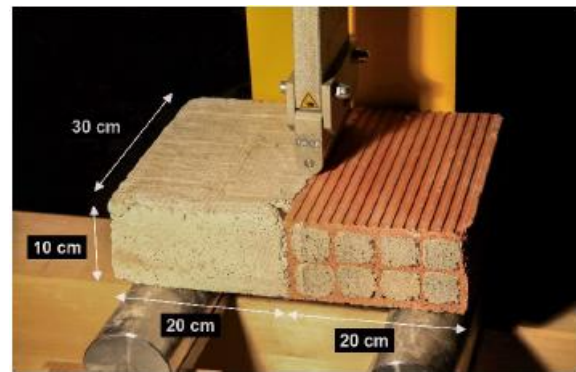
a)   b)

Figure 3-2 Brick-Mortar tests: a) Triplet test ; b) Brikc-Mortar interface test [19]

3.2   Wallet's testing

Wallets are small masonry assemblages used to simulate the behaviour of masonry walls on smaller scale to facilitate their testing. Considered as a second step for studying the mechanical behaviour of masonry after the initial component's characterization.

Different experimental tests have been realized on wallets to study the compressive behaviour of brick masonry walls. Uniaxial compression test in normal and diagonal loading direction have been performed by [2], [19] to determine the compressive strength of brick masonry walls and the influence of loading direction. Biaxial compression tests using on different orientations have been performed earlier [11], studying the effects of the loading angle on the masonry mechanical behaviour.

a)   b)
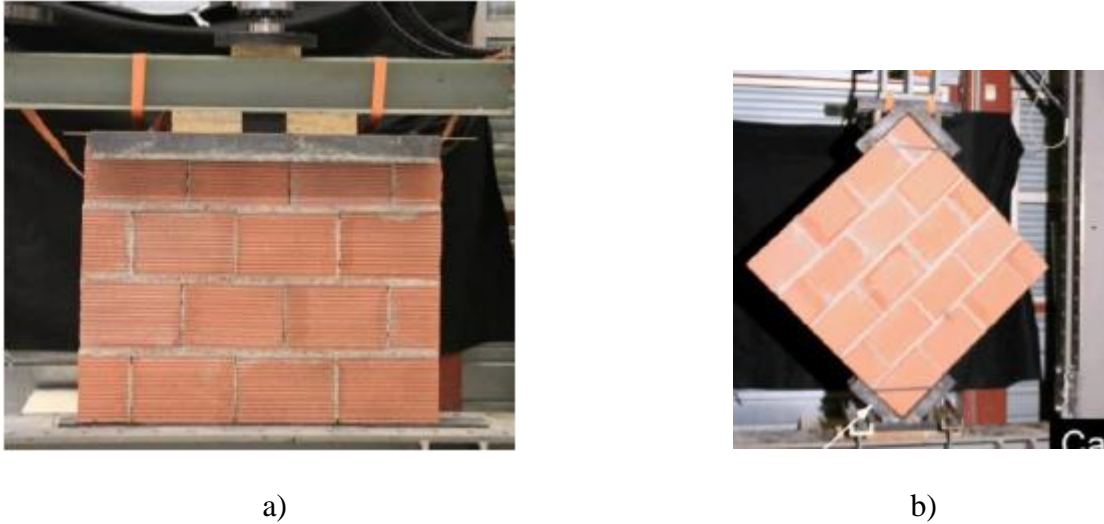
Figure 3-3 Uniaxial compression test on wallets : a)Normal Compression; b)Diagonal compression [19]

Additional test have been conducted by [13] to study the in plane /out of plane behaviour of masonry walls, including four-point flexural test according to EN 1052-1 [20] as illustrated in **Figure 3-4**. Testes were carried out on a two different direction that is previously indicated in **Figure 2-14**. Tests results showed higher flexural strength in the perpendicular orientation to the horizontal bed joints.
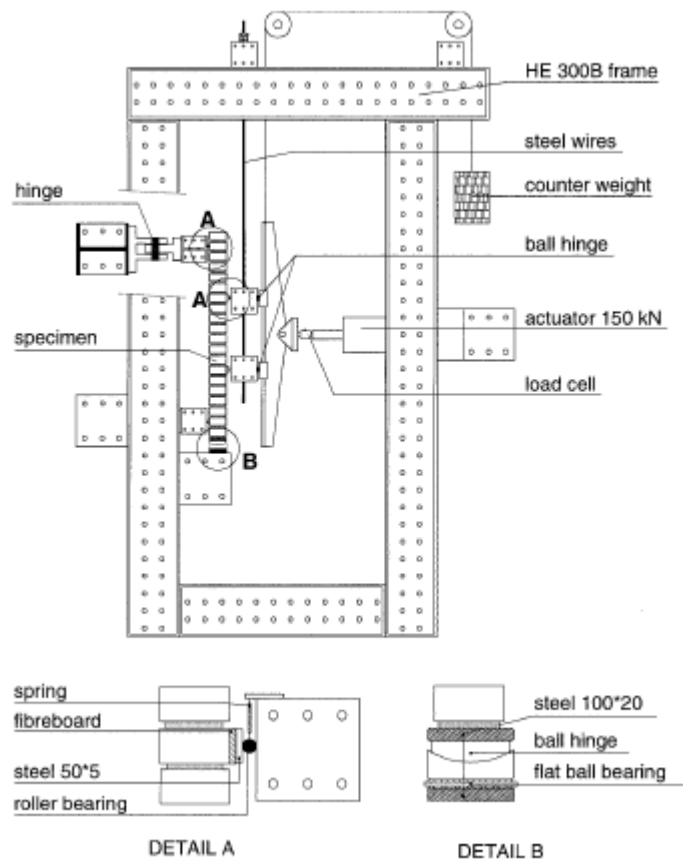
Figure 3-4 Drawing of 4-point bending test arrangement [14]

3.3   Panels testing

Panels are masonry walls with different scale ratio used for the experimental testing, the excessive cost and inconvenience of using such big scale, make it less common. However, it is often used to study the mechanical behaviour of masonry walls under dynamic loading, as the wallets does not fulfil the purposes to obtain accurate and realistic results.

Some researchers tend to carry out tests on walls and panels, in order to study the different failures mechanisms, it is often to use wall instead of wallets in case of studying masonry with openings, and the influence of its geometry on the displacement, shear strength and failure mechanisms, the most common panels tests are:

3.3.1   In plane/ out of plane tests:

It is often to conduct experimental investigations on wall panels to study the seismic behaviour of masonry, [13] especially focusing on the influence of masonry geometry 'with openings' on its mechanical behaviour [21] .

Experimental in plane/ out of plane investigations on unreinforced masonry walls strengthened using polymer textile reinforced mortar has been carried out [22] , revealing three failure mechanisms of TRM reinforced masonry as illustrated in **Figure 3-5**.

a) Cracking at the spandrel-pier connection
b) Spandrels cracking
c) Pier cracking
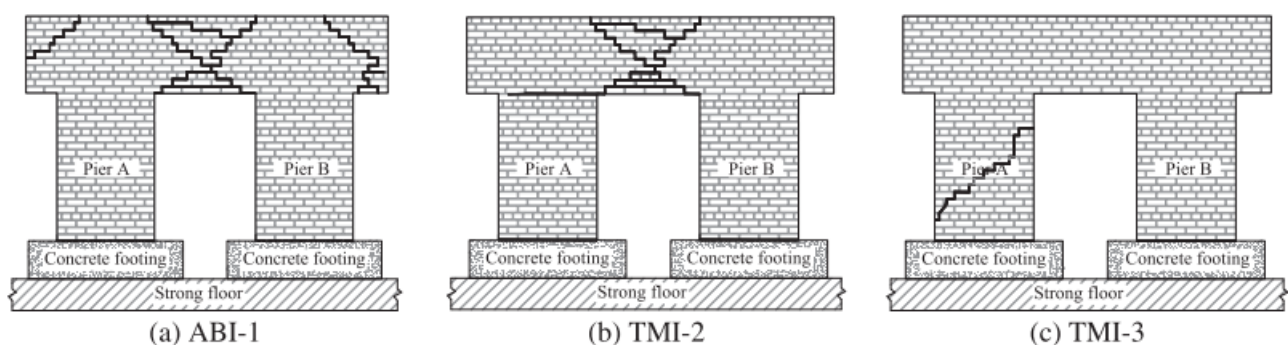
Figure 3-5 Damage paterns of unreinforced masonry walls with openings strengthened using TRM [22]

Other research revealed that the lateral load capacity is inversely proportional to the width of the perforations in the wall whether it is a door or a window opening. Confining the openings with tie columns helps restore the reduced capacity and significantly enhance the wall ductility [23].

3.3.2   Blast loading tests

Several researchers have conducted experimental studies for evaluating the response of masonry against blast loading [24]. The study of mechanical behaviour of masonry walls to blast loading seemed to be often exclusive on panels, and buildings, There has been extensive research on the use of variety of materials such as fibre composite laminate, geotextiles, polymers to improve the performance of masonry for blast protection, [25] made experimental investigation on a total of 700 reinforced masonry element to improve the response of reinforced masonry wall to blast loading.

Unreinforced masonry found to be very brittle under blast loads, and has been demonstrated to fail catastrophically at relatively low load intensity, however because of the ductility supplied by the reinforcement and the mass provided by the grout, even minimally reinforced completely grouted masonry gives a high level of blast resistance [26].

The Air Force Research Laboratory (AFRL) conducted full-scale blast testing on fully grouted masonry walls with no vertical reinforcement, which revealed excellent ductility under blast loading as indicated in Figure 3-6 The testing included panels with and without clay brick veneer and polystyrene foam insulation (typical cavity wall construction) [27].

However, most of this research are supported by many governmental departments and agencies in the U.S and abroad, such as the USA's Government Services Agency (GSA), Department of Défense (DoD), Department of State (DoS), and Department of Energy (DoE), in the aim of creating construction standard for blast-resisting buildings for security purposes.

Figure 3-6 Result of Full-Scale Explosion Testing of Fully Grouted CMU and Cavity walls [27]

3.3.3   Shake Table tests:

The shaking table test is one of the most widely used techniques to assess the seismic performance of structures made of various materials. Commonly, it is widely used for assessing linear/nonlinear and elastic/inelastic dynamic response of structures, in shaking table tests, most researchers used scaled models as specimens.

An earthquake record from a previous occurrence, usually scaled, or a fake accelerogram can be used to perform shaking table experiments.

Shake table tests provide the distinct advantage of accurately representing the dynamic nature of the loading circumstances experienced by a structure during an earthquake, including the combined influence of static and seismic loads, as well as both horizontal and vertical acceleration components (provided that the shake table system is multi-axial). As a result, shake table tests on full-scale specimens can provide crucial information that would otherwise be unavailable for investigating the seismic behaviour of structural members or sub-assemblages, evaluating the efficacy of retrofitting solutions, and validating numerical models in dynamic loading regimes. [28]

Scaled models necessitate similitude laws, which complicate the construction and testing process because they must accurately simulate: I the geometry; ii) the materials' stress-strain relationship; iii) the mass and gravity forces; iv) the initial and boundary conditions [29]

A study carried out by [28] using shaking tables on retrofitted old stone masonry wall indicates that composite materials with inorganic matrices can be effectively used to protect the building stock in earthquake prone areas.
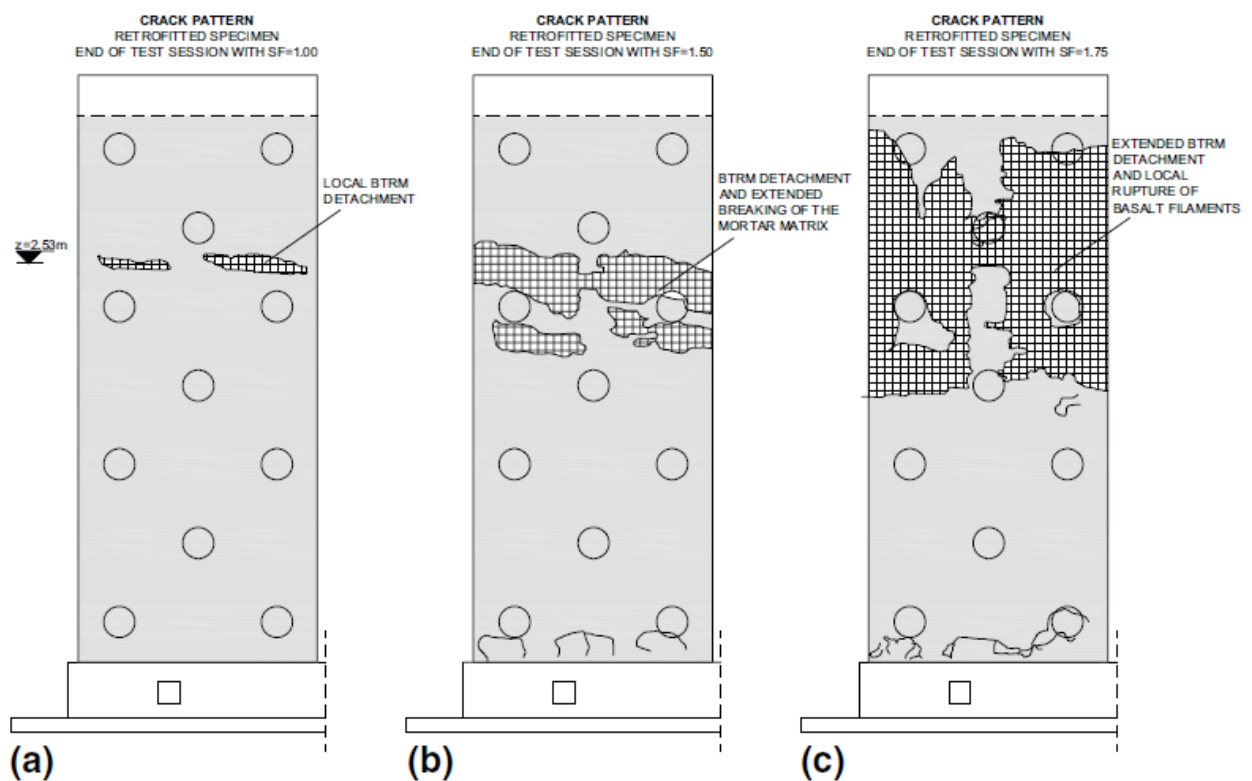
Figure 3-7 Damage pattern of the retrofitted stone wall after test series with SF = 1.00 (a), SF = 1.50 (b) and SF = 1.75 (c) [28]

3.4   Buildings testing

Sometimes, researchers perform the experimental investigation on a real-scale building specimens, build to imitate the behaviour of a building structure. This type is rarely used due to the extremely the excessive cost, and inaccessibility to such equipment. However, it was used multiple times in the assessment of the seismic vulnerability of building structures [30] , [31], [32].

Most of tests conducted on a such a big scale are in the purpose of studying blast response or seismic vulnerability using shaking tables technique.
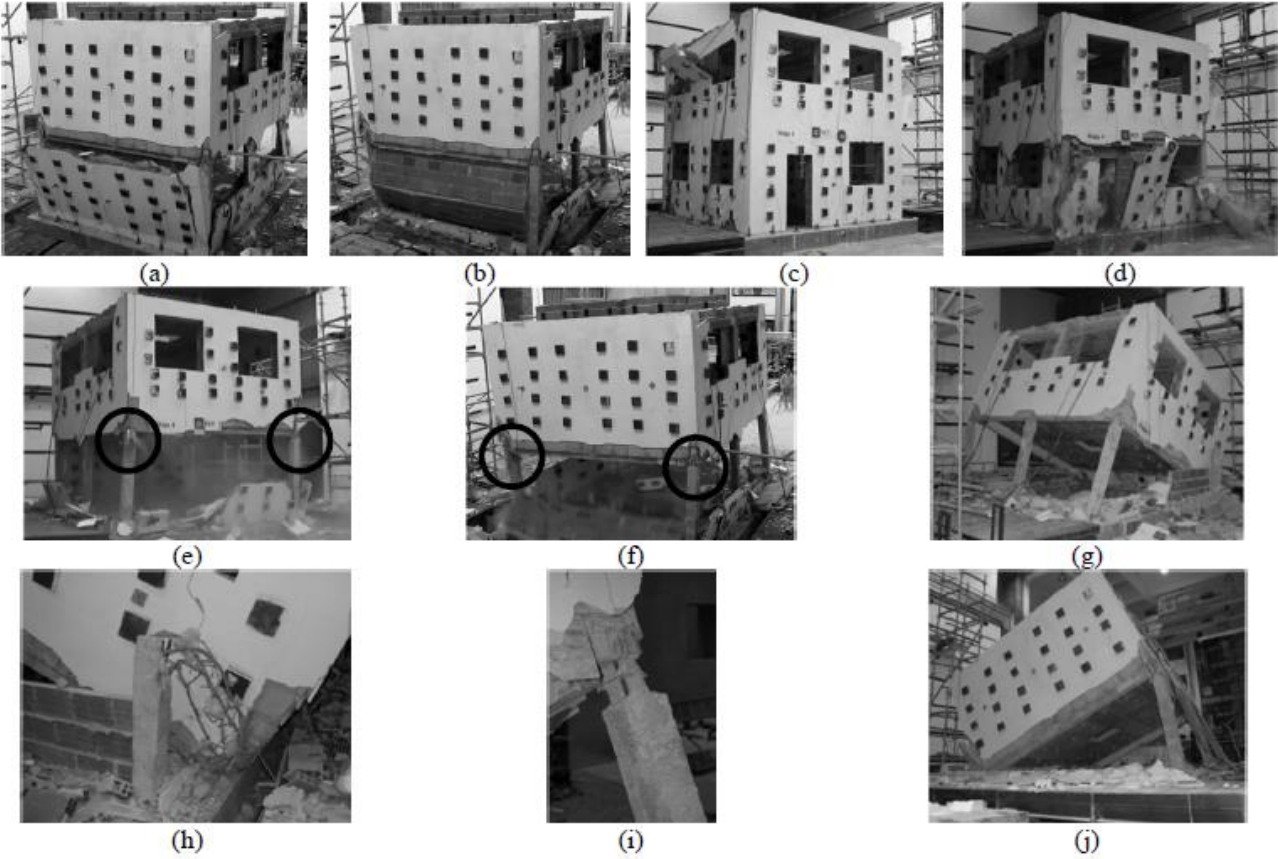
Figure 3-8 Shaking Table test on masonry building [29]

CHAPTER 4

NUMERICAL APPROACHES OVERVIEW

Chapter 4: Numerical Approaches Overview

4.1   Introduction

Numerical simulations are required to study the behaviour of systems whose mathematical models are too complex to provide analytical solutions, as in most nonlinear systems.

Since the 1980s, there has been a considerable increase in the development of material behaviour models [11] [17] [15] [8]. The great diversity of real materials and the need to describe the physical mechanisms that cause the various behaviours has led to the existence of a multitude of behavioural models.

The modelling of the mechanical plastic behaviour of materials is an essential step in the calculation and modelling of structures in general and plastic deformation in particular. The models aim to capture the intrinsic behaviour of the material in order to increase the credibility of the numerical simulation results. For the numerical simulation, Abaqus/CAE Software is used in this study as it is one of the robust and most common software applications for civil engineering mechanical investigations. The interface is easy to use and provides accurate and precise results.

4.2   Modelling Strategies

Masonry is a composite material made of masonry units and mortar that is anisotropic. Using finite element software, numerical models of masonry walls with and without reinforcement were commonly developed by researchers. Depending on the amount of precision, the desired simplicity, the size of the model, and the type of study.

Because of the anisotropy of masonry infill walls, they can be modelled in three main ways: homogenous structures using macro-modelling technique **Figure 4-1-b** , or heterogeneous structures in either detailed micro-modelling as indicated in **Figure 4-1-c** or simplified micro-modelling techniques as indicated in **Figure 4-1-d**.
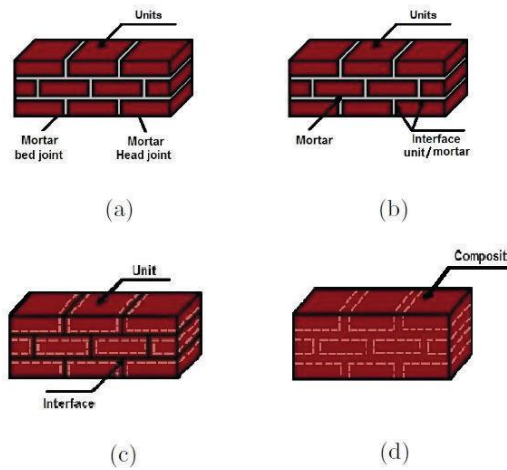
Figure 4-1 Different Modeling strategies for masonry structures : (a) masonry sample (b) detailed micro-modeling (c) simplified micro-modeling (d) macro-modeling. [5]

4.2.1   Macro-modelling

The simplest and more practical way to simulate the behaviour of masonry structures has been done by macro modelling. Masonry walls are composite constructions that can be homogenized with modern techniques in order to be considered as a one material as indicated in **Figure 4-2**.
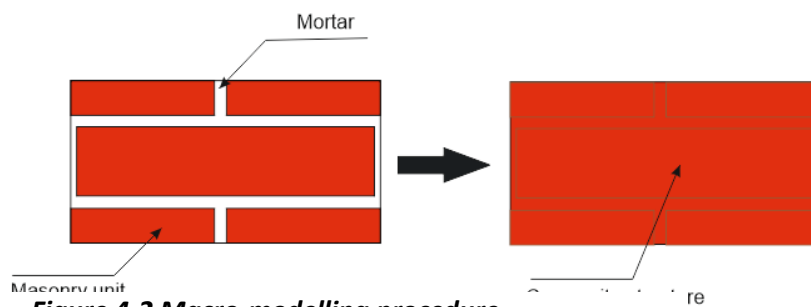
Figure 4-2 Macro-modelling procedure

4.2.2   Micro-modelling

In micro-modelling techniques, masonry walls are modelled heterogeneously. The components of the masonry (Mortar, masonry units) are modelled separately. Interfaces in the joining areas of these elements can be also included in the model **Figure 4-2**.

(a)   *(b)*
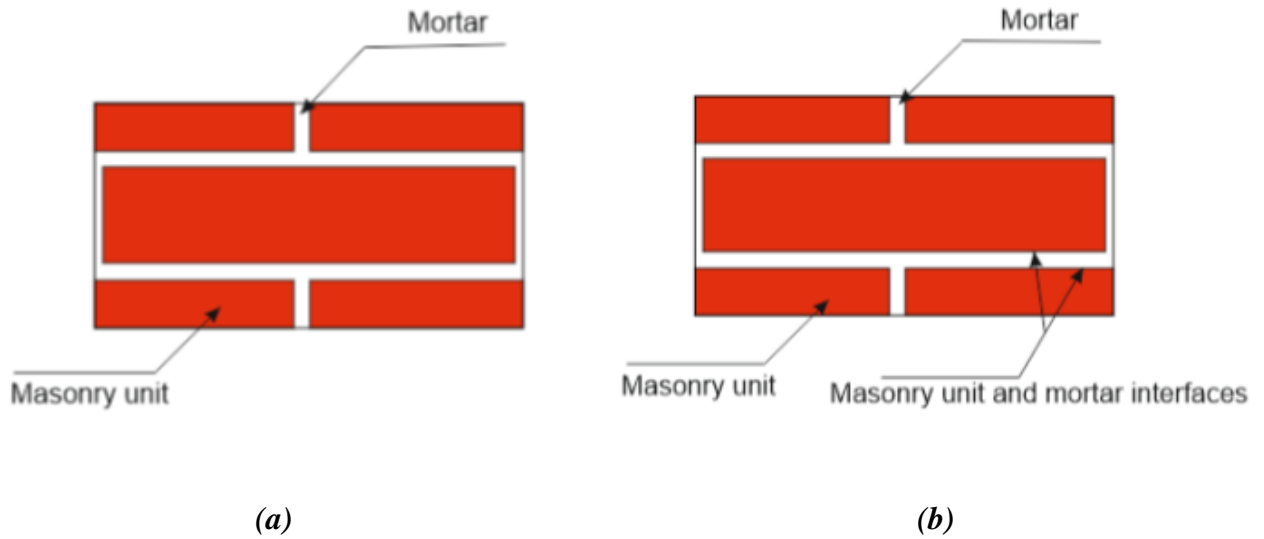
Figure 4-3 Micro-modelling procedure

Detailed micro modeling, is the most precise techniques of the ones listed above **Figure 4-2.b**. The interface between masonry units and mortar is modelled in this case, Young's modulus, Poisson's ratio, and, optionally, inelastic characteristics of both unit and mortar are taken into account. The interface represents a potential crack/slip plane with initial dummy stiffness.

Due to the complexity of this strategy and the unnecessity of such precision when it comes to studying masonry infill, it is uncommon to use. However, some researchers like [33] have used it to study failure mechanisms in masonry **Figure 4-4**.
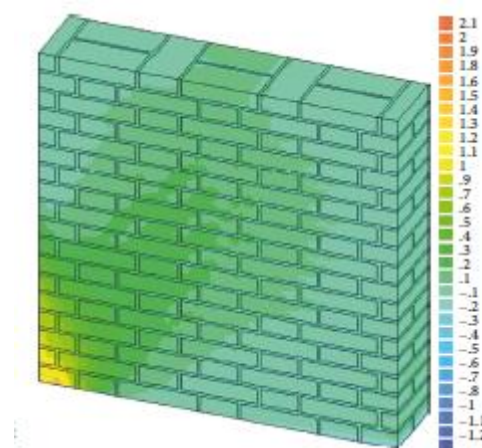
Figure 4-4 Masonry detailed micro-model used [33].

Simplified micro-modelling technique is a less precise version of detailed micro-modeling, it is the most used modelling strategy in similar research, such as [34], [2] , and [13], where joints are combined into

average interfaces, the mortar joints, and the units are enlarged to maintain the geometry **Figure 4-2.a**. Masonry can thus be thought of as a set of elastomeric blocks joined by fracture/slip lines at the joints.

4.2.3   Homogenization techniques

Homogenization techniques of masonry material can be classified into three types [35].

- The traditional empirical approximation based traditional homogenization, which was mostly used before the late 90s, taking into account the effects of volume ratios, physical, and material qualities of brick-and-mortar joints.

- The periodic composite continuum homogenization, using the homogenization theory for periodic media in conjunction with the finite-element approach, it might be suitable for studying large structures, but it is incapable to capture failure mechanisms.

- Micromechanics/Microstructures based homogenization techniques, it uses a symbolic volume to represent all of the masonry's geometric and constitutive characteristics, it is not commonly used as it requires several parameters in micro level, but it is under development method to be adopted more as it might be an alternative to laboratory test.

4.3   Numerical Models Categories

According to [36], modelling strategies were divided into four categories:

4.3.1   BBMs "Block-Based Models":

These models fall within the detailed and simplified-micro modelling techniques, it is the most common to use in similar research [34] as indicated in **Figure 4-5**, Mmasonry is modelled using a block-by-block definition of the structure. As a result, the accurate texture of masonry could be explained. Each block can be treated as a rigid or deformable-body, and the mechanical interaction between them can be modelled using a variety of formulas.
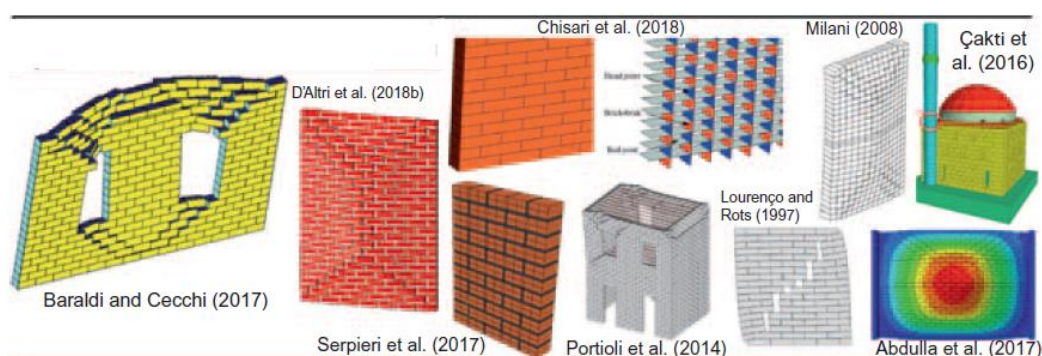
Figure 4-5 Examples of block based models [36]

4.3.2   CMs "Continuum models":

These models fall within the macro-modelling techniques, Masonry is envisioned as a deformable, continuous body with no distinction between blocks and mortar layers as indicated in Figure **4-6**, the masonry material constitutive law could be described using either

  a. Direct approaches, such as constitutive laws tuned, for example, on experimental tests [37] [38]

  b. Homogenization procedures and multiscale approaches [39].
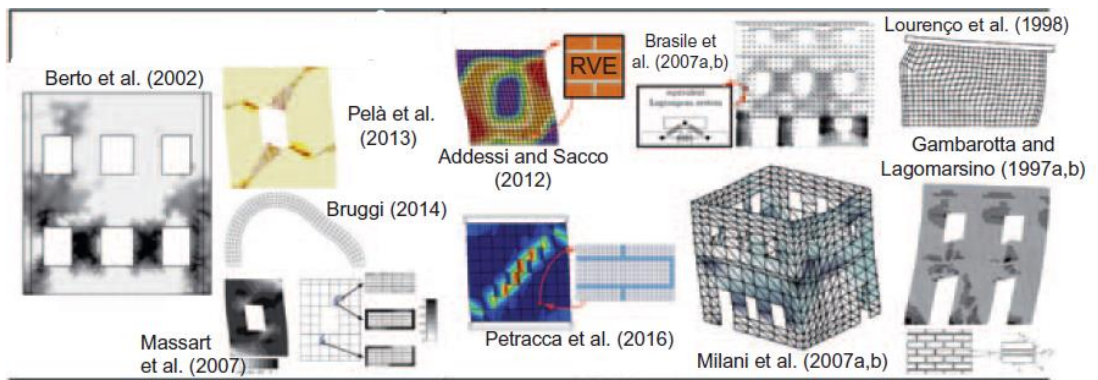
Figure 4-6 Examples of Continuum models [36]

4.3.3   MMs "Macroelements models":

This is another macro-modelling technique indicated in **Figure 4-7**, where "Piers and Spandrels" are the only microelements that can be identified, it uses panel-scale structural components to idealize the structure [40].
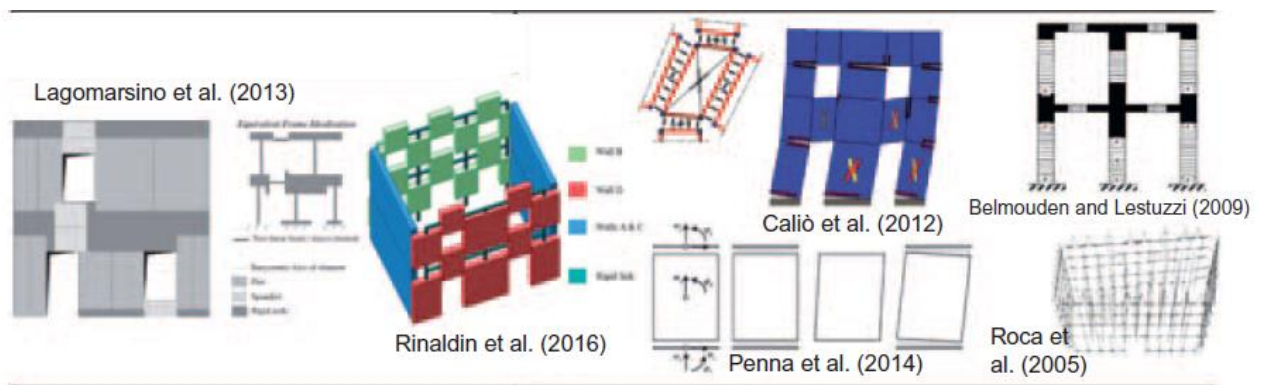
Figure 4-7 Examples of macroelemnt models [36]

4.3.4   GBMs "Geometry Based Models":

A rigid body is employed to model the structure as indicated in **Figure 4-8**. The geometry of the structure represents the only input data required in these modelling approaches, these approaches typically employ

either lower-bound or upper-bound limit analysis-based solutions developed by [41], No block-by-block description of masonry is conceived in this class [42] [43].
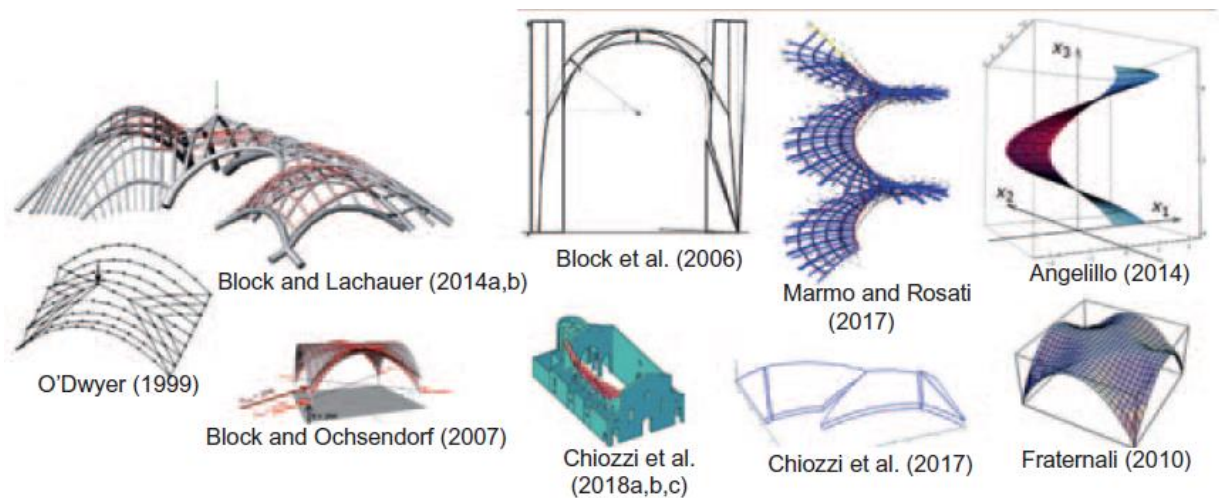
Figure 4-8 Examples of geometry based models [36]

Numerical strategies for masonry structures have been reviewed by [36] with the conclusion that BBMs appear to be the most precise methods for studying the mechanical behaviour of masonry structures. It also can be used to gain in-depth knowledge of specific aspects of masonry construction mechanics, as well as to provide reference results for more simplified strategies.

Isotropic plastic damage and smeared crack constitutive relationships have been extensively used, but in general, no-tension continuum approaches appear to be overly simplified for accurately assessing the structural integrity of masonry structures. It's also worth noting that MM's comprehensiveness is limited to seismic assessments of ordinary masonry structures, GBMs could be very useful, even though their results obtained are incomplete and unusable in displacement-based seismic assessment methods, they can provide important information for structural analysis of masonry arrangements.

4.4   Masonry Existing Material Models:

4.4.1   Drucker Prager Material Model:

The Drucker−Prager model was proposed by Drucker and Prager (1952) as a generalization of the Mohr–Coulomb criterion for soils, to describe the stress–strain behaviour of pressure-dependent materials such as soil, rock, and concrete, therefore it was commonly used to study the mechanical behaviour of masonry walls, especially under dynamic loading [44] [34] [45], to study the impact of cohesion on the displacement of components.

The Drucker–Prager failure criterion is a three-dimensional pressure-dependent model to estimate the stress state at which the soil, rock and concrete reaches its ultimate strength. It is based on the assumption that the octahedral shear stress at failure depends linearly on the octahedral normal stress through material constants. [46]
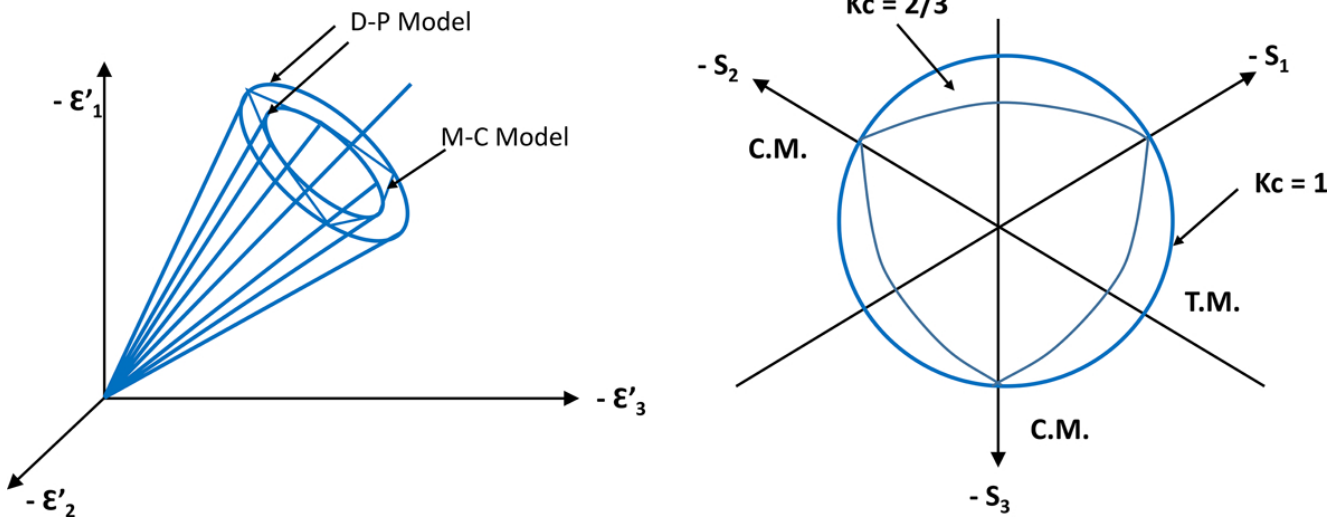
Figure 4-9 ABAQUS modified Drucker-Prager strength domain [45]

The original Drucker–Prager criterion has been modified to include a tension cut-off or a cap model that permits yield to be calculated under hydrostatic pressure.

The generalized Priest criteria and the MSDP$_u$ (Mises– Schleicher and Drucker–Prager unified) criterion are part of the modified Drucker–Prager criterion.

It can be expressed as:

$$\sqrt{J_2} = \lambda I'_1 + k$$

Where:I'_1 Is the first invariant of the stress tensor it is defined as:

$$I'_1 = \sigma'_1 + \sigma'_2 + \sigma'_3$$

Where: σ'_1, σ'_2, and σ'_3, are the principal effective stresses.

J_2 Is the second invariant of the stress deviator tensor it is defined as:

$$J_2 = \frac{1}{6}[(\sigma'_1 - \sigma'_2)^2 + (\sigma'_1 - \sigma'_3)^2 + (\sigma'_3 - \sigma'_1)^2]$$

When expressed to octahedral normal stress σ'_{oct}, and octahedral shear stress τ_{oct} , the criterion is defined as:

$$\tau_{oct} = \sqrt{\frac{2}{3}}\ (3\lambda\sigma'_{oct} + k)$$

Where $\sigma'_{oct} = \frac{2}{3}I'_1$ and $\tau_{oct} = \sqrt{\frac{3}{2}J_2}$

And k and λ are material constants:

$$k = \frac{6c\ cos\phi}{\sqrt{3}(3 - sin\phi)}$$

$$\lambda = \frac{2\ sin\phi}{(3 - sin\phi)}$$

Where c is cohesion intercept, and ϕ is friction angle.

The Drucker-Prager model does not assume that failure is independent of the value of the intermediate primary stress, as the Mohr-Coulomb model does. This model has vertices in the deviatoric plane as indicated in **Figure 4-10**
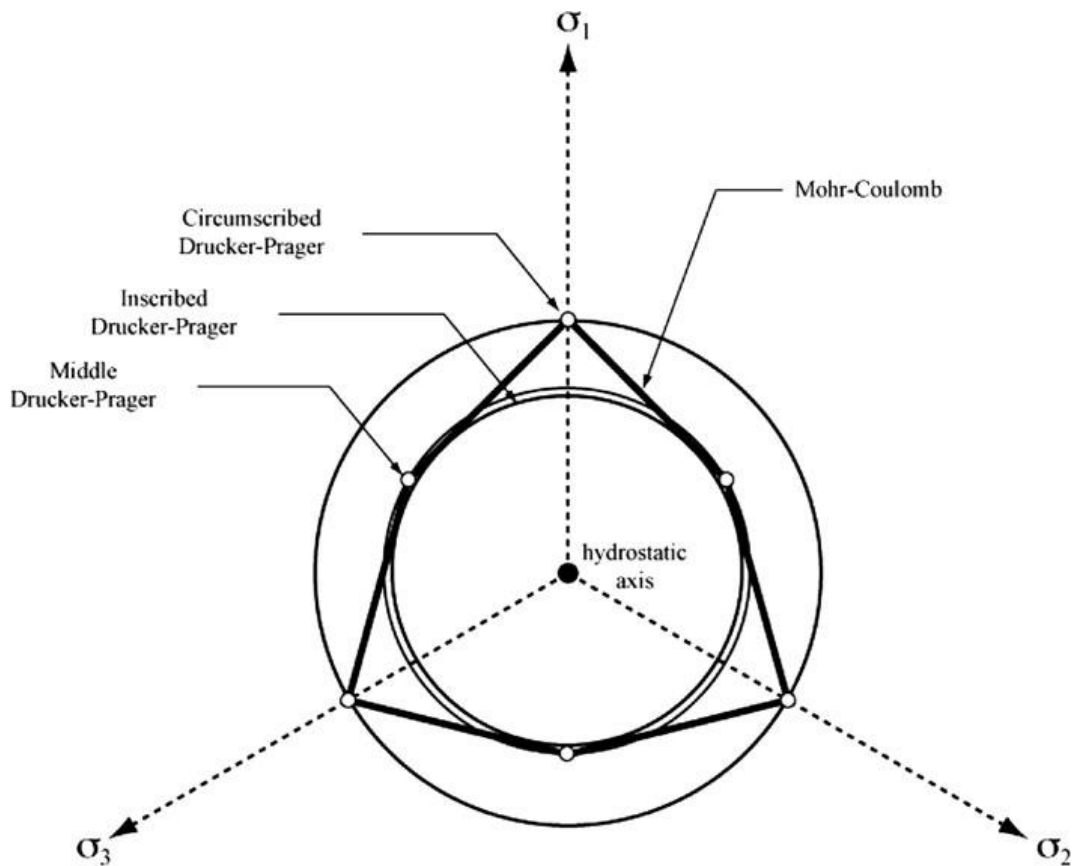
Figure 4-10 Drucker–Prager and Mohr-Coulomb Failyre Criteria in stress space [46]

The result is that when there are two equal principal stress values in a stress state, the flow direction might vary significantly with little or no change in stress. None of the current Abaqus models can offer such behaviour, even the Mohr-Coulomb model has a smooth flow potential. Although this constraint isn't a major concern in many design calculations employing Coulomb-like materials, it can reduce the accuracy of the calculations, particularly in circumstances where flow localization is critical. [47].

4.4.2   Concrete Damage Plasticity Model:

Fundamentally both masonry units (whether brick, concrete, or rock) and mortar are quasi-brittle materials whose mechanical performance will deteriorate (soften) under monotonic or cyclic loading [48].

Abaqus software [47] includes the concrete damaged plasticity (CDP) model, which has been developed for quasi-brittle materials. Lubliner [49] outlines the theory of this model, which was further expanded by Lee and Fenves [50].

The concrete damaged plasticity model is based on the assumption of scalar (isotropic) damage and is designed for applications in which the concrete is subjected to arbitrary loading conditions, including cyclic loading. The model takes into consideration the degradation of the elastic stiffness induced by plastic straining both in tension and compression. It also accounts for stiffness recovery effects under cyclic loading [47].

4.4.2.1   CPD Strain rate decomposition:

For the rate-independent model, an additive strain rate decomposition is assumed:

$$\varepsilon = \varepsilon^{el} + \varepsilon^{pl}$$

Where ε is the total strain rate, ε^{el} is the elastic part of strain rate and ε^{pl} is the plastic part of strain rate.

4.4.2.2   CPD Stress-strain relations:

The stress-strain relations are governed by scalar damaged elasticity:

$$\sigma = (1-d)D_0^{el}:(\varepsilon - \varepsilon^{pl}) = D^{el}(\varepsilon - \varepsilon^{pl})$$

$$D^{el} = (1-d)D_0^{el}$$

Where:

D_0^{el} The initial (undamaged) elastic stiffness of the material

D^{el} Is the degraded elastic stiffness

d Is the scalar stiffness degradation variable [47].

The damage plasticity constitutive model was based on the Cauchy stress relationship:

$$\sigma = (1-d)\overline{\sigma} \;\rightarrow\; \sigma = (1-d_t)\overline{\sigma_t} + (1-d_c)\overline{\sigma_c}$$

Where:

σ Represents the Cauchy stress

$\bar{\sigma}$ The effective Stress.

The damage factors d_c and d_t represent the stiffness degradation rate of the concrete caused by the damage of the concrete during compression and tension, under the condition of uniaxial stress.

The tensile and compressive damage constitutive relationship, as shown in **Figure 4-11.**
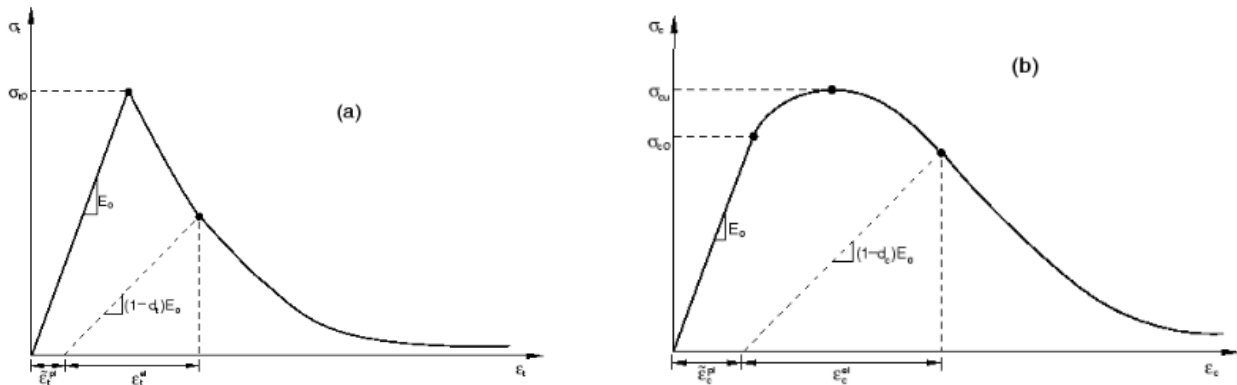
Figure 4-11 Uniaxial damage constitutive curve of concrete : (a) and compression (b)

4.4.2.3 CPD Hardening variables:

Two hardening factors are used to characterize damaged states in tension and compression $\tilde{\varepsilon}_t^{pl}$ and $\tilde{\varepsilon}_c^{pl}$, In tension and compression, these are referred to as equivalent plastic strains [47]

$$\tilde{\varepsilon}^{pl} = \begin{bmatrix} \tilde{\varepsilon}_t^{pl} \\ \tilde{\varepsilon}_c^{pl} \end{bmatrix}$$

The next equation represents the evolution of the hardening variables:

$$\dot{\tilde{\varepsilon}}^{pl} = h(\bar{\sigma}, \tilde{\varepsilon}^{pl}).\dot{\varepsilon}^{pl}$$

4.4.2.4 CPD Yield Function:

The plastic-damage concrete model uses a yield condition based on the yield function proposed by [49] and developed by [50]:

$$F(\bar{\sigma}, \tilde{\varepsilon}^{pl}) = \frac{1}{1-\alpha}(\bar{q} - 3\alpha\bar{p} + \beta(\tilde{\varepsilon}^{pl})\langle\hat{\bar{\sigma}}\text{max}\rangle - \gamma\langle-\hat{\bar{\sigma}}\text{max}\rangle) - \bar{\sigma}_c(\tilde{\varepsilon}_c^{pl}) \leq 0$$

Where α and γ are dimensionless material constants, $\bar{p} = -\frac{1}{3}\bar{\sigma} : I$ is the effective hydrostatic

pressure; $\bar{q} = \sqrt{\frac{3}{2}\,\bar{S}:\bar{S}}$ is the Mises equivalent effective pressure, $\bar{S} = \bar{p}I + \bar{\sigma}$ is the deviatoric

part of the effective stress tensor$\bar{\sigma}$, and $\widehat{\bar{\sigma}}$max is the algebraically maximum eigenvalue of $\bar{\sigma}$. [51]

The function of $\beta(\bar{\varepsilon}^{pl})$ is given as $\beta(\bar{\varepsilon}^{pl}) = \dfrac{\bar{\sigma}_c(\bar{\varepsilon}_c^{pl})}{\bar{\sigma}_t(\bar{\varepsilon}_t^{pl})}(1-\alpha) - (1+\alpha)$, where $\bar{\sigma}_c$ and $\bar{\sigma}_t$ are effective

tensile and compressive cohesion stress, respectively, the coefficient α can be determined from the initial

equibiaxial and uniaxial compressive yield stress, σ_{b0} and σ_{c0} as $\alpha = \dfrac{\sigma_{b0} - \sigma_{c0}}{2\sigma_{b0} - \sigma_{c0}}$,

According to [49] typical value of σ_{b0}/σ_{c0} ratio is in the range of 1.10 to 1.16, therefore the default value for concrete is taken 1.16.

4.4.2.5   CPD Flow Rule:

The relationship between the plastic strain ratio is:

$$\dot{\varepsilon}^{pl} = \dot{\lambda}\frac{\big(\partial G(\bar{\sigma})\big)}{\partial\bar{\sigma}}$$

Where $\dot{\lambda} \geq 0$ is a plastic multiplier?

The flow potential G for this model is the Drucker-Prager hyperbolic function:

$$G = \sqrt{(e\sigma_{t0}\tan\psi)^2 + \bar{q}^2} - \bar{p}\tan\psi$$

Where ψ is the dilation angle measured in the *p–q* plane at high confining pressure, σ_{t0} is the uniaxial tensile stress at failure, *e* is the eccentricity parameter, the flow potential tends to a straight line as the eccentricity tends to a zero [51].

4.4.2.6 K_c and K_t Ratio :

With the value of hydrostatic pressure $\bar{q}$ and $\widehat{\bar{\sigma}}_{max} < 0$ the corresponding yield conditions are:

$$\left(\frac{2}{3}\gamma + 1\right)\bar{q} - (\gamma + 3\alpha)\bar{p} = (1-\alpha)\,\bar{\sigma}_c, \text{(TM)}$$

$$\left(\frac{21}{3}\gamma + 1\right)\bar{q} - (\gamma + 3\alpha)\bar{p} = (1-\alpha)\,\bar{\sigma}_c, \text{(CM)}$$

And:

$$K_c = \frac{\bar{q}(TM)}{\bar{q}(CM)} = \frac{\gamma+3}{2\gamma+3} = \frac{2}{3} \rightarrow \gamma = 3$$

With the value of hydrostatic pressure $\bar{q}$ and $\hat{\bar{\sigma}}_{max} > 0$ the corresponding yield conditions are:

$$\left(\frac{2}{3}\beta + 1\right)\bar{q} - (\gamma + 3\beta)\bar{p} = (1 - \alpha)\,\bar{\sigma}_c, \text{ (TM)}$$

$$\left(\frac{21}{3}\beta + 1\right)\bar{q} - (\beta\bar{p} = (1 - \alpha)\,\bar{\sigma}_c\,, \text{ (CM)}$$

And:

$$K_t = \frac{\bar{q}(TM)}{\bar{q}(CM)} = \frac{\beta + 3}{2\beta + 3}$$
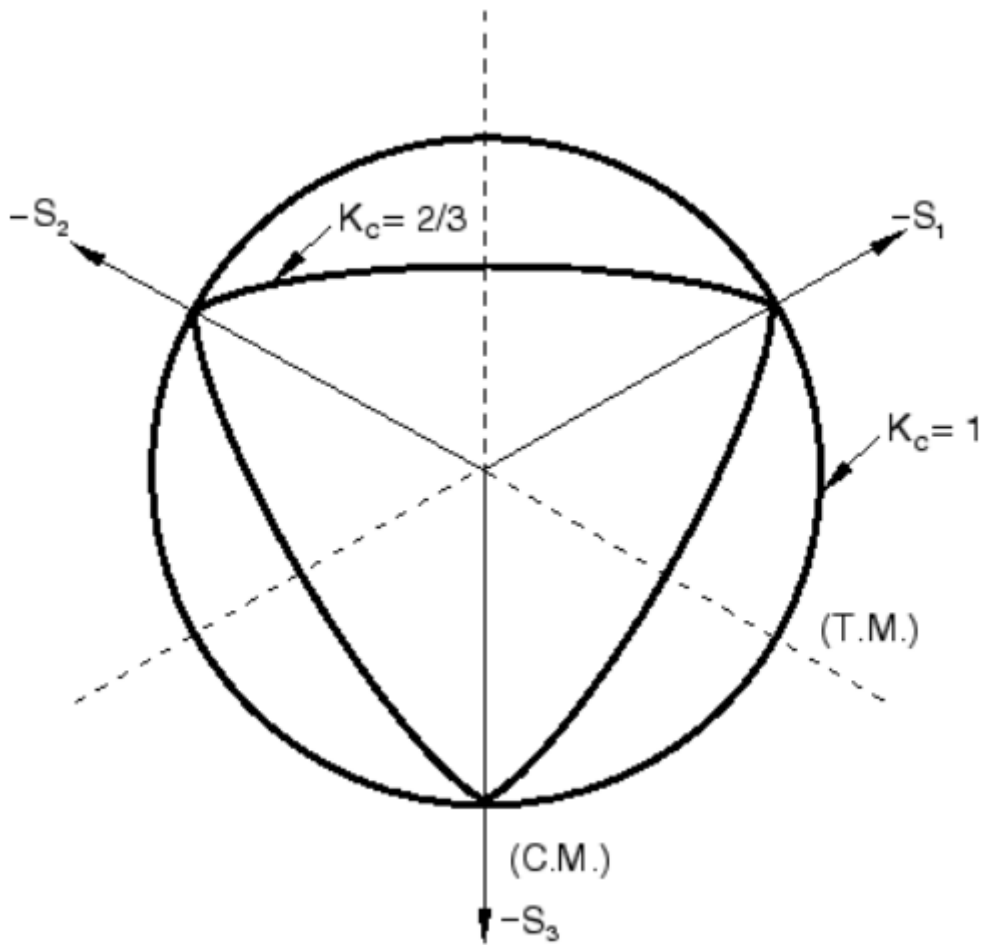
Figure 4-12 Yield surfaces in the deviatoric plane, corresponding to different values of K_c [47]

4.4.2.7 CPD definition in Abaqus/CAE:

Full definition of CDP model in Abaqus includes:

a) The σ−ε relationship for compression of concrete and tension behaviour of concrete in post-critical range.

b) Dilation angle ψ in the p-q plane

c) Flow potential eccentricity ε,

d) The ratio fb0/fc0 of biaxial compressive yield stress to uniaxial compressive yield stress "The default value is 1.16 for concrete" [47],

e) The ratio K_c of the second stress invariant on the tensile meridian $\bar{q}_{(TM)}$ to that on the compressive meridian for the yield function $\bar{q}_{(CM)}$, $K_c = \bar{q}_{(TM)}/\bar{q}_{(CM)}$ It must satisfy the condition 0.5< K_c ≤1.0 "the default value is constant and does not seem to be disputed by experimental evidence [49] it is equal to 2/3 for concrete" [47],

f) The viscosity parameter μ represents the relaxation time of the viscoplastic system and ε^{pl} is the plastic strain evaluated in the inviscid backbone mode, the solution of the viscoplastic system relaxes to that of the inviscid case as t/μ→∞, where t represents the time. Using the viscoplastic regularization with a small value for the viscosity parameter (small compared to the characteristic time increment) usually helps improve the rate of convergence of the model in the softening regime, without compromising results [47], Researches has demonstrated that the masonry wall's in plane capacity is responsive to the viscosity parameter, it increases as the viscosity parameter increases. [52]

CHAPTER 5

EXPERIMENTAL TESTS FOR NUMERICAL

VALIDATION

Chapter 5: Experimental Tests for Numerical Validation

5.1 Introduction

In order to determine the mechanical behaviour of masonry walls under compression, many researchers [2], [19] and [13] have conducted experiments using different scales. The typical methodology is to start with initial material characterization test, mainly compression test on brick and compression and three-point bending test on mortar. Some researchers [19] conduct additional test such as shear test "Triplet test" and brick-mortar interface bending tests. However, testing on wall scales is still the most reliable to obtain accurate results.

This chapter is an overview on the previously performed experimental studies on hollow clay brick masonry as it is the most common to use for internal partition and infill in Algeria. Therefore, the experimental investigation realized by [2] for hollow clay brick masonry under normal and diagonal compression is exposed in this part and used as a reference for this study.

5.2 Test On hollow clay brick

5.3 Compression test on hollow clay brick

Tests conducted by [2] according to EN 772-1 [20], this type of test is used to measure the compressive strength of masonry units, and it involves applying a distributed vertical compressive load to the top surface of the masonry units until failure occurs. The brick samples were prepared by applying a thin layer of mortar on the surface of each specimen to avoid the contact of the hydraulic compressor metal with the fragile surface of the masonry unit. The hollow clay brick was tested in two different load directions as indicated in **Figure 5-1**. The experimental tests were conducted on a total of twelve samples divided as 6 loaded in orthogonal to holes direction, and 6 loaded parallel to holes.

a)   b)

Figure 5-1 hollow brick compression tests: a) compression orthogonal to holes, b) compression
parallel to holes

The measurement was recorded by the internal Linear Variable Differential Transformer (LVDT) of the servo-hydraulic actuator, no additional instrumentation was used to monitor the vertical displacements of the specimens. As a result, the compressive strength was calculated using the equation **[5.1]** and the elasticity modulus for these experiments was not established (Error! Reference source not found.). The stress-strain relationship curves of the tested samples are indicated in Error! Reference source not found. and Error! Reference source not found..

$$f_{c,i} = \frac{F_i}{A_i} \times \delta \ [1]$$

[5.1]

$f_{c,i}$, The compression strength

F_i, is the peak load reached in each test

A_i, is the gross area

δ, The coefficient was determined according to Table A1 of ANNEX A of standard [20]

Table 5-1 compression tests on hollow bricks: summary of results (fc,p=compression strength parallel to holes; fc,o=compression strength orthogonal to holes) [2]

Bricks	$f_{c,\,p}$ [MPa]	$f_{c,\,o}$ [MPa]
Sample 1	10,94	4,04
Sample 2	10,11	3,71
Sample 3	9,34	5,04
Sample 4	12,89	6,48
Sample 5	7,56	4,83
Sample 6	11,57	5,73
Average	10,4	4,97
Standard dev.	1,85	1,03
Minimum	7,56	3,71
Maximum	12,89	6,48
Interval	5,33	2,76
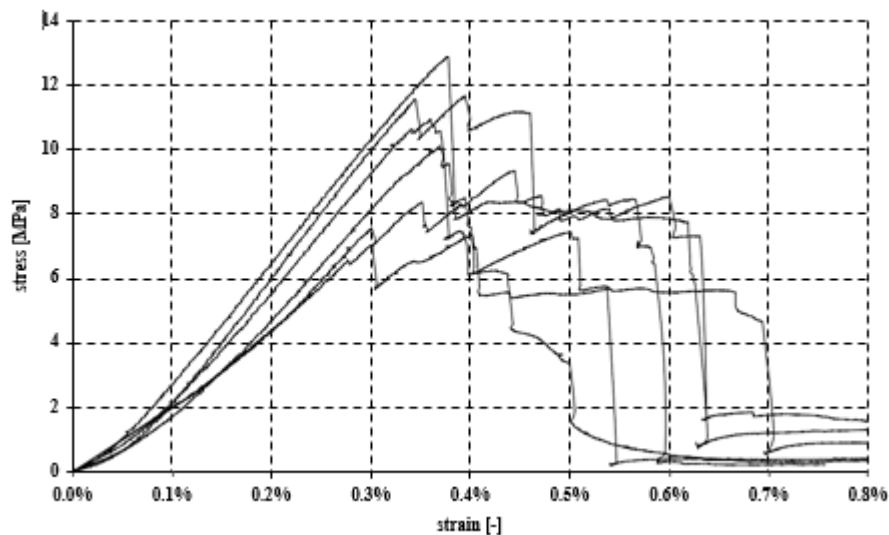
Figure 5-2 hollow bricks stress-strain curve, compression tests parallel to holes [2]
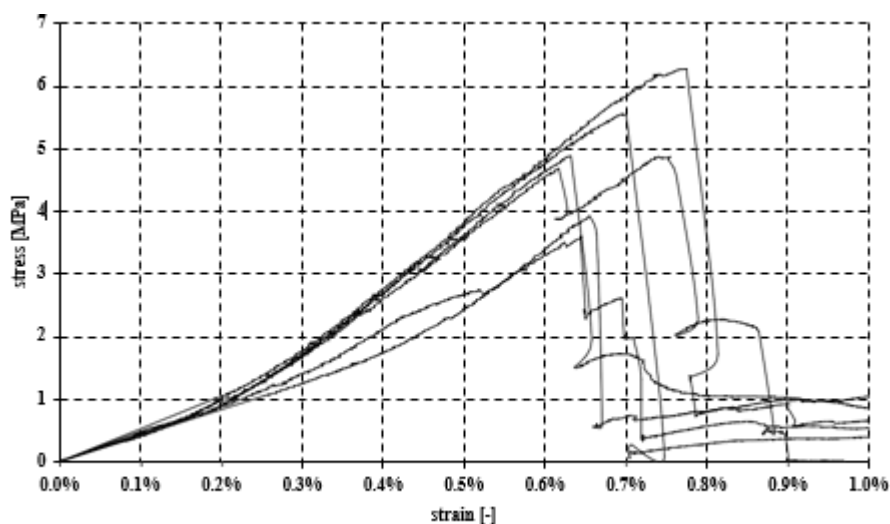
Figure 5-3 Hollow Bricks Stress-strain curve, compression test orthogonal to holes [2]

5.4   Tests on mortar:

The selected mortar for this study, is mortar recipe 1. ¼.¼.4 "1 part of Portland cement (CEM II/B-M(L-S-V)32.5), ¼ of 32.5 cement, ¼ of 12.5 cement, 4 parts of sand (granulometry between 1-4 *mm)*"

To characterise the mechanical properties of mortar, compression and three-point bending tests were conducted by [2] on mortar, two groups of samples have been created:

- 3 prisms 40x40x160 mm for the three-point bending test
- 9 cylinders diameter 100x200 mm for the compression test.

The loading surfaces of cylinders have been carefully flattened and the samples have been instrumented with four 50 mm strain gauges (two horizontal and two vertical).

The previous tests have been performed with the universal machine MTS 810 operating at a constant displacement speed of 0.05 *mm/s* according to EN 1015-11 [20] requirements.

5.4.1   Bending test on mortar:

The test is about applying increasing pressure until failure on a 40x40x160mm specimen as illustrated in Error! Reference source not found. and **Figure 5-4** [1]. This test is performed on a universal testing machine. The main advantage of a three-point flexural test is the convenience of the specimen preparation and testing.

Traction strength *f* has been obtained with the equation [5.2]:

$$f = 1.5 \frac{F.l}{b.d^2} \text{ [2]} \qquad\qquad [5.2]$$

with:

F	maximum load applied	
l	distance between supports	(100±0,5 *mm*)
b	width of the prisms section	(40 *mm*)
d	height of the prisms section	(40 *mm*)

Figure 5-4 bending tests on mortar samples [2]

The tests results were presented by load-displacement curve **Figure 5-5** in addition to the tensile strength of each sample indicated in **Table 5-2**.
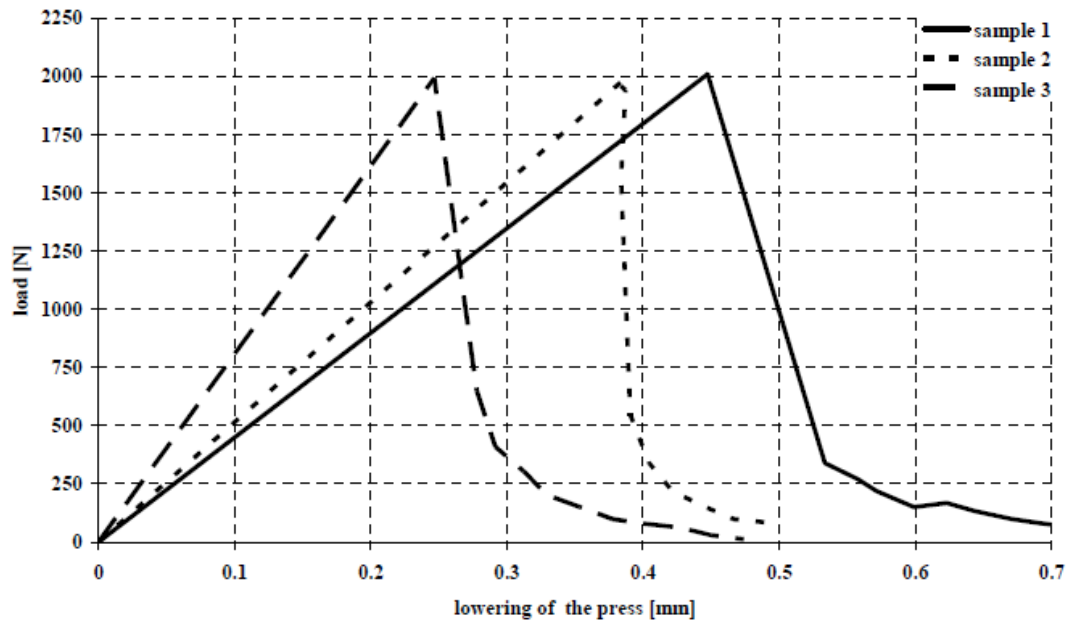
Figure 5-5 Mortar bending tests, load-deformation [2]

Table 5-2 Mortar tensile strength [2]

Prism	*F_{max} [N]*	*f [MPa]*
Sample 1	2009	4,70
Sample 2	1975	4,62
Sample 3	1992	4,66
f_{ctm}		4,66
$f_{ctk}=0.7f_{ctm}$		3,26

5.4.2   Compression test on mortar

To determine the compressive strength of the mortar, a compression test is performed on 9 specimens according to EN 1015-11 [20]. For this test, an increasing monotonic pressure is applied on the cylinder specimen until failure as indicated in Figure 5-6.

Figure 5-6 Compression test on mortar cylinder

The test results were presented by a stress-strain curve illustrated in Error! Reference source not found., and compressive strength, Young modulus, and Poisson's ratio values for each sample indicated in **Table 5-3.**

Table 5-3 Mortar compression test results

Cylinder	f_m[MPa]	E_m[MPa]	v
Sample 1	22.15	-	-
Sample 2	19.48	15157	0.163
Sample 3	24.81	15197	0.181
Sample 4	26.01	18638	0.196
Sample 5	24.09	16900	0.207
Sample 6	26.50	18269	0.207
Sample 7	28.73	17605	0.202
Sample 8	17.96	-	-
Sample 9	21.71	-	-
Average	**23.49**	**16961**	**0.193**
Standard deviation	3.47	1504	0.017

Interval	10.77	3481	0.044
Minimum	17.96	15157	0.163
Maximum	28.73	18638	0.207
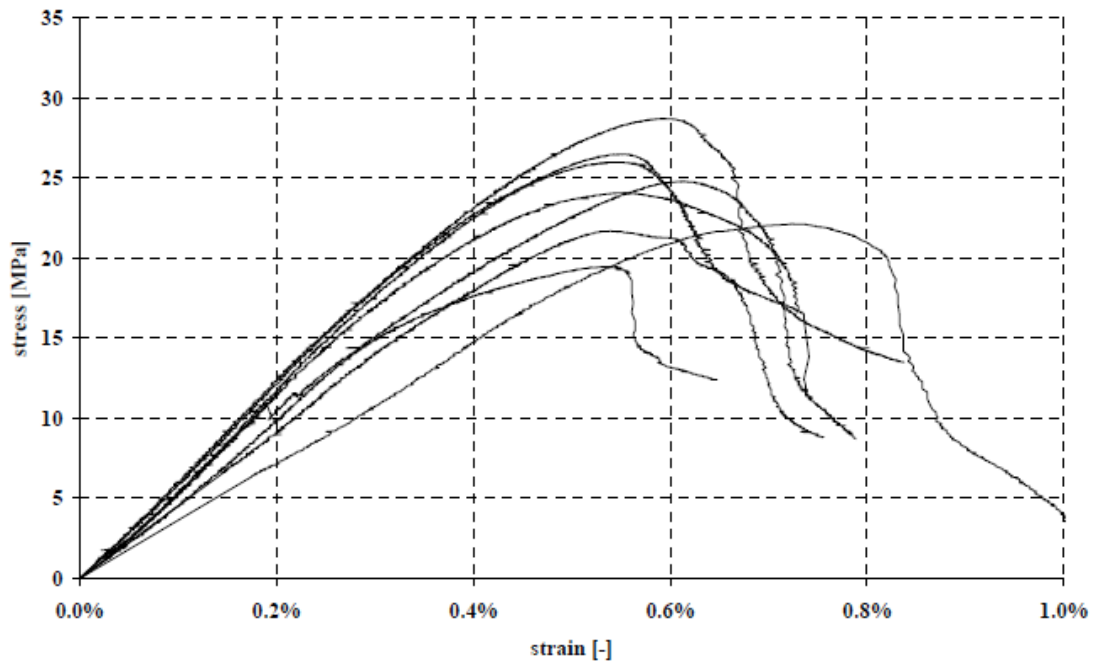
Figure 5-7 Mortar compression test stress-strain curve

5.5   Experimental tests on walls

5.5.1   Tests equipment and samples preparation

In the work of [2] twelve walls have been tested under normal and diagonal compression. The walls were arranged in running bond with a dimension of 101x101x80 cm. The bed and head mortar joints have approximately 10 mm thickness **Figure 5-8**.

The loading surfaces have been levelled with a layer of high-strength mortar to create smooth and parallel surfaces.

Figure 5-8 Hollow clay brick masonry wall specimens [2]

Experiments were carried out by applying a monotonic load to the panels until failure. For both main compression directions, the loading speed was 1.6 kNs-1, which was equivalent to 0.8 kNs-1 for diagonal compression. To avoid accidental loading eccentricities, the applied load was monitored using an external loading cell with a spherical joint. Two HEB 300 steel trusses were placed between the wall samples and press plates used to ensure an even load distribution across sample faces and customized steel saddle were placed in the same way for diagonal compression test to transmit the load to the samples as illustrated in **Figure 5-9**. The equipment is detailed in **Figure 5-9**.
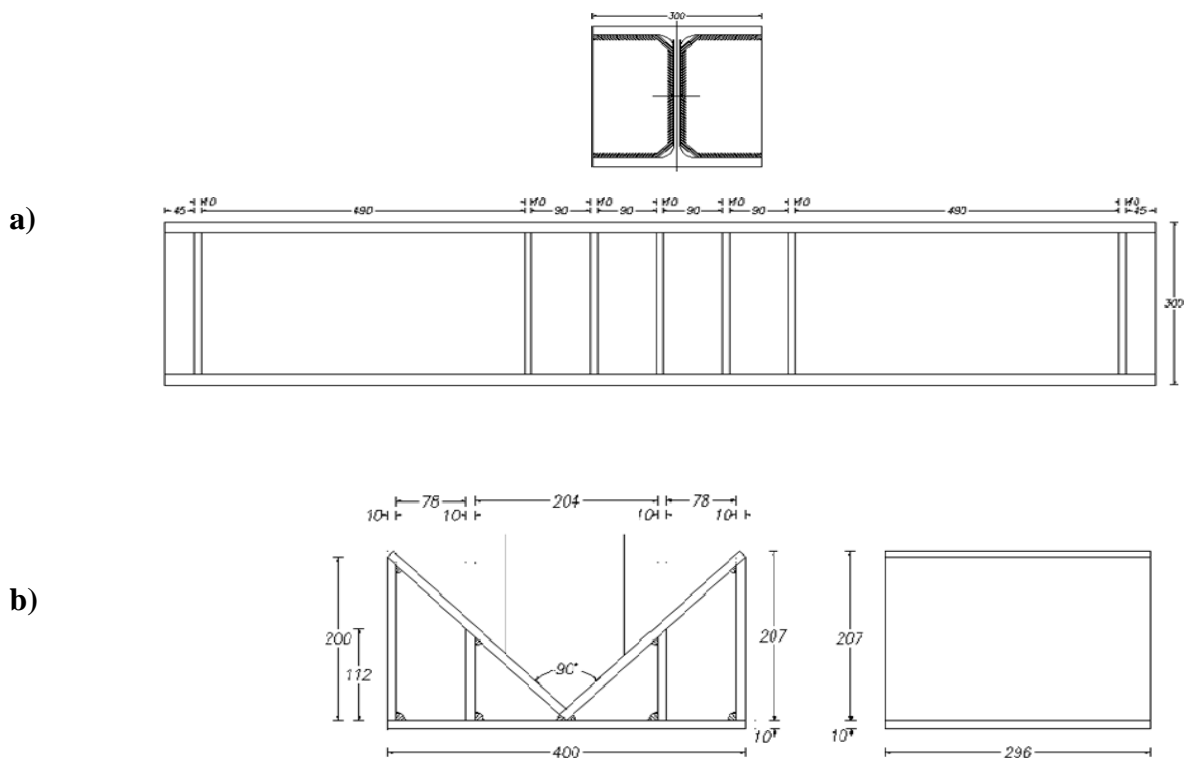
Figure 5-9 Steel saddle/Panel used to transmit loads to walls: a) In normal direction; b) In diagonal Direction

a)   b)
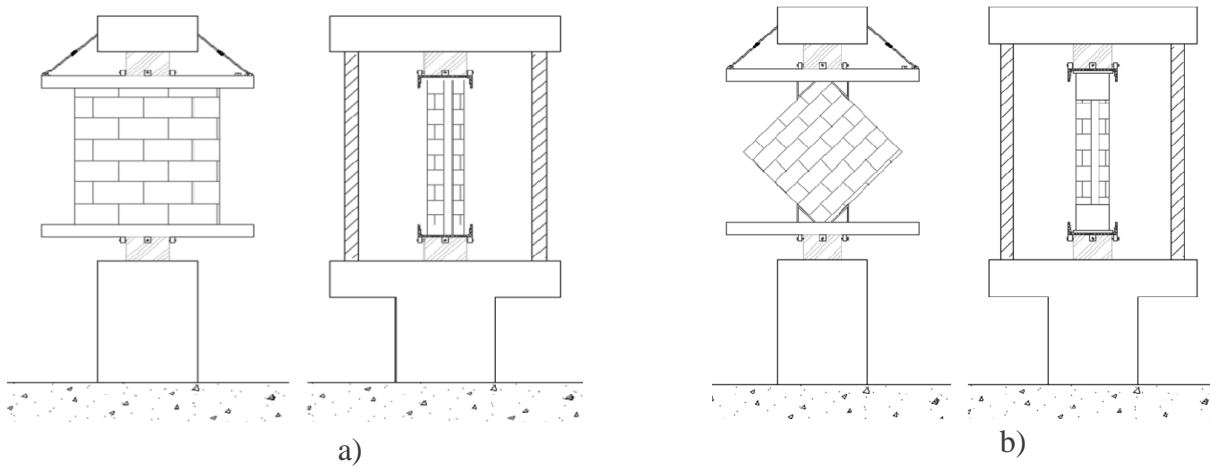
Figure 5-10 Layout of test systems: a) Normal compression test; b) Diagonal compression test

In order to measure vertical plate's translation, a displacement transducers were installed directly on the walls as represented in, the measurements were performed at frequency of 0.1 Hz as illustrated in **Figure 5-11**.

a)

b)

c)
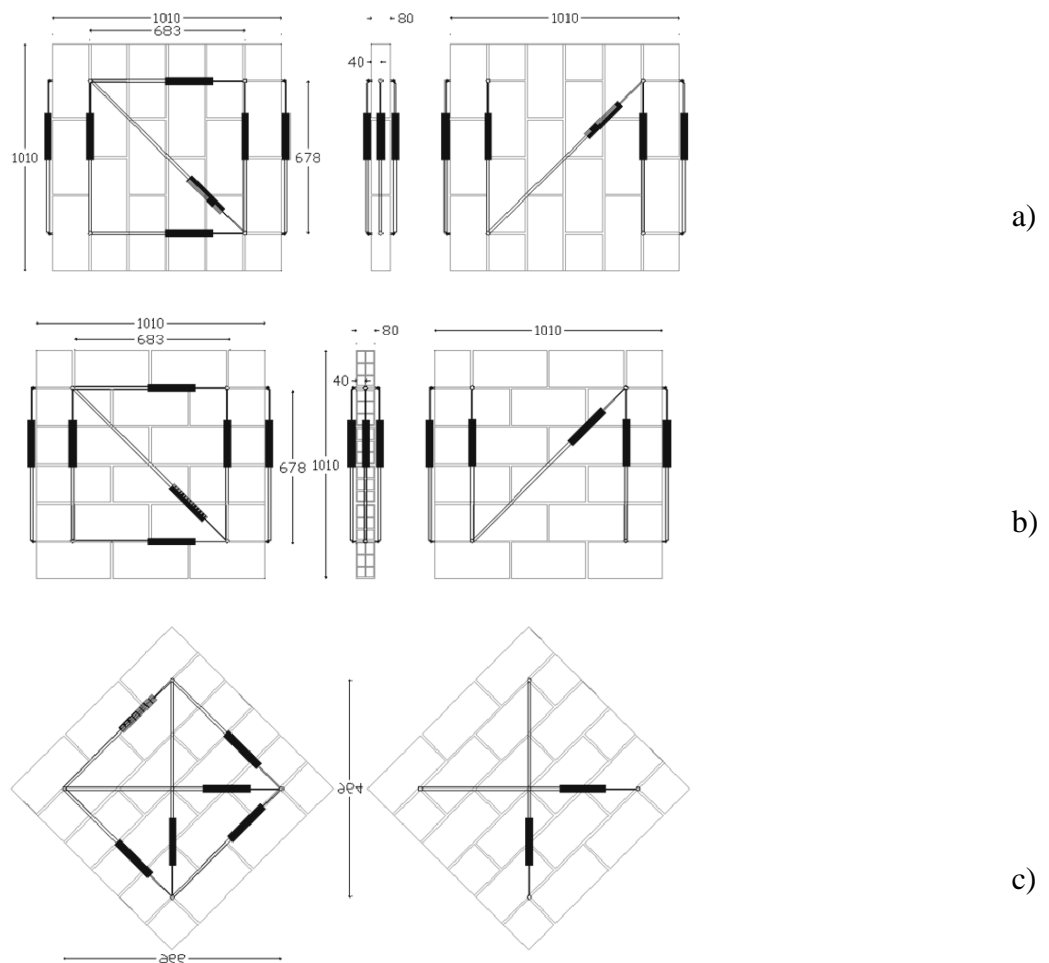
Figure 5-11 hollow brick panels layout of sensors on the wall compressed: a) parallel to holes; b) orthogonally to holes; c) diagonally [mm]

The experimental results obtained from these tests were represented by load-displacement and stress-strain relationship of each tested wall in each of the three-loading directions **Figure 5-12-18**. The compressive strength, Young modulus, shear strength and shear modulus were calculated from the previous tests using the **Table 5-4**.

Table 5-4 results obtained from masonry walls testing calculation [2] [1] [53]

The property	Symbol	Formula	Reference
compression strength in normal direction	f_w	$f_{wi} = F/A_i$ $f_{wh} = F/h.t$ $f_{wv} = F/l.t$	- NF EN 1052-1 "Normal compression test"
Young Modulus	E	$E_i = F/3.\varepsilon.A_i$	- NF EN 1052-1 "Normal compression test"
Shear Strength	f_{w0}	$f_{w0} = F/(\sqrt{2}.l.t)$	- Diagonal compression test
Shear modulus	G_w	$G_w = f_{w0}/\gamma_w$ $\gamma_w = (\varepsilon_{w1} - \varepsilon_{w2})/2$	- Normal compression test - Diagonal compression test

5.5.2   Tests results

The force-displacement and stress-strain relationship were obtained from the previous tests. The results are presented in Figure 5-12 to Figure 5-17. The compressive strength, Young modulus, Shear modulus and Poisson's ratio derived from these curves are summarized in **Table 5-5.**
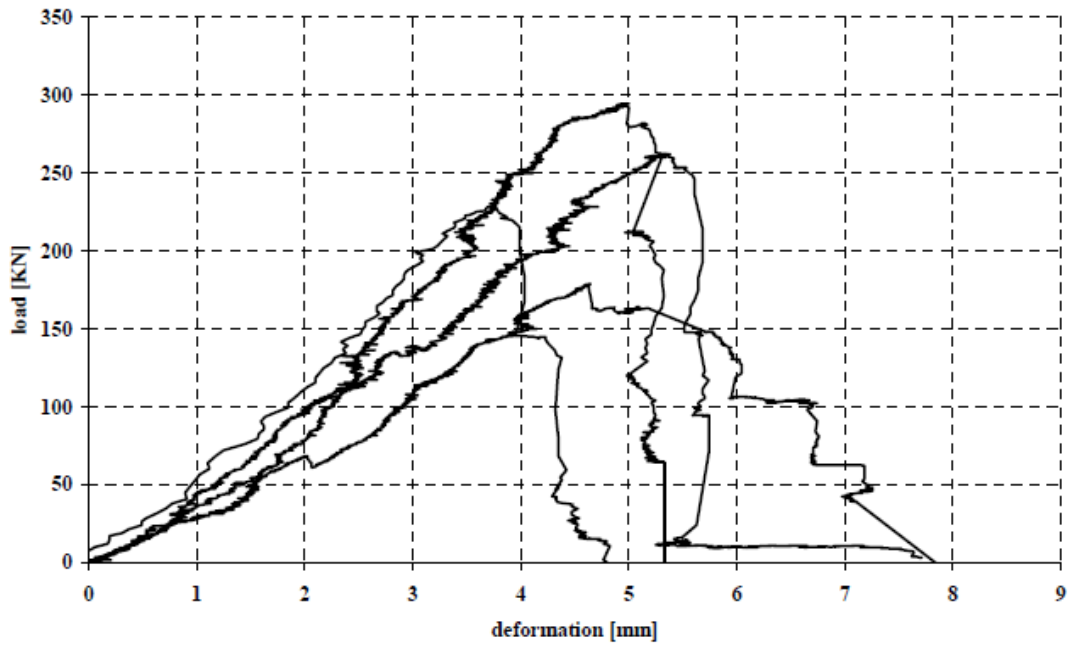
Figure 5-12 compression tests parallel to holes, load-displacement curves
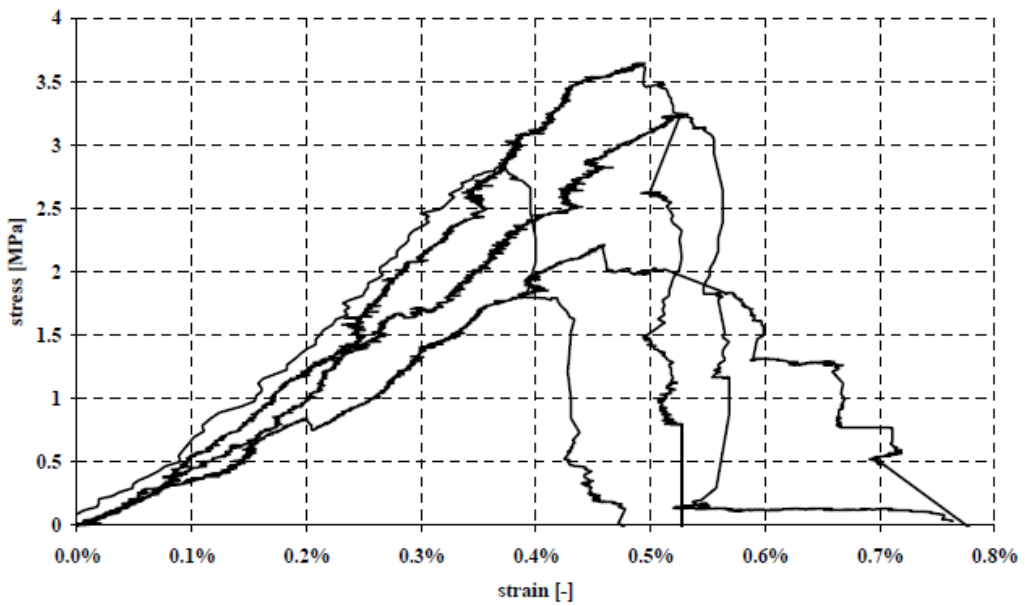
Figure 5-13 Compression tests parallel to holes, stress-strain curves
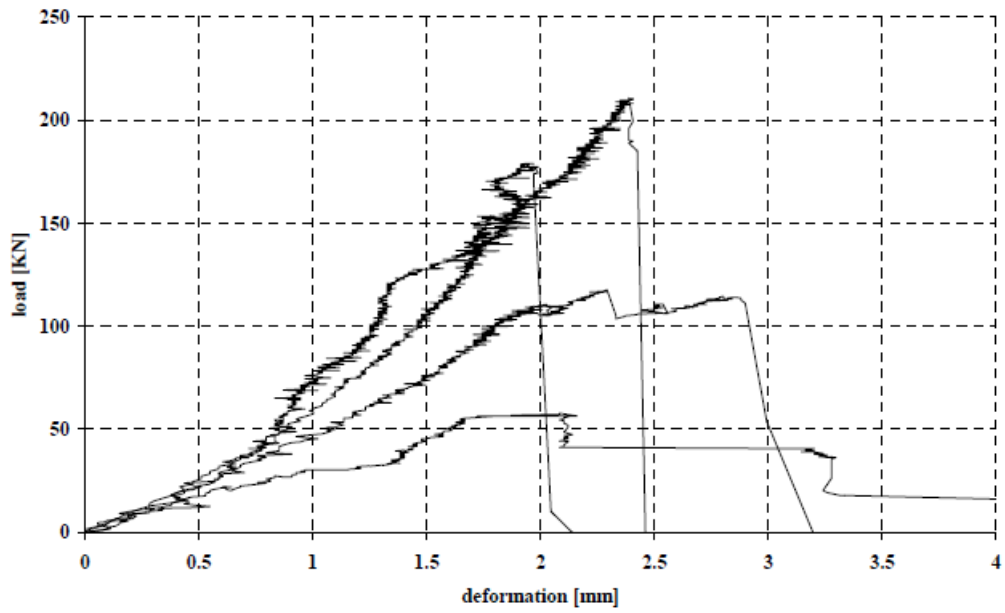
Figure 5-14 compression tests orthogonal to holes, load-displacement curves
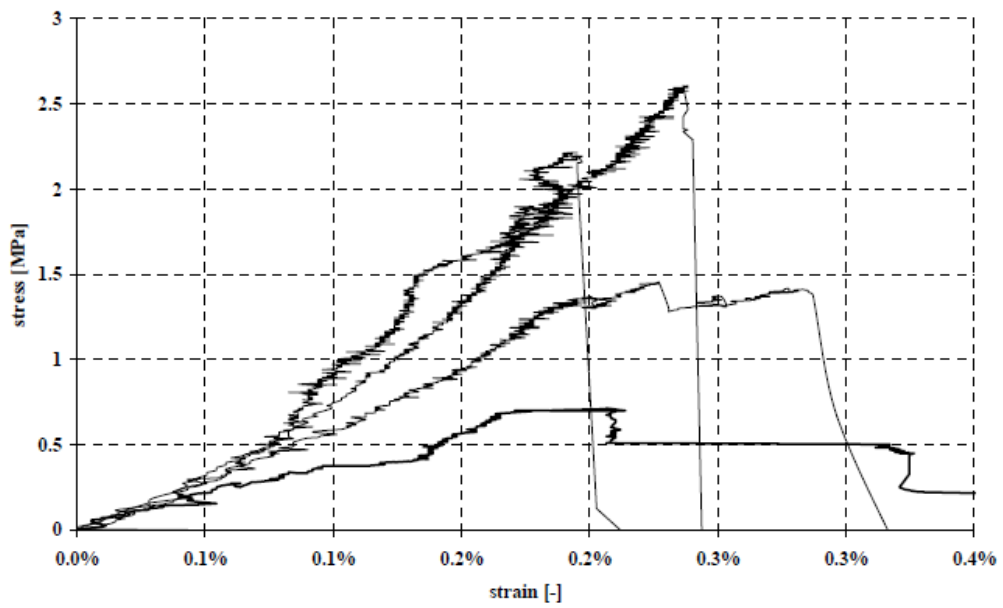
Figure 5-15 compression tests orthogonal to holes, stress-strain curves
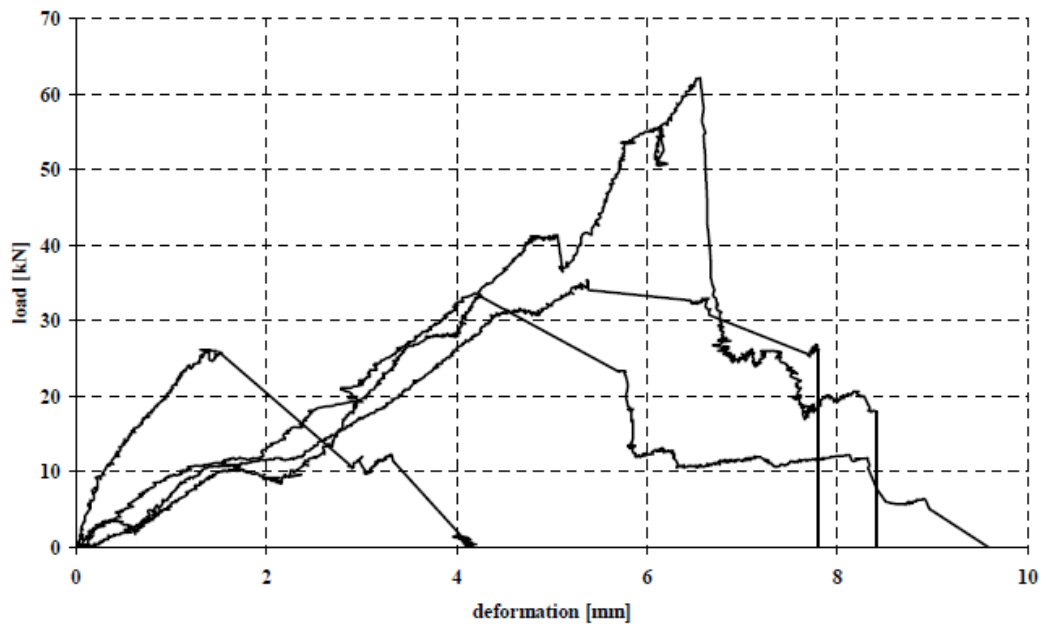
Figure 5-16 diagonal compression tests, load-displacement curves
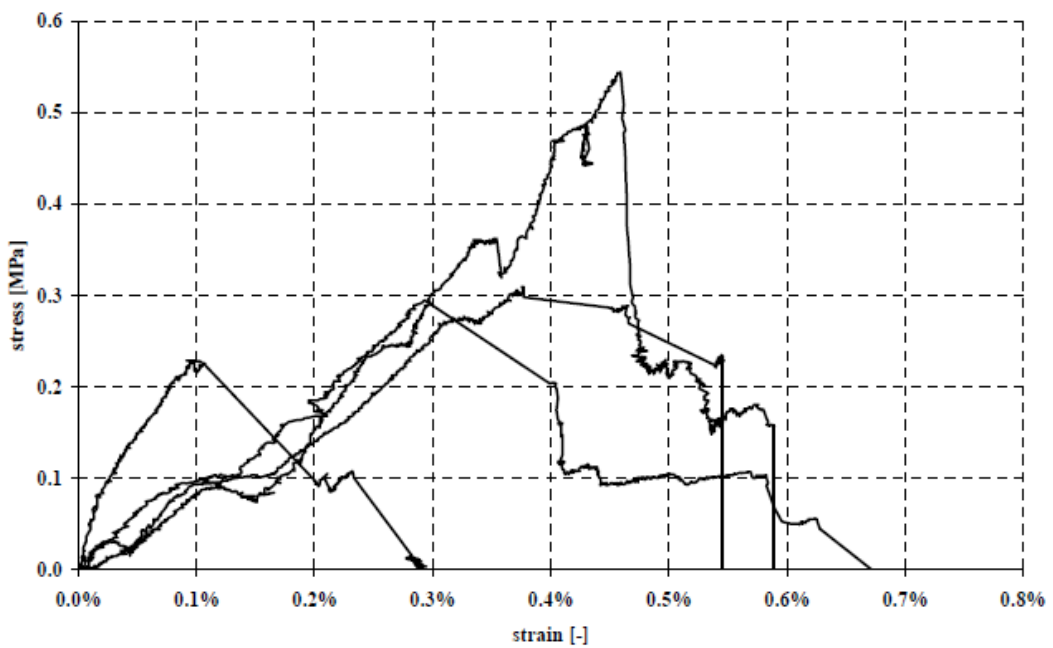
Figure 5-17diagonal compression tests, stress-strain curves

Table 5-5 Tests on walls results summary

Compression strength			
f_{wv}	1.90	MPa	Vertical direction
f_{wh}	3.11	MPa	Horizontal direction
f_{wo}	0.35	MPa	Diagonal direction
Maximum strains			
e_v	0.55	‰	Vertical direction
e_h	0.81	‰	Horizontal direction
e_o	1.17	‰	Diagonal direction
Elastic modulus			
E_v	4804.2	MPa	Vertical direction
E_h	4325.5	MPa	Horizontal direction
E_o	2900.0	MPa	Diagonal direction
G_w	500.0	MPa	Shear modulus
Poisson coefficient			
n_v	0.36		
Ratio between f and E			
f_{wv}/E_v	0.40	‰	
f_{wh}/E_h	0.72	‰	
f_{wo}/E_o	0.12	‰	

CHAPTER 6

DETAILED MICRO-MODELLING OF HOLLOW CLAY BRICK MASONRY WALLS

Chapter 6:   Detailed Micro-Modelling of Hollow Clay Brick Masonry Walls

6.1   Introduction:

For the assessment of the mechanical behaviour of unreinforced brick masonry wall structures, different techniques are available in the literature to simulate the response of masonry walls, from simplified macro models to refined detailed micro-models. For the nonlinear analysis of complex structures when subjected to uniaxial loading, it is most suitable to adopt refined detailed micro-models or simplified micro-models to demonstrate the interactions between the brick units and mortar. Therefore, for the simulation of the mechanical behaviour of hollow clay brick masonry walls under normal compression, considering the interaction of the mortar joints bonding with the brick units, the detailed micro-modelling approach was adopted, using a block-based model.

This chapter aims to simulate the experimental tests presented in the previous chapter, starting by replicating the initial component characterization tests and then simulating the tests on the wallets using a detailed micro-model approach.

6.2   Material's numerical modelling

6.2.1   Identifying properties of mortar

The mortar is considered in this thesis as an elastoplastic quasi-brittle material therefore the Concrete Damaged Plasticity model implemented in Abaqus/CAE [47] was adopted to simulate the mechanical behaviour of mortar. The input of this model consists of elastic behaviour and inelastic behaviour defined in Abaqus with compressive and tensile behaviour. The mechanical characteristics required for this approach are: Elastic parameters obtained by Young Modulus E, Poisson's Ratio v ; Plastic parameters obtained by the compressive behaviour from mortar cylinder compression test realized by [2] and identified by the Yield stress and Inelastic strain. Also, the tensile behaviour extracted from the three-point bending test results realized by [2] identified by the yield stress and cracking strain.

The mortar compression test realized by [2] was simulated using Abaqus/CAE 6.14-5 as illustrated in Error! Reference source not found.**.**
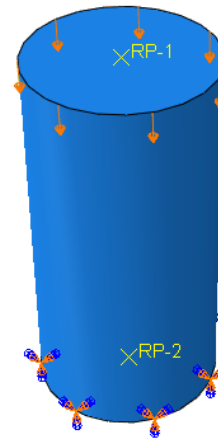
a   b

Figure 6-1 Mortar compression test: a) Real Test ; b)Numerical Model

6.2.1.1 *Identifying the elastic properties of mortar*

For the Poisson's ratio, a classic value of 0.2 was adopted, and the average Young modulus obtained from the experimental curves of the compression test showed a result of 5125.66 MPa. The experimental value was calibrated to 5300 MPa in the Abaqus as illustrated in **Figure 6-2**.
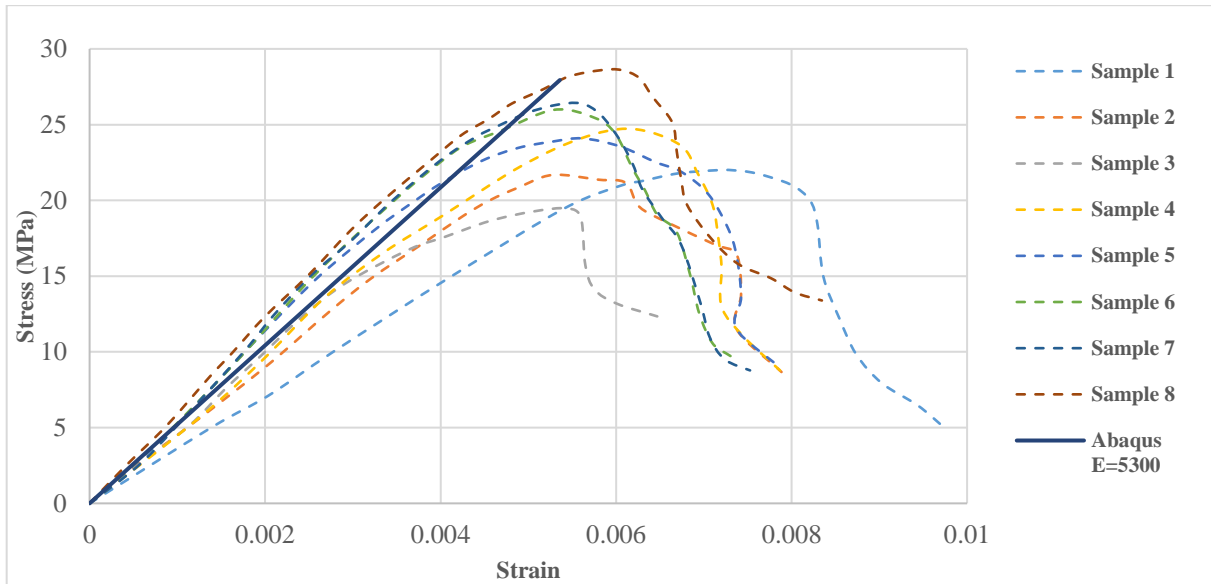
Figure 6-2 Young modulus calibration to mortar compression test curves

6.2.1.2 Identifying Concrete Damaged Plasticity properties of mortar using sensitivity analysis

After identifying the elastic properties of the mortar, the compressive and tensile behaviour of the mortar must be identified based on the experimental curves of the compression and three-point bending test realized by [2].

1) Compressive stress data are provided as a tabular function of inelastic (or crushing) strain where:

$$\varepsilon_c^{-in} = \varepsilon_c - \varepsilon_{0c}^{el} \qquad\qquad [6.1]$$

$$\varepsilon_c^{-in} = \varepsilon_c - \sigma_c/E_0 \qquad\qquad [6.2]$$

Where: ε_c^{-in} is the inelastic strain, ε_c is the total strain, ε_{0c}^{el} is the elastic strain corresponding to the undamaged material, σ_c the Stress corresponding to the strain, and E_0 is the elasticity modulus as indicated in **Figure 6-3**.
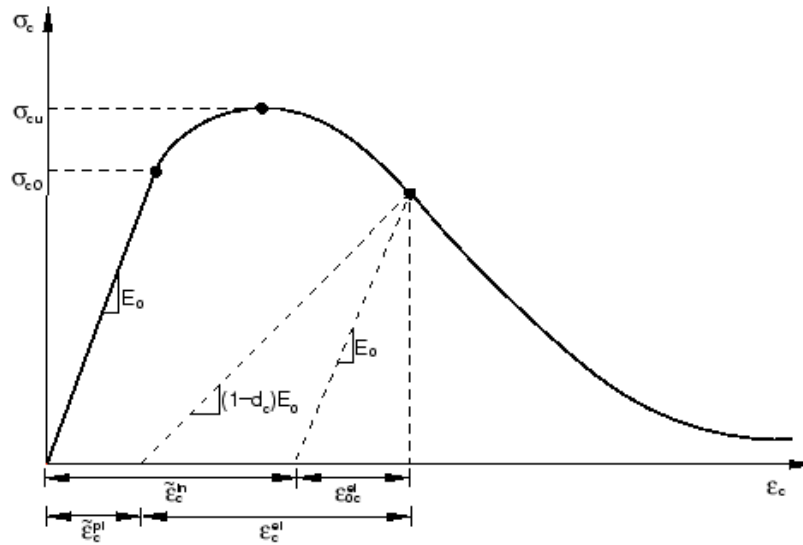
Figure 6-3 Definition of the compressive inelastic (or crushing) strain [47]

2) Tensile stress data are provided as a tabular function of cracking (or crushing) strain where:

$$\varepsilon_t^{-ck} = \varepsilon_t - \varepsilon_{0t}^{el} \qquad\qquad\qquad [6.3]$$

$$\varepsilon_t^{-ck} = \varepsilon_t - \sigma_t/E_0 \qquad\qquad\qquad [6.4]$$

Where: ε_t^{-ck} is cracking strain, ε_t is the total strain, ε_{0t}^{el} is the elastic strain corresponding to the undamaged material, σ_t is the stress corresponding to the strain, and E_0 is the elasticity modulus as indicated in **Figure 6-4**
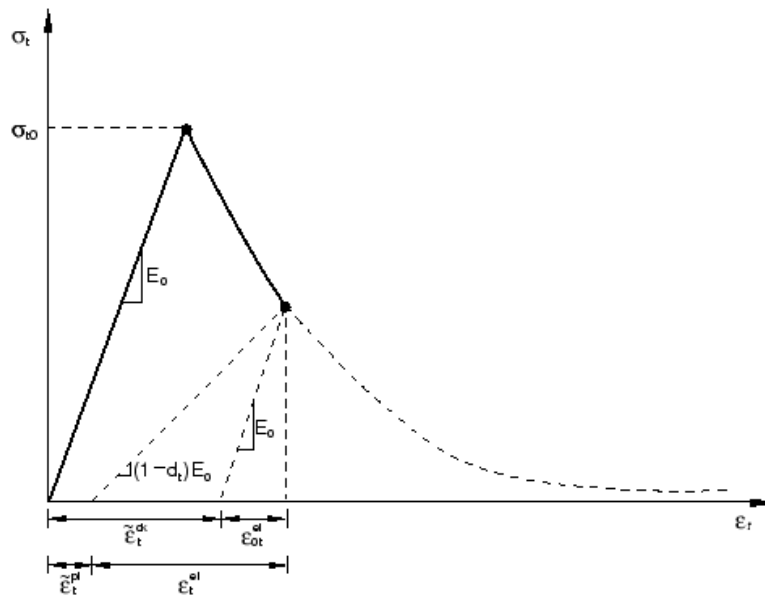
Figure 6-4 Illustration of the definition of the cracking strain [47]

3) Plasticity parameters for the Concrete Damaged plasticity model are presented by:

- The flow rule is the ratio of second pressure invariant to the tensile meridian$K$ "The default value is 2/3"

- Flow potential eccentricity ε =0.05

- The ratio fb0/fc0 of biaxial compressive yield stress to uniaxial compressive yield stress "The default value is 1.16 for concrete"

- Dilation angle ψ in the p-q plan

- The viscosity Parameter

  Where dilatation angle and viscosity parameter are to be defined based on previous research [19] and sensitivity analysis.

  1) The numerical simulation of compression test on mortar cylinder was replicated with a variation in dilation angle « 10°, 30°, 40° », with constant viscosity parameter equal to 0.01

     The dilation angle of 30° meets the post-peak behaviour to a higher extent for the wall with a viscosity parameter coefficient of 0.01

     It was noticed that with the increase of dilation angle, material hardening property increases, and variation of dilation angle property causes variation in the Force-Displacement curve.

     The results presented in **Figure 6-5** shows the variance in the force-displacement relationship for various dilation angles. The post-peak behaviour of the wall varies depending on the dilation

angle. The dilation angle of 30° meets the post-peak behaviour to a higher extent for the wall with a viscosity parameter coefficient of 0.01.
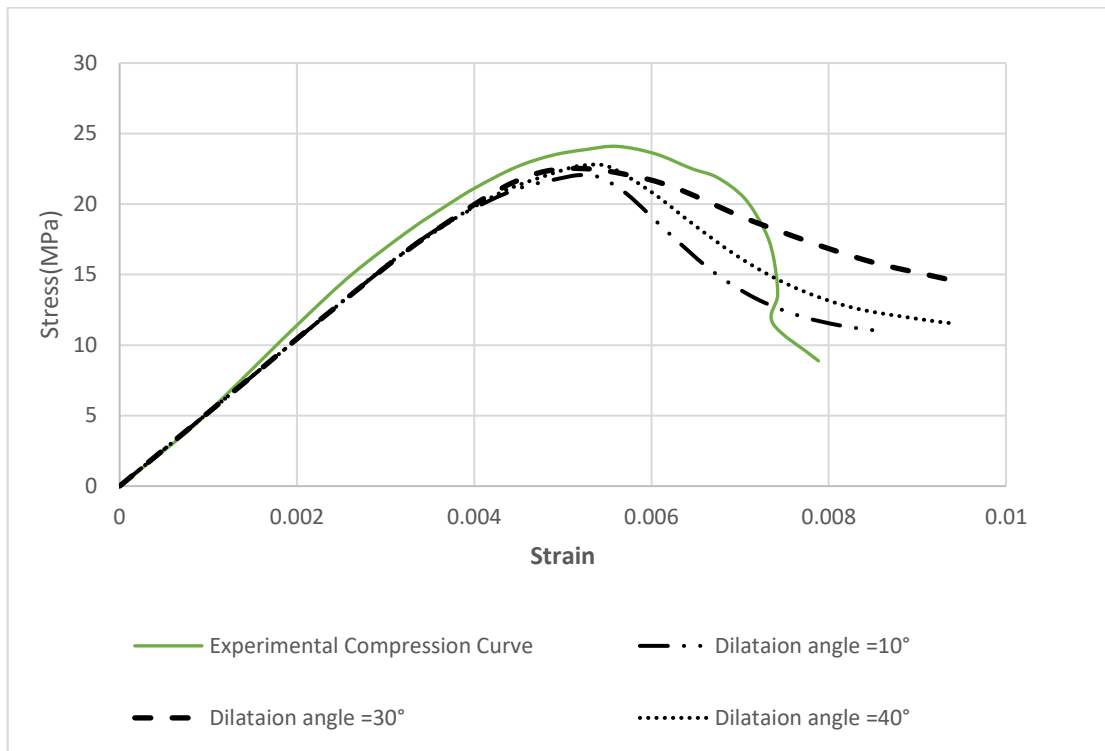
Figure 6-5 Sensitivity Analysis with the variation of dilation angle for Viscosity Coefficient of 0.01

2) The numerical simulation of compression test on mortar cylinder was replicated with a variation in viscosity parameter «0,05; 0,01; 0,1», with constant dilatation angle equal to 30°

- The results presented in **Figure 6-6** shows the variance in the force-displacement relationship for various viscosity coefficient.

- It was noticed that with the increase of dilation angle, material hardening property increases, and variation of dilation angle property causes variation in the Force-Displacement curve

- The viscosity parameter of 0.01 meets the post-peak behaviour to a higher extent for the wall with a dilatation angle of 30°. The experimental failure mode is adequately reproduced with the numerical model.

- For a viscosity parameter= 0.1 there was slight to none relaxation noticed in post peak behaviour

- For viscosity parameter=0.01, the post peak relaxation was similar to the experimental behaviour.

- For a viscosity parameter =0.0001, there was a relaxation noticed after the first inelastic yield, that was too early compared to the experimental results

- The dilation angle of 30° meets the post-peak behaviour to a higher extent for the wall with a viscosity parameter coefficient of 0.01

- the viscosity parameter representing the relaxation time of the viscoplastic system, and is the plastic strain evaluated in the inviscid backbone model, therefore there was a direct correlation between the post-pak relaxation and the viscosity parameter

The post-peak behaviour of the wall is altered by the viscosity coefficient. The viscosity parameter of 0.01 meets the post-peak behaviour to a higher extent for the wall with a dilatation angle of 30°. The experimental failure mode is reproduced with the numerical model as indicated by the stresses contour in **Figure 6-6**.
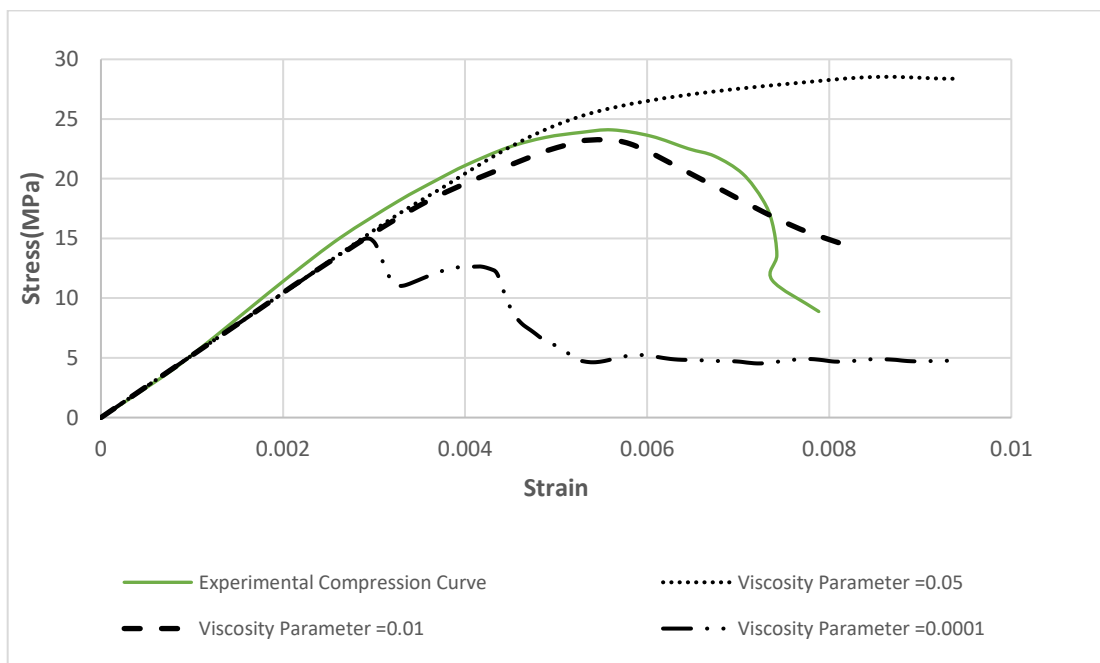
Figure 6-6 Sensitivity Analysis with variation of viscosity parameter for Force displacement relation
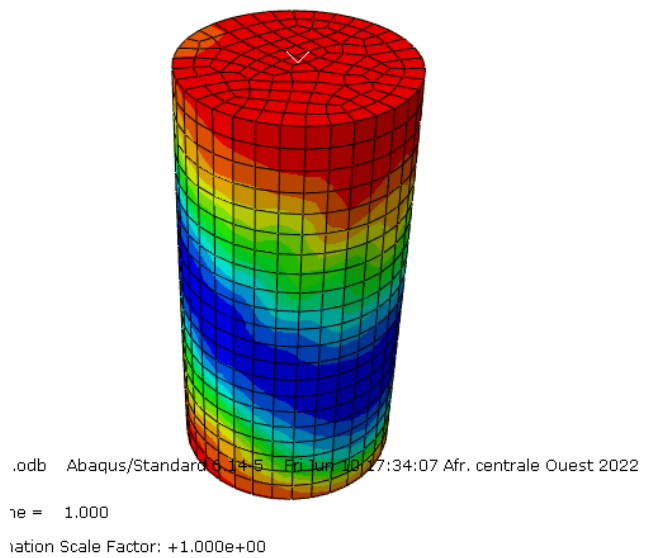
a   b

Figure 6-7 Mortar compression test failure mode : a) Real Test ; b)Numerical Model

6.2.1.3   *Mortar adopted properties:*

After an elastic properties calibration and sensitivity analysis for the mortar's Concrete Damage Plasticity, the properties indicated in **Table 6-1** simulate the experimental results to a great extent.

Table 6-1 Mortar's adopted properties

Mortar's Elasticity		Mortar's plasticity				
E	*v*	ψ	Eccentricity	fb0/fc0	K	Viscosity
5300MPa	0.2	30°	0.05	1.16	2/3	0.01
Mortar's Tensile Behaviour						
Yield Stress		Inelastic Strain				
21.1538461538461		0				
22.6223776223776		0.000794598436389449				
23.4615384615384		0.00106751954513146				

23.8811188811188	0.00139161336176259
24.090909090909	0.00169864960909734
23.5664335664335	0.0022103766879886
22.5174825174825	0.00279033404406535
21.8881118881118	0.003182658137882
20.4195804195804	0.00372850035536599
18.2167832167832	0.00430845771144276
16.3286713286713	0.00471783937455576
13.6013986013986	0.00521250888415065
11.5034965034965	0.00570248756218903
8.88111888111888	0.00644065387348967
Tensile Behaviour	
Yield Stress	Cracking Strain
0.312421371	0
0.1171875	0.00073513035166084

6.2.2   Identifying properties of Hollow clay brick:

The brick compression test realized by [2] is replicated using Abaqus/CAE as indicated in **Figure 6-8 Figure 6-9** , Concrete Damaged Plasticity model was adopted to identify the brick's properties.
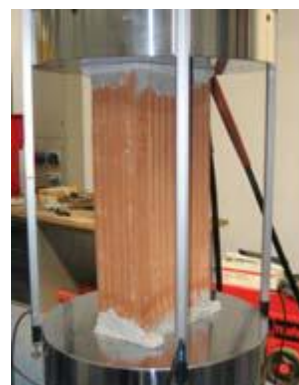
a)   b)

Figure 6-8 Brick Real compression test: a)Orthogonal to holes; b) Parallel to holes [2]

<div align="center">a)   b)</div>
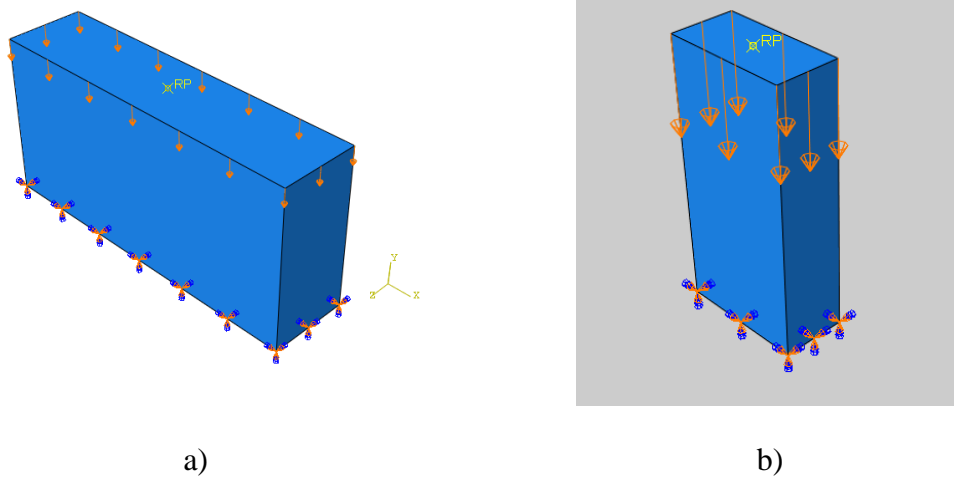
Figure 6-9 Brick compression test numerical model: a) Orthogonal to holes; b) Parallel to holes

6.2.2.1   Identifying the elastic properties of brick:

For the Poisson's ratio, a classic value of 0.2 was adopted, and the average Young modulus calculated from the experimental curves [2] of the compression test showed a result of $E_{bp} = 2911\ MPa$ for brick in the parallel to holes direction, and $E_{bo} = 810\ MPa$ for brick in the orthogonal to holes direction.

6.2.2.2   Identifying Concrete Damaged Plasticity properties of Brick using sensitivity analysis

In order to identify brick material properties using a CPD model, the same method previously explained in **section 6.2.1.2** is performed. However, the tensile behaviour of brick was not provided experimentally. For this reason, the tensile strength was calculated using the equations mentioned in [54]:

$$f_t = 0.3 * (f_c)^{2/3} \qquad\qquad\qquad \textbf{[6.5]}$$

$$\sigma_t = E_c * \varepsilon_t \ \ \text{If } \varepsilon_t \leq \varepsilon_{cr} \qquad\qquad\qquad \textbf{[6.6]}$$

$$\sigma_t = f_c * (\varepsilon_{cr}/\varepsilon_{ct})^{0.4} \ \ \text{If } \varepsilon_t < \varepsilon_{cr} \qquad\qquad\qquad \textbf{[6.7]}$$

After defining the compressive and tensile behaviour, the plasticity properties were adopted as follows:

- The flow rule is the ratio of second pressure invariant to the tensile meridian $K = 2/3$
- Flow potential eccentricity ε =0.05
- The ratio of biaxial compressive yield stress to uniaxial compressive yield stress fb0/fc0 = 1.16
- Dilation angle in the p-q plan identified by a sensitivity analysis ψ = 30°

-    Viscosity coefficient parameter identified after a sensitivity analysis equal to 1E-5.

The model successfully reproduced the experimental behaviour characterized by a linear pre-peak slope followed by a brittle failure **Figure 6-10** and **Figure 6-11**. The defined parameters are summarized in **Table 6-2**. The numerical failure modes are in good agreement with experimental tests as indicated in the **Figure 6-0**.
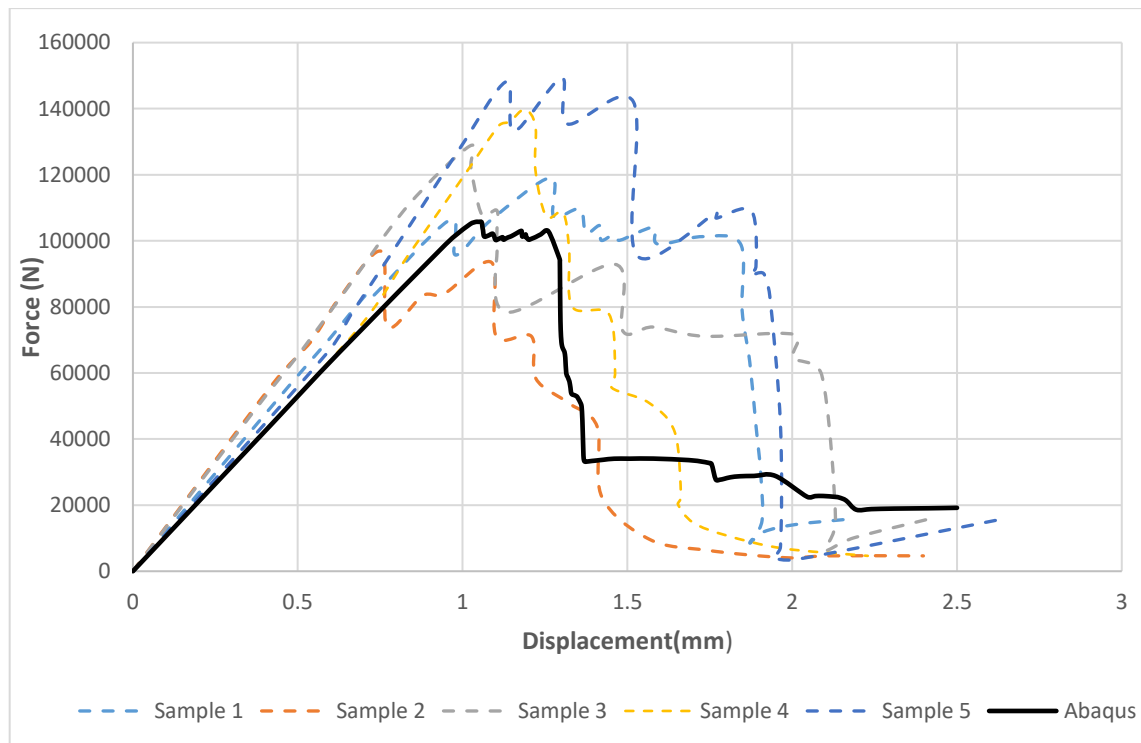
Figure 6-12 Numerical Brick Compression test results "Parallel to holes"
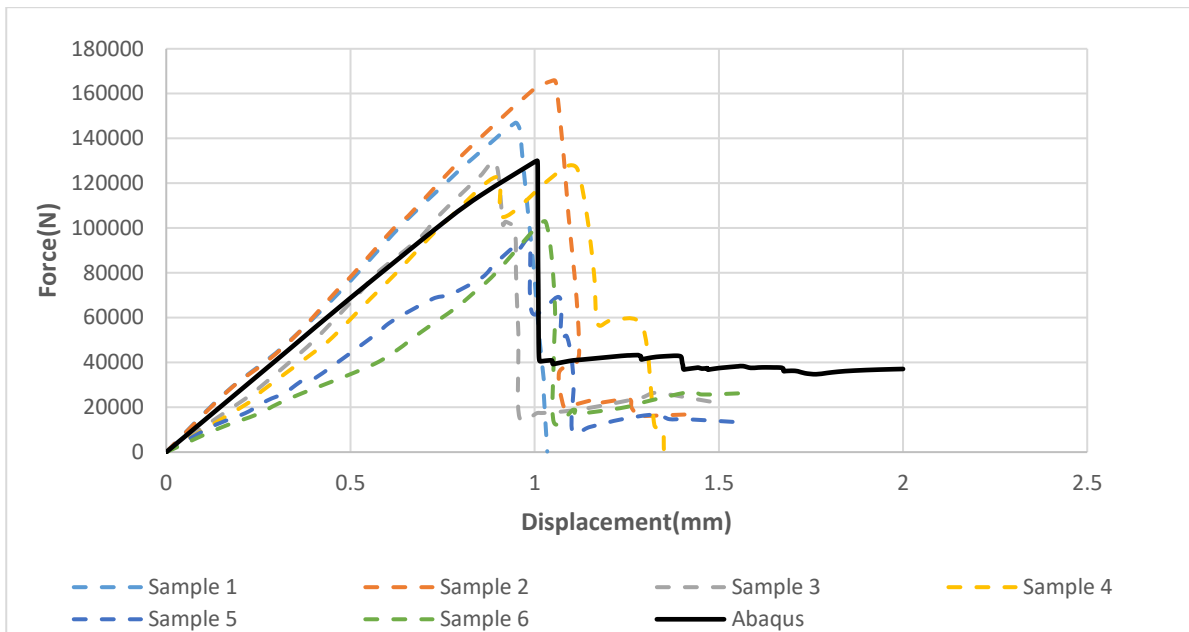
Figure 6-13 Numerical Brick Compression test results "Orthogonal to holes"

a)   b)
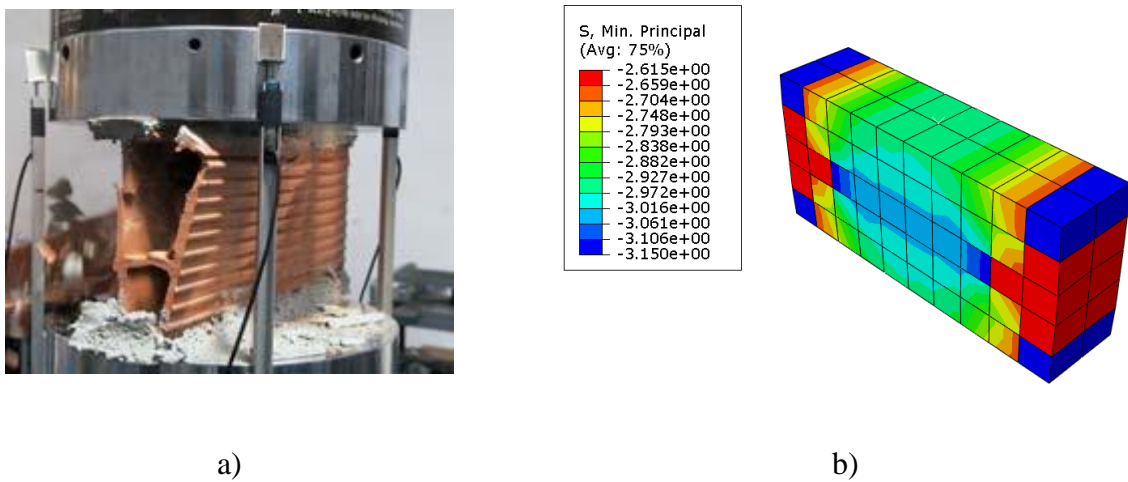
Figure 6-14 Brick orthogonal compression test failure mode : a) Real Test ; b)Numerical Model

a)   b)
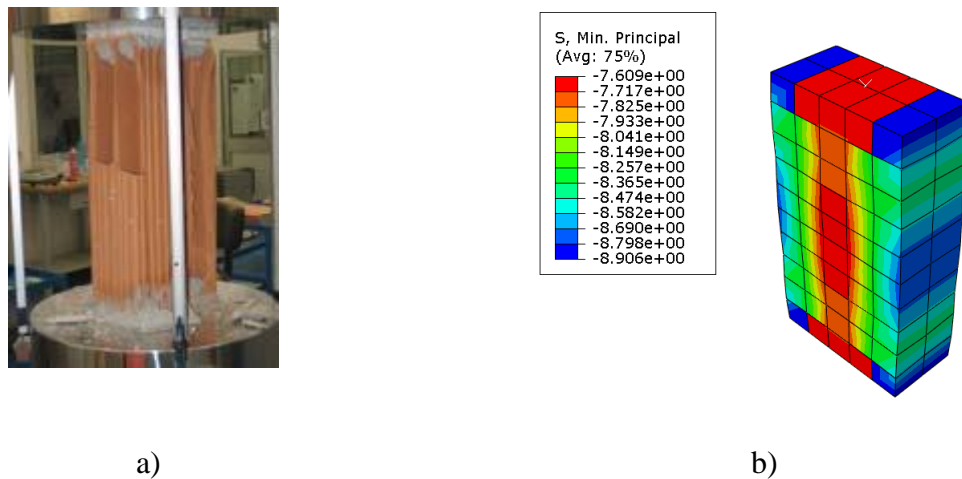
Figure 6-15 Brick parallel compression test failure mode : a) Real Test ; b)Numerical Model

A good accuracy between the experimental results and the numerical

6.2.2.3   Brick Adopted Properties

After an elastic properties calibration and sensitivity analysis for the brick's Concrete Damaged Plasticity the properties indicated in **Table 6-3** simulate the experimental results to a great extent.

Table 6-3 Properties of Brick

Plastic Properties				
ψ	K	fb0/fc0	Eccentricity	Viscosity Parameter
30°	2/3	1.16	0.05	1E-5
Parallel to holes brick			Orthogonal to holes brick	
Elastic Properties				
E_{bp}	v_{bp}		E_{bo}	v_{bo}
2911MPa	0.2		810MPa	0.2
Compressive Behaviour			Compressive Behaviour	
Inelastic strain	Yield Stress		Inelastic strain	Yield Stress

9.02	0	3.99999978106953	0
9.09499999999999	0.000468126164493256	4.65217393208091	0.000613975689532798
8.34499999999999	0.000833870109129906	4.88695627615626	0.000672699369813567
8.6	0.000919856268299462	3.84347807239899	0.00178224389675555
7.925	0.00125047910566969	3.89565182933552	0.00187297203431342
8.14999999999999	0.00129528879425101	3.76521743699418	0.00205731297070533
7.77499999999999	0.00145636145861086	3.034782650578	0.00276970798507662
7.91	0.00151328187383578	2.46086957283236	0.00333375299287618
8.165	0.00177850678733059	2.01739088742807	0.00377417086829522
7.805	0.00196258983231328	1.65217371315044	0.00422032389241976
7.91	0.00240947564546207	0.582608193063977	0.00535414853796592
0.905	0.00567816076656909	0.660869704190643	0.00538131129469423
1.01	0.00575203619909505	0.660869704190643	0.00546166819669994
1.16	0.00600636145861062	0.686956582658911	0.00579855044777117
1.28	0.00661189779079056	0.76521721806372	0.00626678608929428
1.265	0.00681172478040994	0.921739364595193	0.00690191613665739
1.265	0.00695220920947568	1	0.00708890127239248
1.31	0.00716172478040994	0.843477853468527	0.00820153856434164
Tensile Behaviour			
Yield Stress	**Cracking Strain**	**Yield Stress**	**Cracking Strain**
1,334309199MPa	0	0,863933319MPa	0

6.3   Walls numerical modelling

The panels' tests realized by [2] were simulated in detailed micro-model technique using blocks based model as indicated in **Figure 6-17** and **Figure 6-16**. The dimension of the experimental tests were

respected, the previous results in **6.2.1.1** and **6.2.1.2** were used to define the brick and mortar properties, the interaction was considered a tangential with a friction coefficient equal to 0.75 [34].
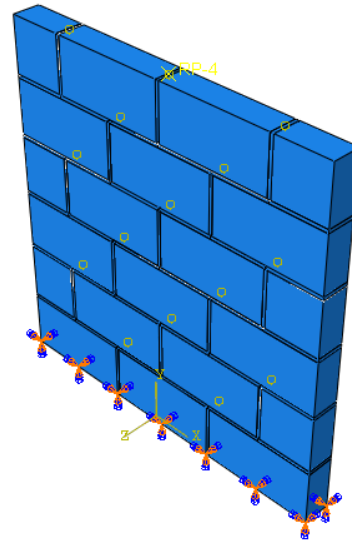
a)   b)

Figure 6-16Wall compression test model (Orthogonal to holes): a) Experimental ; b)Numerical
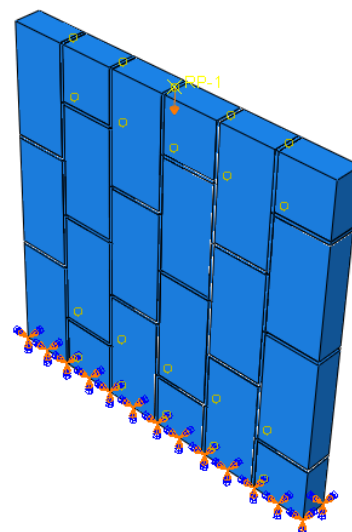
a)   b)

Figure 6-17 Wall compression test model (Parallel to holes): a) Experimental ; b)Numerical

6.3.1 Wall compression test Orthogonal to holes

The simulation of compression test showed a big variation compared to the experimental results, where the simulation showed a bigger elastic range, but with a similar elasticity modulus.

The numerical tests were replicated with a variation reduction in the brick's elastic range by reducing the plastic strain values, results indicated in **Figure 6-18** it is seen that the experimental result is satisfied to a greater extend with an elastic range of 40% of the brick's initial properties. The experimental failure mode was characterized by masonry crushing an out of plane buckling of the wall **Figure 6-19a**. In the case of the numerical model, the stress contour indicated a crushing mechanism in the masonry wall without any buckling **Figure 6-19b**. As a result, the wall properties used to simulation the experimental tests were as indicated in **Table 6-4**.
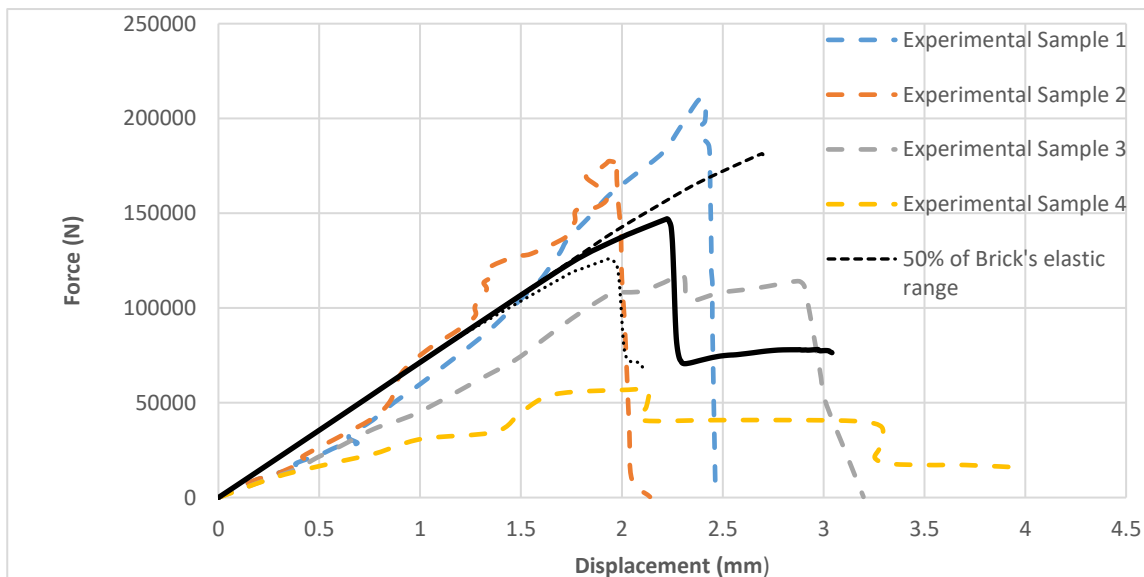
Figure 6-18 Numerical wall compression test (Orthogonal to holes) with variation reduction in brick's elastic range

a)   b)

Figure 6-19 Wall compression test failure mode (Orthogonal to holes): a) Experimental ;
b)Numerical

Table 6-4 Properties of Constituve materials of wall under normal compression

Elastic Properties			
Mortar		**Brick**	
E_m	v_m	E_{bo}	v_{bo}
5300MPa	0.2	810MPa	0.2
Plastic Properties			
ψ	K	fb0/fc0	Eccentricity	**Viscosity Parameter**	
30°	2/3	1.16	0.05	Brick=1E-5	Mortar=0.01
Mortar Compressive Behaviour		**Mortar Compressive Behaviour**	
Yield Stress	**Yield Stress**	**Yield Stress**	**Cracking Strain**
21.1538461538461	0	1.59999991242781	0
22.6223776223776	0.000794598436389449	1.86086957283236	0.000613975689532798

23.4615384615384	0.00106751954513146	1.9547825104625	0.000672699369813567
23.8811188811188	0.00139161336176259	1.5373912289596	0.001178224389675555
24.090909090909	0.00169864960909734	1.55826073173421	0.001872972034313342
23.5664335664335	0.0022103766879886	1.50608697479767	0.002057312970703533
22.5174825174825	0.00279033404406535	1.2139130602312	0.002769707985076662
21.8881118881118	0.003182658137882	0.984347829132944	0.003333752992876188
20.4195804195804	0.00372850035536599	0.806956354971228	0.003774170868295222
18.2167832167832	0.00430845771144276	0.660869485260176	0.004220323892419766
16.3286713286713	0.00471783937455576	0.233043277225591	0.005354148537965922
13.6013986013986	0.00521250888415065	0.264347881676257	0.005381311294694233
11.5034965034965	0.00570248756218903	0.264347881676257	0.0054616668196699944
8.88111888111888	0.00644065387348967	0.274782633063564	0.005798550447771177
		0.306086887225488	0.006266786089294288
		0.368695745838077	0.006901916136657393
		0.4	0.0070889012723924488
		0.337391141387411	0.00820153856434164
Mortar's tensile Behaviour		**Brick's tensile Behaviour**	
Yield Stress	**Yield Stress**	**Yield Stress**	**Cracking Strain**
0.312421371	0	0.864842286946615	0
Contact Properties			
μ			
0.75			

6.3.2 Wall compression test parallel to holes

The simulation of compression test showed a big variation compared to the experimental results, where the simulation showed a significantly bigger elastic modulus estimated to almost 5 times bigger than the experimental test as indicated in **Figure 6-20**.

Due to the inaccurate previous results, the test was replicated with a variation of brick's young modulus reduction, is seen that the experimental result is satisfied to a greater extend with a 15% of the initial Brick's young modulus as indicated in **Figure 6-21**.
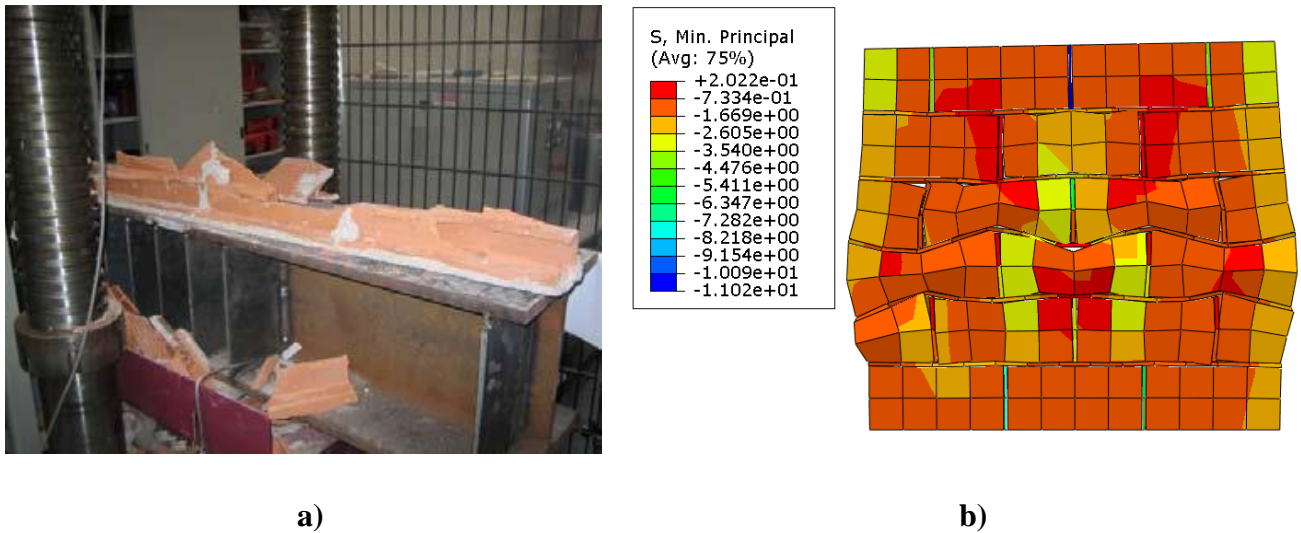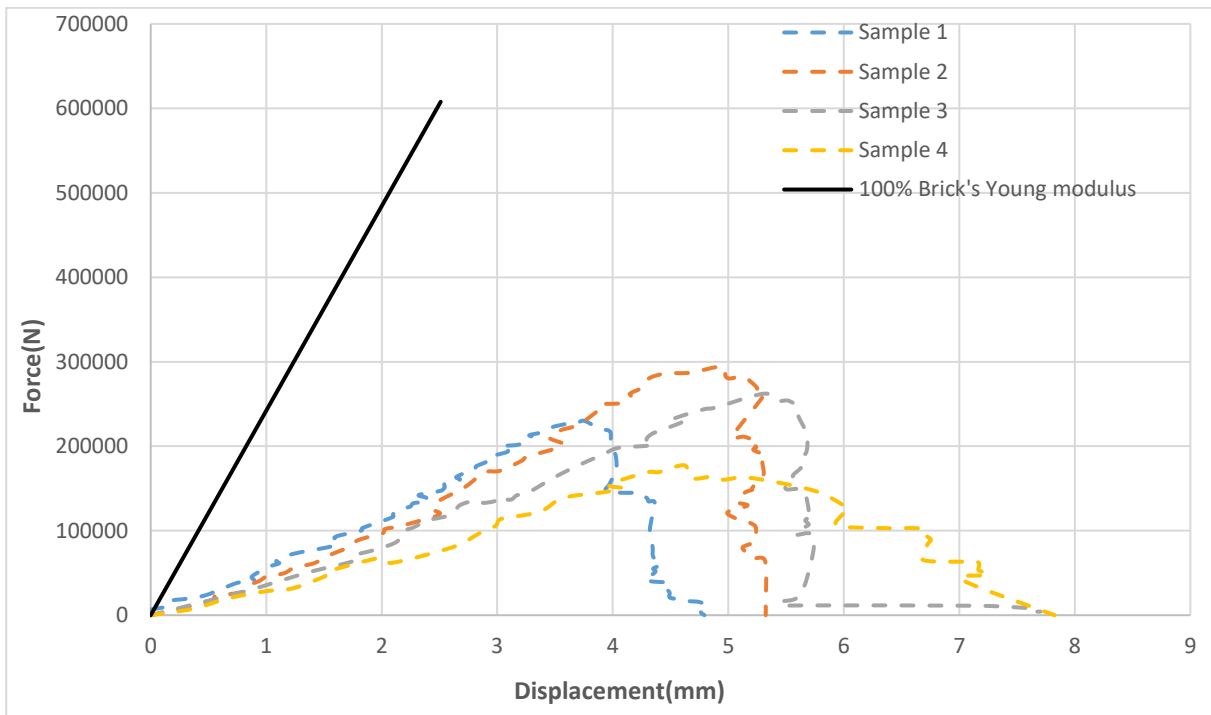

Figure 6-20 Numerical walll compression test(Parallel to holes) results
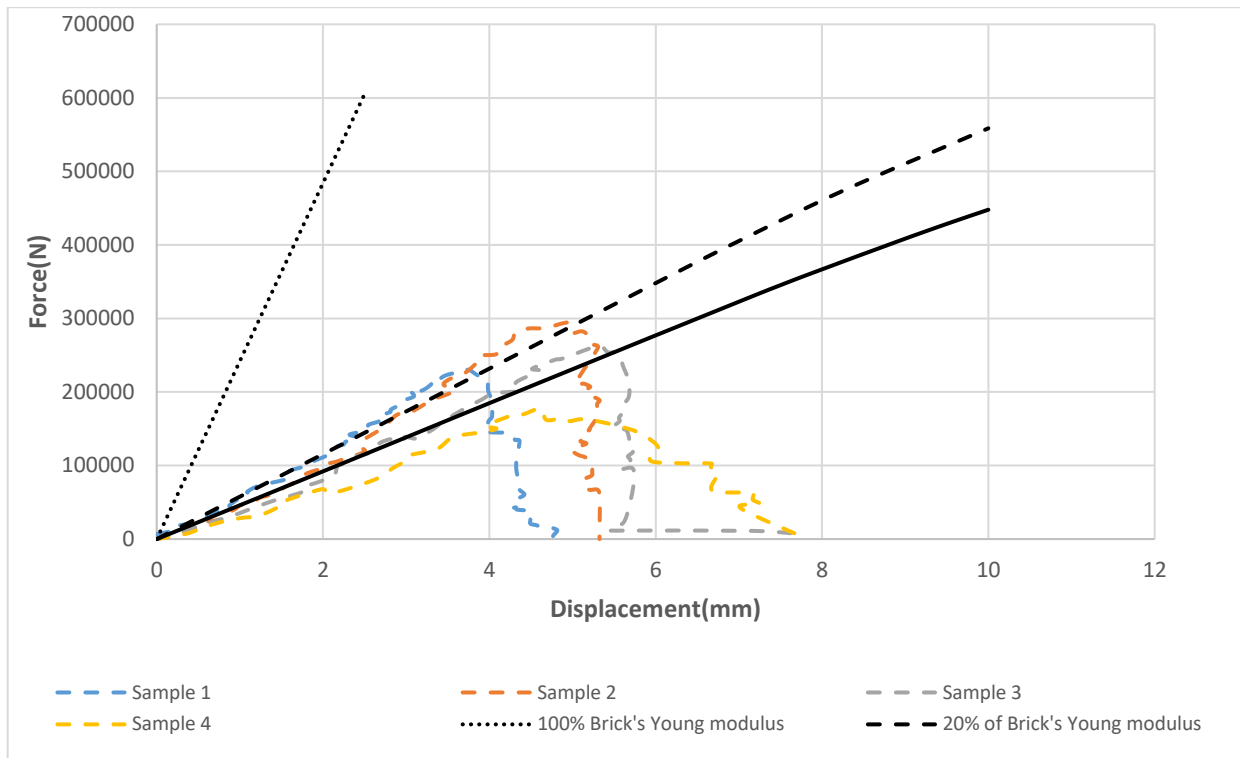
Figure 6-21 Numerical wall compression test (Parallel to holes) results with variation of Young Modulus

After defining a suitable elastic modulus, the test was replicated with a variation in compressive peak stress reduction as indicated in **Figure 6-22**. It is seen that 25% of the initial peak value of brick compression test satisfy the experimental results to a great extent.
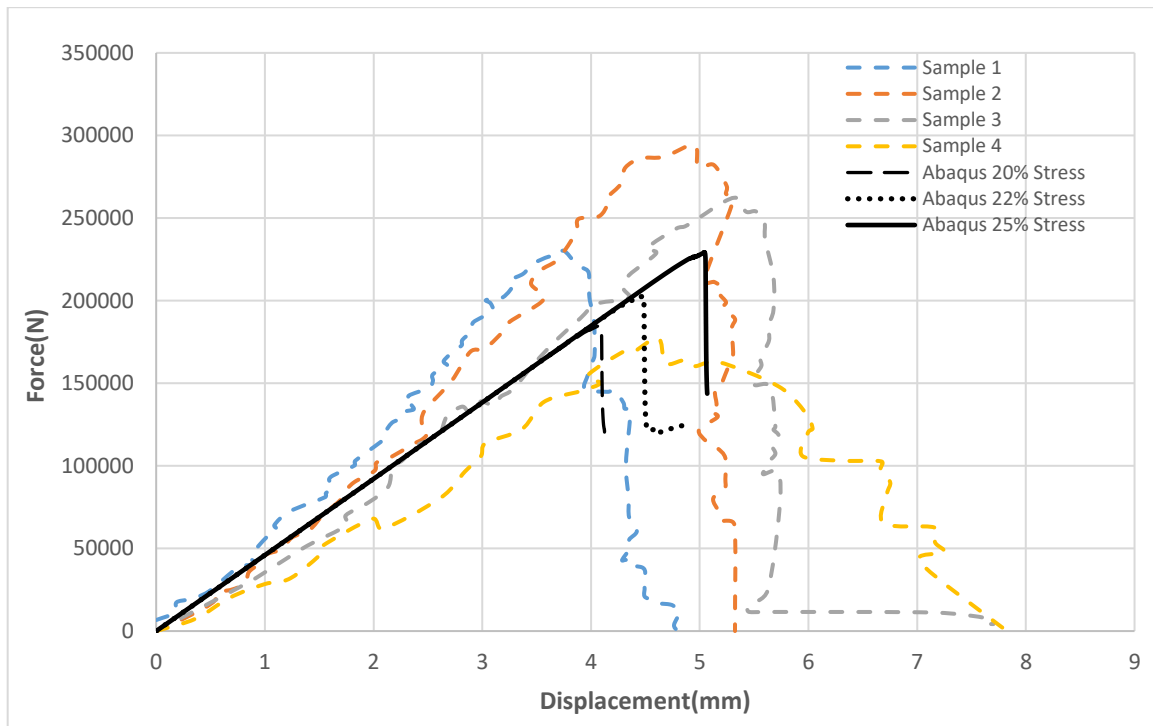
Figure 6-22 Numerical wall compression test(Parallel to holes) with variation reduction in brick's peak stress

The experimental failure mode was characterized by masonry crushing and separation of the wall **Figure 6-23**Figure 6-18**a**. The stress contour in the numerical model indicated a good agreement with the experimental results. The crushing and separation of the wall mechanism are well reproduced **Figure 6-23b**. As a result, the wall properties used to simulate the experimental tests were as indicated in **Table 6-5**.
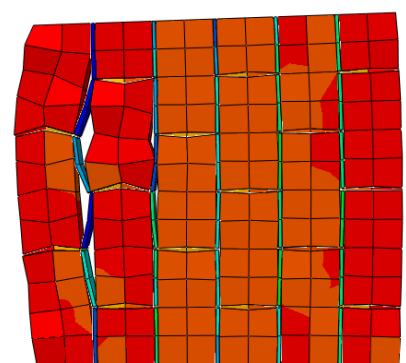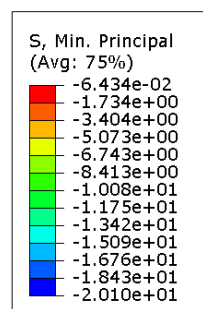
a)   b)

Figure 6-23 Wall compression test failure mode (Parallel to holes): a) Experimental ;
b)Numerical

*Table 6-5 Properties of Constituve materials for wall under horizontal compression*

Elastic Properties			
Mortar		**Brick**	
E_m	v_m	E_{bo}	v_{bo}
5300MPa	0.2	436.65 MPa	0.2
Plastic Properties			

ψ	K	fb0/fc0	Eccentricity	Viscosity Parameter	
30°	2/3	1.16	0.05	Brick=1E-5	Mortar=0.01

Mortar Compressive Behaviour		Mortar Compressive Behaviour	
Yield Stress	**Yield Stress**	**Yield Stress**	**Cracking Strain**
21.1538461538461	0	2.255	0
22.6223776223776	0.000794598436389449	2.27375	0.000468126164493256
23.4615384615384	0.00106751954513146	2.08625	0.000833870109129906
23.8811188811188	0.00139161336176259	2.15	0.000919856268299462
24.090909090909	0.00169864960909734	1.98125	0.00125047910566969
23.5664335664335	0.0022103766879886	2.0375	0.00129528879425101
22.5174825174825	0.00279033404406535	1.94375	0.00145636145861086
21.8881118881118	0.003182658137882	1.9775	0.00151328187383578
20.4195804195804	0.00372850035536599	2.04125	0.00177850678733059
18.2167832167832	0.00430845771144276	1.95125	0.00196258983231328
16.3286713286713	0.00471783937455576	1.9775	0.00240947564546207
13.6013986013986	0.00521250888415065	0.22625	0.00567816076656909
11.5034965034965	0.00570248756218903	0.2525	0.00575203619909505
8.88111888111888	0.00644065387348967	0.29	0.0060063614586106 2
		0.32	0.00661189779079056

		0.31625	0.00681172478040994
		0.31625	0.00695220920947568
		0.3275	0.00716172478040994
Mortar's tensile Behaviour		**Brick's tensile Behaviour**	
Yield Stress	**Yield Stress**	**Yield Stress**	**Cracking Strain**
0.312421371	0	0.864842286946615	0
Contact Properties			
μ			
0.75			

CHAPTER 7

CONCLUSION

Chapter 7: Conclusion

7.1   Discussion

7.1.1   Experimental and Numerical results discussion:

- The initial experimental characterization test performed by [2] showed a variety in the results between tested samples; The brick loaded in parallel to hole direction presented a 200% higher compressive strength than the brick loaded in orthogonal to holes direction, whereas the failure of all brick samples was found brittles, however, the post plastic failure curves have presented a roughness due to the heterogeneous nature of hollow clay brick unit's, where the collapsed brick's stacks over the next level and creates an additional compression resistance as the compressor goes down.

- The initial experimental characterization test on mortar presented proximate results between tested samples, with a much bigger compressive strength than the tensile strength, the experimental compressive strength falls within the range of the Algerian regulations "3.5<f_{ctm}=23.49<55 MPa".

- The compression test on the wall showed the influence of load direction on the walls failure mechanisms, different load directions 'Orthogonal, Parallel to brick holes and diagonal at 45°' presented three different failure mechanisms same as found by [11], however, the compression test on walls showed a variation in results between the samples loaded in the same direction that reaches up to 53% of the maximum value in the experimental elasticity modulus.

- The orthogonal to holes compression test on walls presented a lower value of the compressive strength and elasticity modulus compared to the parallel to holes loading.

- The sensitivity analysis of the brick in orthogonal and parallel to holes direction and mortar presented a similar value of dilatation angle for both constitutive materials.

- The numerical modelling of the wall compression test based on the properties of the initial material presented an overestimation of compressive strength compared to the results of the experimental tests, a calibration process was required and performed to improve the simulation results.

- The numerical simulation of the orthogonal to holes compression test on walls based on the constitutive material properties showed accuracy in the elasticity modulus values, however, the parallel to holes loading simulation did present an overestimation of the elastic modulus that is up to 500% of the experimental value that was calibrated to obtain the correct simulation.

- The calibrated numerical simulation of the walls compression tests presented mechanical behaviour "Load-displacement and stress-strain relationship" and failure mechanisms similar to the experimental results.

7.1.2 Theoretical results discussion:

- The Algerian Construction Regulation [1] recommend a few equations to determine the resistance of a masonry wall based on the initial materials test.

$$R = 0.55\sqrt[3]{\sigma_m . \sigma_b}$$ [7.1]

R : Wall average compressive breaking strength expressed in MPa

σ_m: Mortar compressive strength expressed in MPa

σ_b: Brick compressive strength expressed in MPa

$$E_M = \frac{E_b . E_m (h + e)}{(h . E_m + e . E_b)}$$ [7.2]

E_b : Elasticity modulus of the brick expressed in MPa.

E_m : Elasticity modulus of the mortar expressed in MPa;

E_M : Elasticity modulus of the wall expressed in MPa;

h: height of the product expressed in mm ;

e: thickness of the product.

Using **[7.1]** and **[7.2]** the elastic modulus and compressive strength were calculated theoretically the are presented in Table 7-1 Theoretical resistance of masonry wall**Table 7-1** .

Table 7-1 Theoretical resistance of masonry wall

Theoretical	**Experimental**
Wall under orthogonal to holes compression	
$R_{Orth\ min} = 2.229 MPa$ $R_{Orth\ max} = 3.14 MPa$	$R_{Orth\ Exp} = 1.895 MPa$
$E_{M.Orth} = 3767.30 MPa$	$E_{M.Orth.Exp} = 4804.2 MPa$
Wall under parallel to holes compression	

$R_{Par\,min} = 2.826 MPa$ $R_{Par\,max} = 3.94 MPa$	$R_{Par\,Exp} = 3.11 MPa$
$E_{M.Par} = 3010.6 MPa$	$E_{M.Par.Exp} = 4325.5 MPa$

- It is noted that the wall average experimental compressive strength is out of the theoretical rage in the orthogonal loading case, it is found to be less than 50% of the minimum theoretical value in certain samples, however, the theoretical results seem to satisfy the experimental results in case on the parallel to holes loading.

- The experimental elasticity modulus is greater than the theoretical one in both cases of loading.

- The theoretical results showed an inaccuracy and unreliability compared to the experimental values.

7.2   Conclusion:

Initial experimental studies on hollow clay brick and mortar, and masonry walls under compression load in orthogonal and parallel to brick holes direction were carried out. Stress-strain and Force-Displacement relationship were extracted [2]. Numerical modelling using FEM software ABAQUS is developed, and non-linear behaviour is captures using CDP model.

The previous results were compared to theoretical results obtained using [1]. It was found that the hollow clay brick has a higher compressive strength under parallel to holes loading compared to orthogonal to holes loading. The compressive strength of constituent materials-brick and mortar are quite high as compared to masonry walls due to the anisotropy induces combined use of constituent materials.

The theoretical methods to determine the wall resistance to compression were found unreliable, as the experimental compressive strength in case of the orthogonal to holes compression were found less than 50% of the minimum theoretical value.

FE analysis results of masonry walls under compression load shows a disagreement with experimental results, presenting an overestimation of the walls compressive strength. The calibrated CDP model parameters used for FE analysis works well and are capable to capture non-linear force-displacement behaviour under compression as it shows good agreement vis-à-vis experimental studies and presenting a similar failure mechanism.

The Direction of loading has an influence on the value of the modulus of elasticity and compressive strength. Masonry walls loaded in the direction parallel to brick holes had higher values of the modulus of elasticity and compressive strength than the walls loaded in the direction orthogonal to brick holes.

Because of the limited number of tested walls all presented results and comments should be regarded mainly from qualitative point of view. More tests data are required to confirm validate or rebut the previous results.

Works Cited

[1] Règles de conception et de calcul des maçonneries D.T.R C2.45, Centre National d'Etudes et de Recherches Intégrées du Bâtiment, 2005.

[2] A. V. Bergami, Implementation and experimental verification of model for nonlinear analysis of masonry infilled r.c frame, 2007.

[3] DTU Travaux de bâtiment , Travaux d'enduits de mortiers, Partie 1-1 : Cahier des clauses techniques, 2008.

[4] D. d. t. e. méthodes, RECUEIL DES FICHES D'IDENTIFICATION DES MALFAÇONS, Version Septembre 2019.

[5] M. Tabbakhha, Multiscale methodology for vulnerability assessment of masonry structures, Ecole Centrale Paris, 2013.

[6] D. M. Farshchi, Numerical modelling of in-plane behaviour of URM walls and an investigation into the aspect ratio, vertical and horizontal post-tensioning and head joint as a parametric study., 2009.

[7] N. N. T. a. J. Thomas, Behaviour and strength assessment of masonry prisms, 2018.

[8] L. M, Modelling of the non-lineaire behaviour of masonry, 1990.

[9] H. a. al, Effect of mortar grade on the uniaxial compression strength of low-strength hollow concrete block masonry prisms, 2020.

[10] H. B. K. a. al, Stress-Strain Characteristics of Clay Brick Masonry under Uniaxial Compression, 2007.

[11] A. W. PAGE, The biaxial compressive strength of brick masonry, 1981.

[12] Méthodes d'essai de la maçonnerie Partie 3 : Détermination de la résistance initiale au cisaillement NF EN 1052-3, France : l'Association Française de Normalisation (AFNOR), AVRIL 2003.

[13] A. F. C. A. FURTADO, Seismic vulnerability assessment and retrofitting strategies for masonry infilled frame buildings considering in-plane and out-of-plane behaviour, 2020.

[14] Out-of-plane bending of masonry : behaviour and strength, Technische University of Technology, 01/01/1999.

[15] P. B. Lourenco, Computational Strategy for Masonry Structures, Netherlands: Delft University Press, 1996.

[16] JHOMPSON and THOMPSON, Development of diametral testing procedures to provide a measure of strength characteristics of masonry assemblages, Int. Conf. of Masonry Structural System, Austin, Texas, 1967.

[17] M. DHANASEKAR and A. PAGE, The influence of brick masonry infill properties on the behavior of infilled frames, 1986.

[18] R. Nowak, Strength Parameters of Clay Brick Walls with Various Directions of Force, Testing of Materials and Elements in Civil Engineering (2nd Edition), September 2021.

[19] I. Layadi, Effet de remplissage en maçonnerie sur lecomportement de portique en béton armé sous chargement latérale, 2019.

[20] Méthodes d'essai des éléments de maçonnerie- Partie 1 : Détermination de la résistance à la compression, Janvier 2001.

[21] F. Parisi, Full scale testing of unreinforced masonry walls with openings, 2012.

[22] N. Ismail and J. M. I. , In-plane and out-of-plane testing of unreinforced masonry walls, 2016.

[23] A. A. A. A. M. M. Hussein Okail, Experimental and analytical investigation of the lateral load response of confined masonry wall, 2016.

[24] E. Badshah, Response of masonry systems against blast loading, 2021.

[25] Chr.Mayrhofer, Reinforced masonry walls under blast loading, 2001.

[26] J. S. J. S. H. B. B. a. D. J. Hoemann, Minimally Reinforced CMU Cavity Walls Against Blast Demands, Part II: Performance Under Impulse Loads. ASCE Journal of Performance of Constructed Facilities, 2014.

[27] J. H. J. S. H. S. J. D. R. H. M. B. B. Davidson, Full-Scale Experimental Evaluation of Partially Grouted, Minimally, Air Force Research Laboratory ReportAFRL-RX-TY-TR-2011-0025, 2011.

[28] G. D. C. ,. G. d. F. Stefano De Santis, "Out-of-plane seismic retrofitting of masonry walls with Textile Reinforced Mortar composites," *Springer Nature,* 2019.

[29] Paulo B Lourenço, "Shaking table testing for masonry infill walls: unreinforced versus reinforced solutions," *Earthquake Engineering & Structural Dynamics,* November 2016.

[30] F. Messali and J. Rots, In-plane drift capacity at near collapse of rocking unreinforced calcium silicate and clay masonry piers,, vol. Volume 164, 2018,.

[31] R. Esposito and F. Messali, Seismic assessment of a lab-tested two-storey unreinforced masonry Dutch terraced house, Springer, 2019.

[32] A. D'Alessandro and A. Meoni, Full-scale testing of a masonry building monitored with smart brick sensors, November 2018.

[33] F. Sciarretta, S. Russo and C. Casalegno, Experimental Analysis of Failure Mechanisms in Masonry-PFRP Profile Connection, Department of Design and Planning in Complex Environments, IUAV University of Venice, Dorsoduro 2206, 30123 Venice, Italy, 2018.

[34] K. F. Abdulla, Simulating masonry wall behaviour using a simplified micro-model, 2017.

[35] H. Hao and Y. L. , Homogenization of Masonry Using Numerical Simulations, 2001.

[36] G. M. Bahman Ghiassi, Numerical Modeling of Masonry and Historical Structures, Woodhead Publishing Series in Civil and Structural Engineering, 2019.

[37] J. M. F. E. R. J. S. M. Rots, "Computational modeling of masonry with a view to groningen induced seismicity," in *10th International Conference onStructural Analysis of Historical Constructions, SAHC,*, 2016.

[38] P. R. J. B. J. Lourenc¸o, "Continuum model for masonry: parameter estimation and validation. J. Struct. Eng," 1998.

[39] E. M. G. C. S. Bertolesi, Homogenization towards a mechanistic rigid body and spring model (HRBSM) for the non-linear dynamic analysis of 3D masonry structures, 2018.

[40] Y. L. P. Belmouden, An equivalent frame model for seismic analysis of masonry and reinforced concrete buildings., 2009.

[41] A. M. G. T. A. Chiozzi, A genetic algorithm NURBS-based new approach for fast kinematic limit analysis of masonry vaults., 2017.

[42] A. M. G. G. N. T. A. Chiozzi, A fast and general upper-bound limit analysis approach for out-of-plane loaded masonry walls., 2018 .

[43] A. G. N. M. G. T. A. Chiozzi, UB-ALMANAC: an adaptive limit analysis NURBS-based program for the automatic assessment of partial failure mechanisms in masonry churches, 2018.

[44] N. D. Agüera, "Structural Response of Unreinforced Masonry Walls," *Journal of Civil Engineering and Architecture 10 (2016) 219-231,* 2016.

[45] A. B. Habieb, "Low Cost Frictional Seismic Base-Isolation of Residential New Masonry Buildings in Developing Countries: A Small Masonry House Case Study," *The Open Civil Engineering Journal,* December 2017.

[46] L. Alejano, "Drucker–Prager Criterion," *Rock Mechanics and Rock Engineering,* November 2012.

[47] "Abaqus/CAE ver. 6-12.2," Dassault Systemes Simulia Corp, 2012.

[48] M. .. Gilbert, Fatigue in Railway Infrastructure, 2009.

[49] ,. J. O. S. O. E. O. J. Lubliner, A plastic-damage model for concrete, International Journal of Solids Structures, 1989.

[50] G. L. F. J. Lee, Plastic-Damage Model for Cyclic Loading of Concrete Structures, Journal of Engineering Mechanics, 1998.

[51] H. F. Wei Demin, Investigation for plastic damage constitutive models of the concrete material, 2017.

[52] A. R. B. R. K. M. ,. G. B. M. Achyut Paudel, Homogenization of Masonry Wall using Sensitivity Analysis, International Journal of Engineering and Innovative Technology (IJEIT), February 2021.

[53] N. E. 1052-1, norme européenne, norme Fraiçaise : Méthodes d'essai de la maçonnerie Parite 1, Octobre 1999.

[54] J. A. Dauda and O. Iuorio, Numerical analysis and experimental characterisation of brick masonry, 2020.

[55] N. E. 1052-3, norme européenne, norme Fraiçaise : Méthodes d'essai de la maçonnerie Parite 03, Juillet 2007.

[56] M. S. Zulim, Anisotropy Effect of Masonry on the Behaviour and Bearing, 2020.

[57] F. S. a. al, Experimental Analysis of Failure Mechanisms in Masonry-PFRP, 2018.

[58] M. Hafezolghorani, Simplified Damage Plasticity Model for Concrete, 2017.

[59] A. Anandarajah, The Drucker–Prager Model and Its Integration, 2010.

[60] P. C. Association, Types and Causes of Concrete Deterioration, 2002.

[61] A. E. G. rimmer, A Glossary of Historic Masonry Deterioration Problems and Preservation Treatments, Library of Congress Cataloging in Publication Data, 1984.